Washington University in St. Louis
Washington University Open Scholarship

All Theses and Dissertations (ETDs)

January 2009

# A Phenotypic And Genetic Characterization Of The Cell Adhesion Molecules Echinoid And Friend-Of-Echinoid In The Directed Cell Movements Of Ommatidial Rotation During Drosophila Eye Development.

Jennifer Fetting
*Washington University in St. Louis*

Follow this and additional works at: https://openscholarship.wustl.edu/etd

Recommended Citation
Fetting, Jennifer, "A Phenotypic And Genetic Characterization Of The Cell Adhesion Molecules Echinoid And Friend-Of-Echinoid In The Directed Cell Movements Of Ommatidial Rotation During Drosophila Eye Development." (2009). *All Theses and Dissertations (ETDs)*. 109.
https://openscholarship.wustl.edu/etd/109

This Dissertation is brought to you for free and open access by Washington University Open Scholarship. It has been accepted for inclusion in All Theses and Dissertations (ETDs) by an authorized administrator of Washington University Open Scholarship. For more information, please contact digital@wumail.wustl.edu.

WASHINGTON UNIVERSITY IN ST. LOUIS

Division of Biology and Biomedical Sciences

Program in Developmental Biology

Dissertation Examination Committee:
Tanya Wolff, Chairperson
Aaron DiAntonio
James J. Havranek
Stephen L. Johnson
Kathryn G. Miller
James B. Skeath
Susan A. Spencer

# A PHENOTYPIC AND GENETIC CHARACTERIZATION OF THE CELL ADHESION MOLECULES ECHINOID AND FRIEND-OF-ECHINOID IN THE DIRECTED CELL MOVEMENTS OF OMMATIDIAL ROTATION DURING *DROSOPHILA* EYE DEVELOPMENT.

By

Jennifer Lynn Fetting

A dissertation presented to the
Graduate School of Arts and Sciences
of Washington University in
partial fulfillment of the
requirements for the degree
of Doctor of Philosophy

August 2009

Saint Louis, Missouri

# Acknowledgements

I am grateful to my thesis advisor, Dr. Tanya Wolff, for her help and mentoring during my time in the lab. Tanya allowed me to be an independent scientist, giving me the freedom and opportunity to design my own project. I particularly appreciate Tanya's support and understanding during this past year.

I would like to thank Ryan Fiehler, Justina First, Bree Grillo-Hill, Jake Guinto, Sara Larson, and Amy Rawls, my colleagues in the Wolff lab. They were incredible labmates and good friends, generous with their time and advice. Thank you, also, to my thesis committee: Dr. Aaron DiAntonio, Dr. James J. Havranek, Dr. Stephen L. Johnson, Dr. Kathryn G. Miller, Dr. James B. Skeath and Dr. Susan A. Spencer for their advice and guidance with my project. I especially want to thank Dr. Susan Spencer for being so incredibly generous with suggestions, reagents, and unpublished data.

My friends, both here at Wash U and elsewhere, were an amazing source of support. In particular Jennifer Taylor, Justina First, Bree Grillo-Hill, Jessica Esparza, and Suzanne Brady were indispensible for helping me get through grad school.

Most of all, I would like to thank my family: Fritz, Sally, and Jeffrey Fetting, for their unwavering love and support during my time in graduate school. They were always willing to listen, and to offer assurance, and most importantly, to change the subject when the question, "So how are things going in the lab?" was answered with "I don't want to talk about it". I dedicate this dissertation to them, with love and thanks.

# Table of Contents

# List of Tables and Figures

# Abstract of the Dissertation

A Genetic Analysis of Cell Adhesion Molecules in Directed Cell Movements During Drosophila Eye Development: the Role of Echinoid and Friend-of-Echinoid in Ommatidial Rotation.

By

Jennifer Lynn Fetting

Doctor of Philosophy in Biology and Biomedical Sciences (Developmental Biology)

Washington University in St. Louis, 2009

Professor Tanya Wolff, Chairperson

Correct development of multicellular organisms relies on the precise patterning of cells, which must respond to and interpret specific cues that instruct the cells to differentiate and often undergo directed cell movements and rearrangements to give rise to functional tissues and organs. Differential adhesion between the stationary and mobile cells permits and promotes these cellular movements, effecting patterning of cells and tissues. During *Drosophila* eye development, groups of cells, the ommatidial precursors, undergo a 90° rotational movement within a matrix of stationary cells, providing the cell motility readout of tissue polarity. The mechanisms that regulate ommatidial rotation are not well understood.

In order to better understand how ommatidia coordinate cell signaling and cell adhesion to regulate the directed cell movement of ommatidial rotation, I investigated the roles of two cell adhesion molecules, Echinoid (Ed) and Friend-of-Echinoid (Fred), in this process. Initially, I characterized the misrotation phenotypes resulting from loss-of-function mutations in these two genes, and used a genetic approach to ascertain that they function during larval development and cooperate to regulate rotation.

To understand the underlying mechanism by which *ed* and *fred* regulate rotation, I performed a row-by-row analysis of Ed and Fred protein localization during ommatidial rotation, and found that these proteins localize in patterns that are consistent with an affect on cell-cell adhesion. This observation led to the hypothesis that different levels of Ed or Fred in rotating vs. nonrotating cells provide a permissive environment for cell movement at the beginning of ommatidial rotation. Beginning midway through ommatidial rotation, equalizing levels of these proteins in the ommatidial cells and the interommatidial cells leads to a restrictive environment, thus slowing ommatidial rotation. In support of this hypothesis, I demonstrate that manipulating levels of these proteins and interfering with the establishment of the early permissive environment slows ommatidial rotation.

My work also provides evidence that Ed and Fred may regulate signaling in the slow phase of ommatidial rotation. Mosaic analysis identified a requirement for *ed* and *fred* in photoreceptors R1, R6, R7 and the cone cells for proper ommatidial rotation. In addition, I used a genetic approach to identify potential interactors of *ed* and *fred* in rotation, and found that both genes interact with two downstream effectors of Egf signaling: the Mapk/Pnt transcriptional output and the Cno cytoskeletal/junctional output.

Furthermore, my analysis of the *cno* loss-of-function phenotype provides the first indication that Cno inhibits ommatidial rotation.

Egf signaling promotes ommatidial rotation, although the underlying mechanism is unclear. I hypothesize that Egfr signaling promotes ommatidial rotation by inhibiting Cno activity in the ommatidial cells. As ommatidial rotation slows, Ed and Fred cooperate to regulate the Egf receptor in R1, R6, R7 and the cone cells, and increased inhibition of the Egf receptor as Ed levels rise leads to an increase in Cno activity and the cessation of ommatidial rotation.

Using a genetic approach, I also identified the tissue polarity genes as interactors of *ed* and *fred* in rotation. Intriguingly, *ed* and *fred* specifically modify different subsets of the TP genes. Mosaic analysis of the tissue polarity gene *strabismus* (*stbm*) identified a requirement for *stbm* in photoreceptor R7, thus providing the first indication of a role for a tissue polarity gene outside of photoreceptors R3 and R4 to regulate some aspect of tissue polarity.

.

# CHAPTER ONE

## An introduction to *Drosophila* eye development, tissue polarity, and ommatidial rotation

# Abstract

Throughout the development of multicellular organisms, manipulation of cell-cell adhesion is vital for cell signaling, cellular movements, and tissue maintenance. Proper development also requires the precise patterning of cells, which must interpret and respond to specific molecular cues that instruct them to assume distinct identities, initiate an appropriate differentiation program, and arrange themselves in the three dimensional space of a tissue. The study of tissue polarity in the *Drosophila* eye provides an excellent model system for studying the patterning of cells in response to molecular signals, and understanding how cell-cell adhesion integrates with signaling to regulate directed cell movements during pattern formation.

## The *Drosophila* compound eye

The adult *Drosophila* compound eye consists of approximately eight hundred unit eyes, or ommatidia, arranged in a precise hexagonal lattice (Fig. 1-1). Each ommatidium contains approximately 20 cells: eight photoreceptor neurons (R1-R8), four cone cells, and primary, secondary, and tertiary pigment cells. The rhabdomeres, or light-sensing organelles, of the photoreceptors are arranged into trapezoids, with R3 occupying the point of the trapezoid (Fig. 1-1). These trapezoids assume one of two chiral forms, such that all ommatidia on the dorsal half adopt the same form, with R3 pointing toward the dorsal pole, and all the ommatidia on the ventral half of the eye adopt the opposite orientation. This divides the eye into dorsal and ventral halves separated by a midline, called the equator (Fig. 1-1) (Wolff and Ready, 1993).

The functional consequence of this chirality, combined with the curvature of the eye, is the appropriate mapping of the photoreceptor neurons to specific regions of the brain. This arrangement is necessary for correct image formation. Due to the way the eye curves, corresponding photoreceptors in adjacent ommatidia (for example, R1 in a group of adjacent ommatidia) all see the same point in space and project their axons to the same space in the brain. If the photoreceptors are not precisely aligned, the axons project to incorrect parts of the brain, disrupting vision and processing of images.

## *Drosophila* eye development

The precise organization of ommatidia originates during larval development. The eye imaginal disc is initially an undifferentiated epithelial monolayer covered by a sac called the peripodial membrane. During the third larval instar, a wave of differentiation,

the leading edge of which is marked by an indentation in the epithelium called the morphogenetic furrow (MF), originates at the posterior edge of the eye disc and sweeps across to the anterior edge. In its wake, cells are recruited into the developing ommatidia in a stepwise manner: first R8, followed by R2/R5, R3/R4, R1/R6, and R7, and finally the non-neural cone cells which secrete the lens of each unit eye. Thus, a temporal gradient exists such that the most developmentally mature ommatidia reside in the posterior part of the disc (Ready et al., 1976; Wolff and Ready, 1993).

Initially the arrangement of ommatidia is identical on both halves of the eye. Cells within the ommatidia are symmetric and are assembled so that the R3/R4 precursors face the anterior edge. By row 5 behind the furrow, the R3 and R4 cells adopt their respective fates and ommatidia begin a 90° rotation movement (Fig. 1-2). Here, the initial symmetry and uniformity of pattern are broken as the ommatidia on the dorsal half of the eye rotate counterclockwise, and those on the ventral half rotate clockwise to give rise to the mirror image symmetry seen in the adult. Rotation begins between rows 4 and 5 and is complete by row 15 (Fiehler and Wolff, 2007).

The cells in the rotating ommatidia move together, as a unit, within a matrix of undifferentiated, stationary cells (Fiehler and Wolff, 2007). They must therefore reduce their adhesion to these immobile neighbors, while remaining embedded in the eye disc. As R1/6/7 and the cone cells join the rotating ommatidia, they also need to decrease their adhesion to the stationary interommatidial cells (IOCs), bind tightly to the other ommatidial cells, and rotate as part of the unit. After rotation, the cone cells move up over the apical surface of the photoreceptors, covering them and forming stereotypical contacts (Wolff and Ready, 1993).

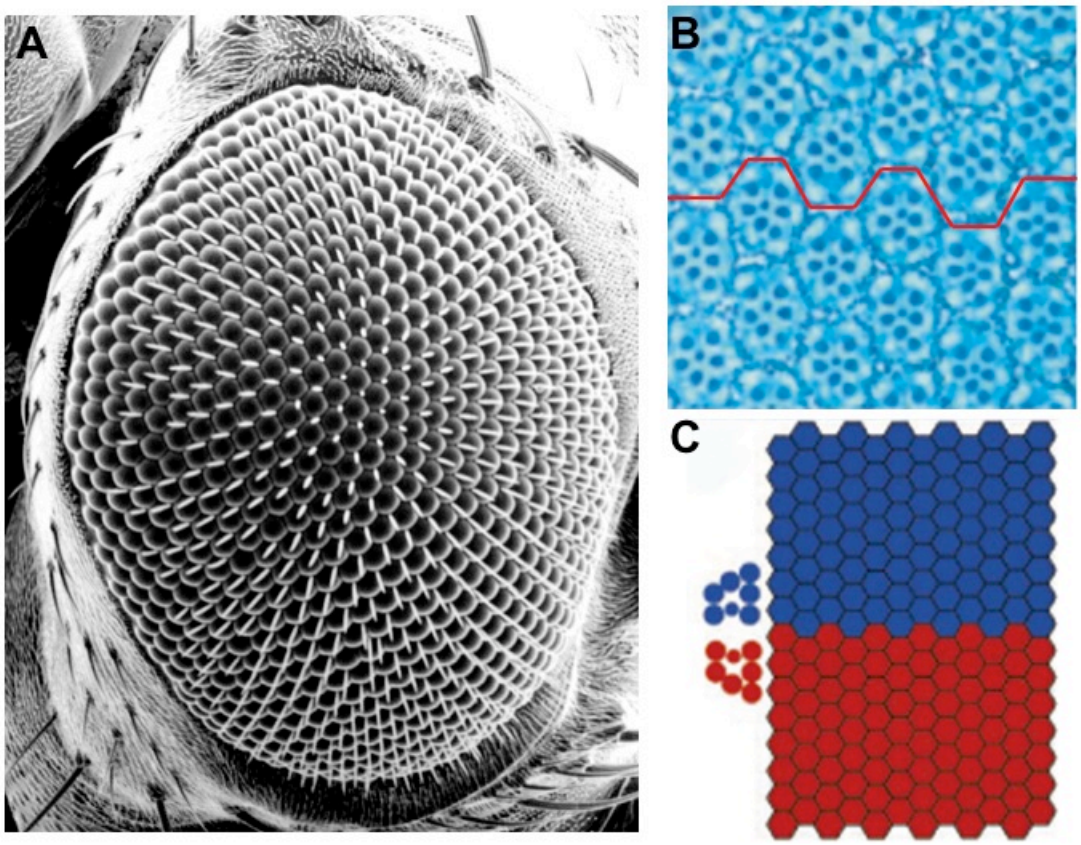


**Figure 1-1. The *Drosophila* compound eye.** (A) A scanning electron micrograph of the wild-type adult *Drosophila* eye. Ommatidia are precisely arranged into rows. (B) In each ommatidium, the rhabdomeres of seven of the eight photoreceptor cells are visible as darkly-staining dots arranged into trapezoids. On either side of the equator (red line), the point of the trapezoid faces in opposite directions, giving rise to mirror image symmetry. (C) A schematic representation of this symmetry and the two chiral forms of trapezoid found on the dorsal (blue) and ventral (red) halves of the eye. All figures are oriented such that dorsal is toward the top, ventral is toward the bottom, posterior is to the left, and anterior is to the right.

During pupal life, the eye disc everts and transforms from a sac-like structure into the flattened, dome-shaped adult eye. Even during the complex and dramatic morphological changes that occur during disc eversion, the ommatidia remain locked into place, and the connections between the eye and the brain are unchanged. After eversion, a subset of undifferentiated cells in the pupal eye join the ommatidia and become primary, secondary, or tertiary pigment cells or bristle cells. The remaining undifferentiated cells undergo programmed cell death, which removes the excess IOCs and sets the final hexagonal pattern (Wolff and Ready, 1993).

## Tissue Polarity

A universal characteristic of metazoans is the arrangement of cells into organized tissues. Epithelia are polarized along an apical-basal axis, with different junctions, proteins, and subcellular structures confined to apical or basal parts of the cell, allowing signaling events, absorption, and secretion to occur within the proper spatial context. Some tissues are also polarized along an axis perpendicular to the apico-basal axis, within the plane of the epithelium, known as tissue polarity or planar cell polarity.

Tissue polarity is vital for the development of multicellular organisms, and in numerous patterning and cell motility events. In vertebrates, tissue polarity is easily seen in the arrangement of hair follicles on the mouse epidermis, which are all uniformly oriented along the rostral/caudal axis (Guo et al., 2004). Similarly, tissue polarity is essential for the correct orientation of the stereocilia of the inner ear hair cells in the cochlea (Curtin et al., 2003; Lewis and Davies, 2002; Montcouquiol et al., 2003).

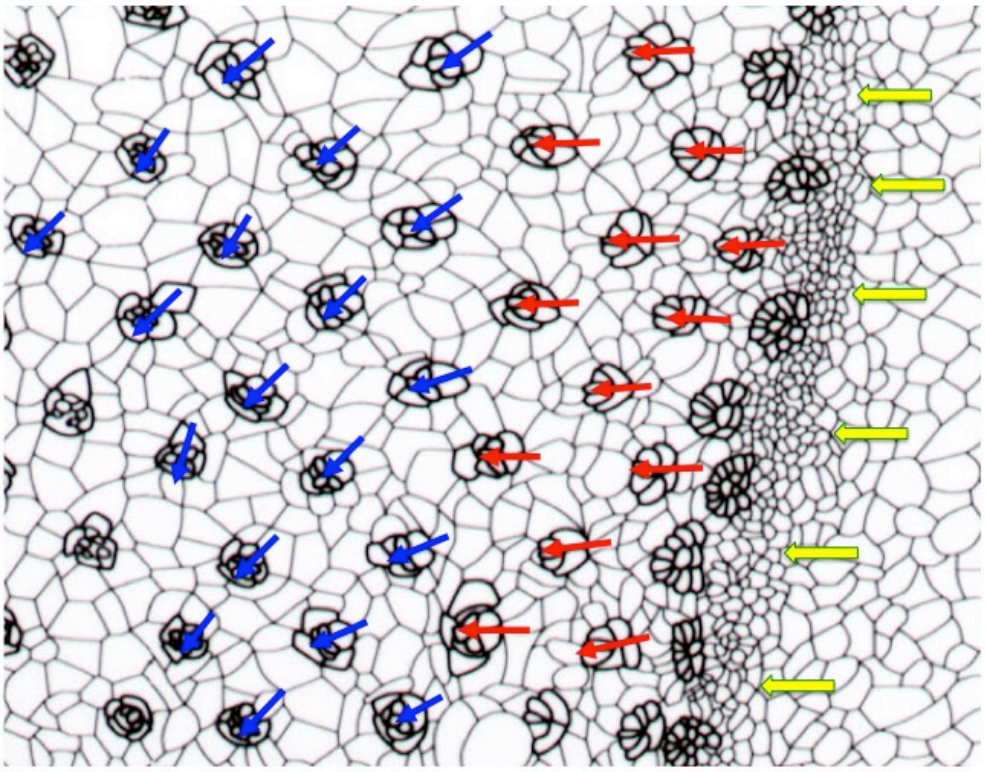

**Figure 1-2. Ommatidial rotation in the dorsal half of the *Drosophila* larval eye disc.** Posterior to the morphogenetic furrow (yellow arrows), cells differentiate and form ommatidial clusters (dark outlined cells). These clusters are initially oriented in the same direction on both dorsal and ventral halves of the eye, with the R3/R4 cell pair facing the anterior edge of the eye disc (red arrows). Five rows past the morphogenetic furrow, dorsal ommatidia begin to rotate counterclockwise (blue arrows) and ventral ommatidia begin to rotate clockwise (not shown). Rotation ceases after the ommatidia rotate a full 90°.

These stereocilia form a chevron on each hair cell, and that of each hair cell all point in the same direction. Disruption in the pattern results in defects in hearing.

Tissue polarity is not confined to epithelial cells. Mesenchymal cells in vertebrates including *Xenopis*, zebrafish, and mice rely on tissue polarity for the cell intercalation movements that drive convergent extension and lengthen the body axis during gastrulation (Darken et al., 2002; Djiane et al., 2000; Formstone and Mason, 2005; Goto and Keller, 2002; Montero et al., 2005). Similarly, tissue polarity organizes the epithelial cells that again undergo convergent extension during neural tube closure (Curtin et al., 2003; Jessen et al., 2002; Kibar et al., 2001; Park and Moon, 2002). Defects in these processes have catastrophic consequences for the embryo, including embryonic death and neural tube closure defects.

## Tissue polarity in the *Drosophila* eye

Much of our understanding about mechanisms that generate tissue polarity came from studies using *Drosophila*. Tissue polarity is most evident in the ommatidia, wing hairs, and abdominal hairs. A conserved group of genes, including *frizzled* (*fz*), *disheveled* (*dsh*), *strabismus* (*stbm*), *prickle* (*pk*), *diego* (*dgo*), and *flamingo* (*fmi*), are know as the core tissue polarity genes because they are essential for proper polarization of these tissues (Adler, 2002; Boutros and Mlodzik, 1999; Chae et al., 1999; Feiguin et al., 2001; Gubb et al., 1999; Klingensmith et al., 1994; Theisen et al., 1994; Usui et al., 1999; Vinson et al., 1989; Wolff and Rubin, 1998; Zheng et al., 1995). In eye, wing and abdominal tissue, the output of tissue polarity signaling is the polarized localization of the tissue polarity proteins to different sub-cellular domains of each cell. In the wing, Fz,

Dsh, Dgo, and Fmi form a complex on distal tip of the cell, while Stbm, Fmi, and Pk form a complex on the proximal face of the cells (Bastock et al., 2003; Klein and Mlodzik, 2005; Strutt, 2001; Strutt, 2002)(Fig. 1-3). This ultimately gives rise to the localization of an actin-based structure, the wing hair, at the distal tip of the wing cell (Eaton, 2003; Winter et al., 2001).

In the *Drosophila* eye, expression and activity of two atypical cadherins, Fat (Ft) (Mahoney et al., 1991) and Dachsous (Ds) (Clark et al., 1995), and Four-jointed (Fj), a Golgi kinase (Ishikawa et al., 2008), are thought to set up a global positional signal that is interpreted by the tissue polarity complex (Cho and Irvine, 2004; Rawls et al., 2002; Simon, 2004). Ds localizes in a gradient such that the highest levels are at the D and V poles and lowest at the equator. Fj localizes in a complementary pattern – high at the equator and low at the poles (Yang et al., 2002). Fat is expressed uniformly throughout the eye disc, but is modified by Fj activity in the Golgi so it effectively acts in a gradient as well (Strutt et al., 2004). These gradients are thought to bias Fz activity in the equatorial cell, although the mechanism by which this information is interpreted by the tissue polarity complex is unknown (Yang et al., 2002).

Tissue polarity in the eye is manifest in the adoption of one of two chiral trapezoid forms, and relies on proper execution of three earlier developmental events: fate specification (R3/R4 fate); direction of rotation (clockwise or counter-clockwise); and degree of rotation (from 0° to 90°) (Wolff et al., 2007). Different subsets of tissue polarity genes are required in R3 and R4 to determine R3/R4 cell fate, reminiscent of the distinct localization patterns seen in the wing (Fig. 1-3). *fz*, *dsh*, *dgo*, and *fmi* are required in R3, while *stbm*, *pk*, and *fmi* are required in R4 (Jenny et al., 2005; Strutt et al., 2002;

Strutt, 2002; Wolff and Rubin, 1998). One transcriptional target of Fz signaling in R3 is Delta (Dl), which binds and activates Notch (N) on the R4 cell (Cooper and Bray, 1999; Fanto and Mlodzik, 1999; Tomlinson and Struhl, 1999). This differential level of N activity results in different fates through the downstream effector Enhancer of *split* (E(spl))(Cooper and Bray, 1999). The direction of rotation has been shown to be tightly linked to fate specification, and it was assumed that degree of rotation was, too. For a long time, R3 and R4 have been thought of as the cells that control all aspects of tissue polarity.

Other tissue-specific effectors of tissue polarity in the eye include proteins that only affect the degree to which ommatidia rotate, while cell fates are specified properly and ommatidia initiate rotation in the correct direction. These molecules include the serine/threonine kinase Nemo (Nmo), DE-cadherin, DN-cadherin, and Egf signaling pathway members (Brown and Freeman, 2003; Choi and Benzer, 1994; Fiehler and Wolff, 2008; Gaengel and Mlodzik, 2003; Mirkovic and Mlodzik, 2006; Strutt and Strutt, 2003). In *nmo* mutant eyes, ommatidia adopt the correct chirality but generally fail to rotate the full 90° (Fig 1-4). *nmo* is required in R1, R6, and R7 for proper ommatidial rotation (Fiehler and Wolff, 2008).

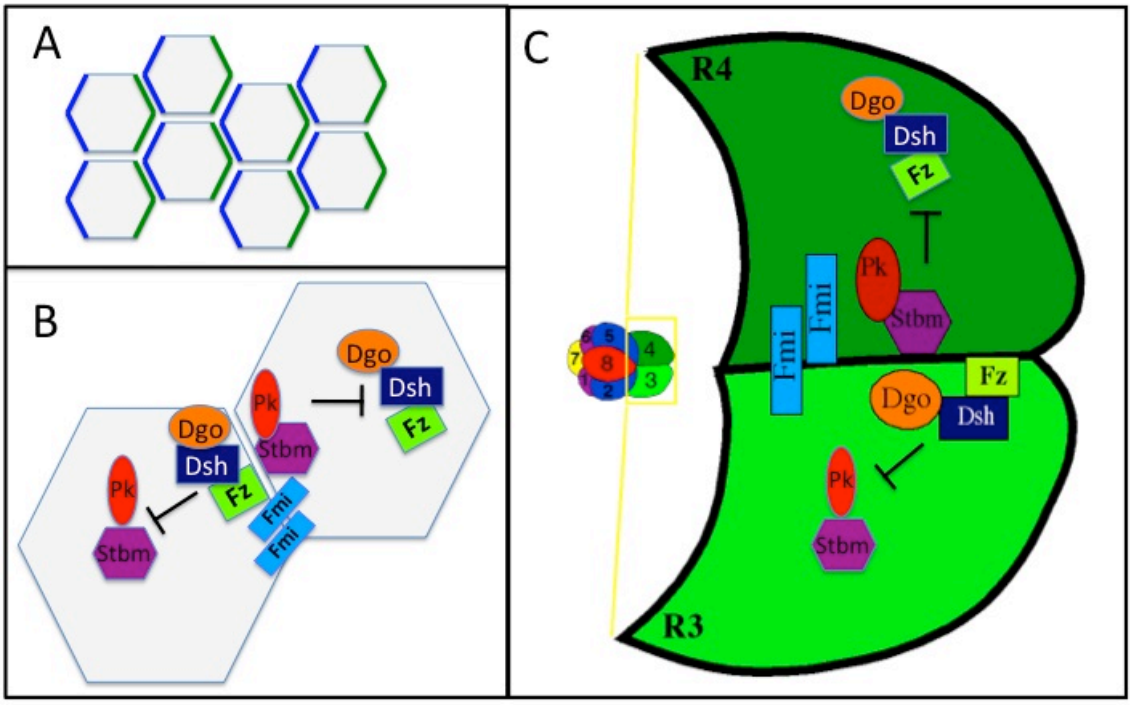


**Figure 1-3. Asymmetric localization of the tissue polarity proteins.** (A) The Fz/Dsh/Dgo complex (green) localizes to the distal membrane of pupal wing cells, while the Stbm/Pk complex (blue) localizes to the proximal membranes. Fmi is the only core tissue polarity protein that localizes to both faces. (B) The Fz/Dsh/Dgo complex blocks the Pk/Stbm complex from localizing to the distal membrane, while the Pk/Stbm complex prevents the Fz/Dsh/Dgo complex from localizing to the proximal membranes. (C) In the R3/R4 cell pair, the Fz/Dsh/Dgo complex localizes to the R3 cell and again prevents localization of Stbm/Pk at this membrane. Stbm/Pk, in turn, localize to the R4 membrane and block the localization of Fz/Dsh/Dgo at this membrane.

## Cell adhesion molecules and ommatidial rotation

Cell adhesion molecules play vital roles in cell movement: excess adhesion between two populations of cells inhibits or prevents movement (Hermiston et al., 1996; Lecuit, 2005). Previously, two cell adhesion molecules, E-cadherin and N-cadherin, were shown to be important during rotation (Mirkovic and Mlodzik, 2006). E-cad is the major cadherin in the *Drosophila* eye, localizing throughout the eye disc. It forms *trans* homodimers and localizes to adherens junctions (AJs), where it binds β-catenin to form and stabilize the AJs (Tepass and Harris, 2007). N-cadherin performs a similar function, but is confined to neurons and in the *Drosophila* eye disc is localized only to the R3/R4 boundary (Mirkovic and Mlodzik, 2006). Loss-of-function studies reveal that DE-cadherin promotes rotation, while DN-cadherin has the opposite effect, and it is the precise balance between levels of these two molecules that is essential for correct rotation (Mirkovic and Mlodzik, 2006). Additionally, the cadherins are thought to integrate signals from both the Egf signaling pathway and the tissue polarity pathway to control rotation, as they interact genetically with members of both pathways (Mirkovic and Mlodzik, 2006).

## Egfr signaling in eye development and rotation

The Egf signaling pathway is involved in almost every stage of *Drosophila* eye development, including photoreceptor recruitment (Dominguez et al., 1998; Freeman, 1997; Kumar et al., 1998; Spencer et al., 1998)), and recent work identified a role for the

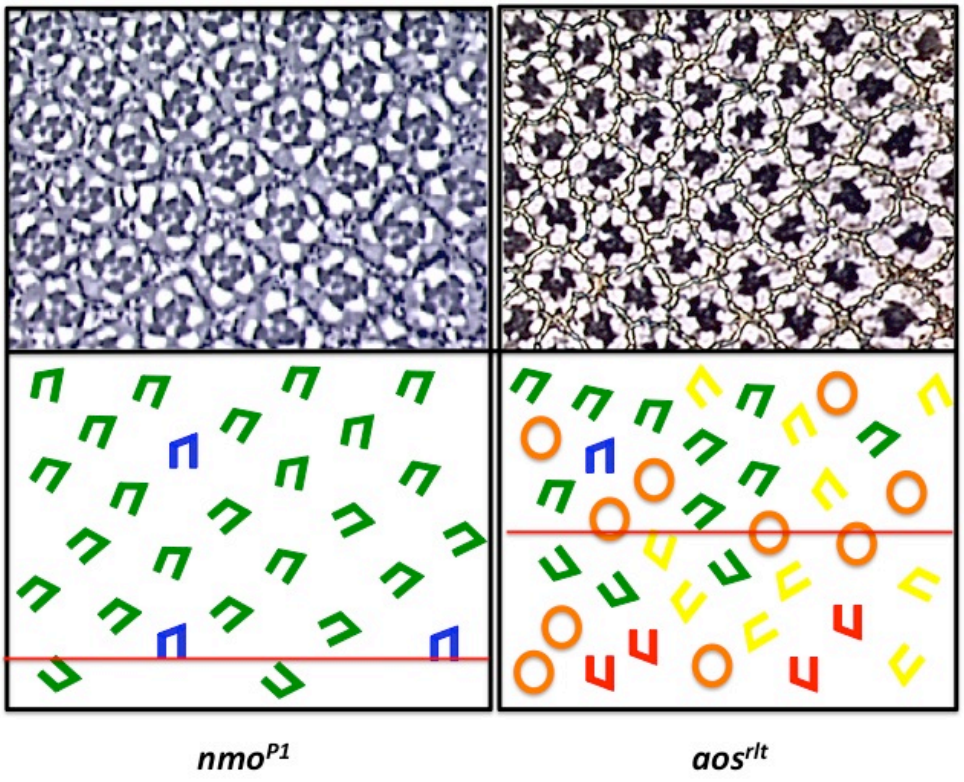


**Figure 1-4. Ommatidial rotation defects in *nmo*$^{P1}$ and *aos*$^{rlt}$ mutant eyes.** (A, B) Sections through adult eyes and (A', B') corresponding schematics. Mutations in *nmo* and Egf signaling pathway members, including *aos*$^{rlt}$, specifically affect the degree of ommatidial rotation component of tissue polarity. (A, A') *nmo*$^{P1}$ mutant ommatidia under-rotate (MAO = 60°, SD = 22 (Fiehler and Wolff, 2008) and data not shown). (B, B') *aos*$^{rlt}$ mutant ommatidia both over- and under-rotate (MAO = 80°, SD = 40). Green trapezoids represent under-rotated ommatidia and yellow trapezoids represent over-rotated ommatidia. Blue trapezoids and red trapezoids represent wild-type ommatidia in the dorsal and ventral halves of the eye, respectively. Orange circles represent ommatidia with an incorrect number of photoreceptors. Orange lines indicate the approximate location of the equator.

Egf signaling pathway in ommatidial rotation (Brown and Freeman, 2003; Gaengel and Mlodzik, 2003; Strutt and Strutt, 2003). The main Egfr ligand essential for proper rotation is Spitz, with Keren playing a redundant, nonessential role (Brown and Freeman, 2003; Brown et al., 2007). After ligand binding, the Egfr acts through an adaptor molecule and the GEF Sos, ultimately resulting in Ras activation (reviewed in (Shilo, 2003)). In rotation, both the Ras/Raf/Mapk transcriptional cascade (resulting in activation of the transcription factor Pointed (Pnt) (Gabay et al., 1996)) and the Ras/Canoe (Cno) cytoskeletal/junctional modification effector pathways transduce the Egf signal (Brown and Freeman, 2003; Gaengel and Mlodzik, 2003).

Cno is the *Drosophila* homolog of the mammalian AJ protein Afadin/AF-6, and has several PDZ domains, a Ras interaction domain, and an actin-binding domain (Matsuo et al., 1997; Miyamoto et al., 1995). Afadins localize to AJs, where they bind nectins (see below) and initiate AJ formation (Mandai et al., 1997; Pokutta et al., 2002; Tachibana et al., 2000). While different molecules such as E-cadherin and β-catenin are associated with stable AJs, afadins are particularly known for forming AJs in tissues that are continually being remodeled (Takai et al., 2003), such as those that must be at the cellular interface between motile and non-motile cells in order to allow the moving cells to slip past their stationary neighbors.

Three different models have been proposed to explain the role of Egfr signaling during ommatidial rotation. Brown and Freeman suggest that Egfr signaling acts as a "lock", or error correction mechanism during pupal development (Brown and Freeman, 2003). In this model, Egfr signaling acts to keep ommatidia locked into place during

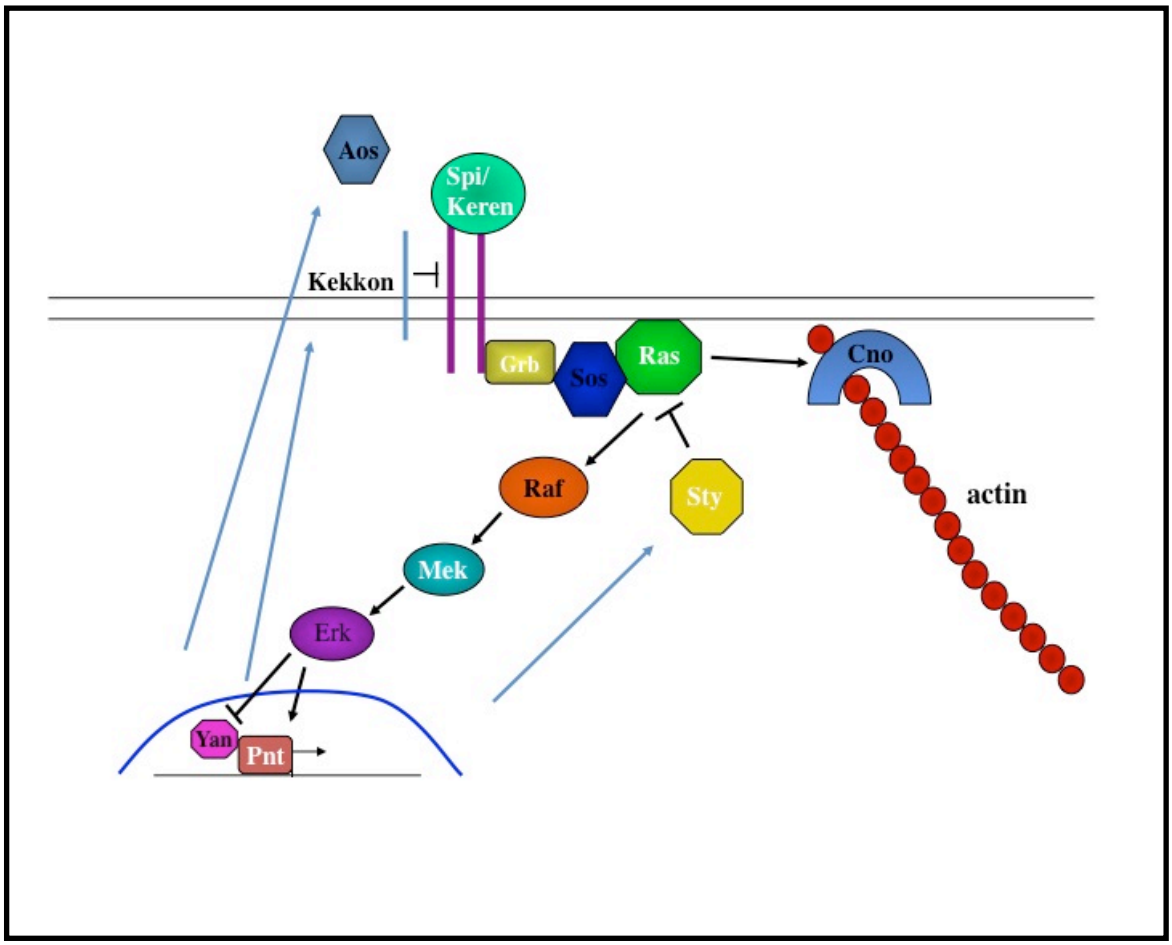


**Figure 1-5. The Egf signaling pathway during ommatidial rotation**. Upon Spi binding, the Egfr dimerizes and transautophosphorylates. This recruits the adaptor molecule Grb and the GEF Sos to the plasma membrane. Sos activates Ras, which then stimulates the Mapk pathway (Raf, Mek, Erk), resulting in changes in transcription via the transcription factor Pnt. Transcriptional targets of Pnt include the inhibitors Aos, Sty, and Kekkon1, forming a negative feedback loop. Ras also interacts with the actin-binding molecule Cno during ommatidial rotation.

later morphogenetic events. Gaengal and Mlodzik suggest that Egfr signaling acts as a "gas" pedal during the second 45º of rotation, regulating the strength of signaling from some other source (Gaengel and Mlodzik, 2003). They see significant over- and under-rotation of ommatidia before the end of larval development in Egf signaling pathway mutant eyes. Strutt and Strutt suggest that the rotation phenotypes seen in Egfr pathway members are due to the partial transformation of the mystery cells into R3/R4, resulting in inappropriate Fz localization, which contributes to the rotation phenotype (Strutt and Strutt, 2003).

Sections through adult Egf pathway mutant eyes reveal that ommatidia both over- and under-rotate (Fig. 1-4) (Brown and Freeman, 2003; Gaengel and Mlodzik, 2003; Strutt and Strutt, 2003). The mean angle of orientation (MAO) is 90°, but few ommatidia actually rotate this amount. There is a wide variance in the degree to which individual ommatidia rotate. This is true whether the mutation results in an increase or a decrease of Egf signaling, which made it difficult to determine whether the Egf pathway promotes or inhibits rotation. Genetic interactions between DE-cadherin and *spitz* suggest that the Egf pathway acts in a positive direction on rotation (Mirkovic and Mlodzik, 2006).

The Egf signaling pathway has multiple levels of regulation (Shilo, 2003). Transcriptional targets include its own inhibitors *argos* (*aos*), *kekkon1*, and *sprouty* (*sty*) thus forming a negative feedback loop (Casci et al., 1999; Ghiglione et al., 1999; Golembo et al., 1996; Klein et al., 2004). These mutations in Egfr inhibitors display defects in ommatidial rotation in addition to photoreceptor cell number defects. Other regulators of Egf signaling are not transcriptionally regulated by Egfr activation. These genes include two cell adhesion molecules, Echinoid (Ed) and Friend-of-Echinoid (Fred),

which cooperate to negatively regulate the Egf receptor during R8 selection (Rawlins et al., 2003b; Spencer and Cagan, 2003) (Spencer in preparation).

## Ed and Fred in *Drosophila* development

*ed* and its paralog *fred* both encode large transmembrane cell adhesion molecules (CAMs) with extracellular immunoglobin (Ig) C2 repeats and fibronectin type III domains (Bai et al., 2001; Chandra et al., 2003). While the extracellular domains of Ed and Fred share 69% identity, their intracellular domains are only 30% identical (Chandra et al., 2003). The intercellular tail of Ed contains a C-terminal PDZ-binding motif (PDZBM) and a Jaguar (Jar) binding domain, while the Fred intracellular domain has no conserved motifs (Chandra et al., 2003; Lin et al., 2007; Wei et al., 2005).

Ed negatively regulates Egfr upstream of Ras during R8 selection (Rawlins et al., 2003b; Spencer and Cagan, 2003). Mutations in *ed* lead to extra photoreceptor cells. Ed is putatively phosphorylated by, and may form a complex with, the Egfr. In addition, the Ed intracellular domain is cleaved, and undergoes endocytosis, which regulates Egf signaling (Spencer and Cagan, 2003). Additionally, Ed forms homophilic and heterophilic *trans* dimers with Fred, and this dimerization is necessary to keep Ed properly localized to the cell membrane (Spencer and Cagan, 2003) (Spencer, in preparation). In the wing, the PDZBM of Ed has been shown to bind both the AJ protein Bazooka (Baz) and the Ras effector Canoe (Cno) at their PDZ domains, and this binding is important for AJ stabilization (Wei et al., 2005).

Fred also functions to regulate Egf signaling. Recent evidence indicates that Fred binds Ed and inhibits Ed activity (Spencer, in preparation). Ed and Fred form

transheterodimers, and these are thought to promote Ed retention at the membrane and interfere with Ed cleavage and endocytosis and thus prevent Ed's inhibition of Egf signaling (Spencer, in preparation). *In vitro*, cells with high levels of either Ed or Fred segregate away from cells with low levels of Ed or Fred (Spencer, in preparation)(Spencer and Cagan, 2003). *In vivo*, Ed or Fred is not detectable at the interface between two cells with different levels of Ed or Fred (Laplante and Nilson, 2006).

In addition to their roles in eye development, *ed* and *fred* have additional tissue-specific functions that suggest a general role in attenuating Egfr and Notch signaling. For example, Ed and Fred modulate N signaling in the *Drosophila* notum, and are involved in the process of SOP selection through influencing Dl endocytosis (Chandra et al., 2003)(Ahmed, Chandra et al. 2003)(Escudero et al., 2003; Rawlins et al., 2003a). In this process, Ed and Fred do not interact with the Egf signaling pathway, even though it too plays a role in SOP patterning. In the wing, Ed acts redundantly with E-cadherin, binding Bazooka (Baz), an AJ protein, and Cno, to form and stabilize AJs (Wei et al., 2005). In this tissue, Ed is necessary for the correct localization of Cno and Baz; neither protein is membrane associated when Ed is not present. In the oocyte and embryo, differential Ed expression in adjacent cell types is thought to trigger actin cable formation, promoting dorsal closure (Laplante and Nilson, 2006). Also in the embryo, Ed binds Jar, the fly unconventional myosin VI, to promote its dimerization, and regulate dorsal closure (Lin et al., 2007).

The closest mammalian homologs of Ed and Fred are the nectins (Wei et al., 2005), Ig superfamily members that bind to Afadin/Af-6, and initiate formation of AJs

(Rikitake and Takai, 2008; Sakisaka et al., 2007; Tachibana et al., 2000; Takahashi et al., 1999; Takai et al., 2003). In mammals, Afadin and its binding partners, nectins and α-actinin, build and stabilize those dynamic AJs that undergo remodeling (Ooshio et al., 2007; Takahashi et al., 1999). Nectins and afadins have been implicated in numerous human diseases and developmental defects, including breast cancer, metastasis, and cleft palate (Sozen et al., 2001; Suzuki et al., 2000).

# Scope of this Dissertation

The complete mechanism underlying ommatidial rotation remains unclear. Manipulation of cell-cell adhesion and response to cell signaling are clearly vital for correct ommatidial rotation, but the means by which ommatidia coordinate these components to orchestrate the complex directed cell movements of ommatidial rotation is not known. To address this issue, I have investigated the roles played by two paralogous genes, *ed* and *fred*, in ommatidial rotation. First, I characterized the phenotypes of both genes, and found that they act during larval development to regulate the movements of the ommatidial cells. I next conducted a row-by-row analysis of the Ed and Fred protein localization during ommatidial rotation, and found that they localize in strikingly different patterns. From this analysis, I show that Ed levels are reduced in ommatidial cells prior to rotation, and that this reduction necessary for ommatidial rotation to occur. In contrast, I find that Fred is enriched in ommatidial cells compared to interommatidial cells, and that its expression pattern phenocopies those of two tissue polarity proteins Stbm and Fmi.

Using standard mosaic analysis, I demonstrate that *ed* and *fred* are required in R1, R6, R7, and the cone cells for correct ommatidial rotation. Furthermore, I show that both *ed* and *fred* interact genetically with members of the Egf signaling pathway during ommatidial rotation, and that unlike in the wing, Ed does not localize Cno to the membrane in eye discs. In addition, I show that *ed* and *fred* interact genetically with different subsets of tissue polarity genes: *ed* interacts with R3 genes, and *fred* interacts with R4 genes. I demonstrate a role for at lease one tissue polarity gene, *stbm*, in R7, providing the first evidence that a tissue polarity gene acts outside of R3/R4 to regulate tissue polarity. Finally, I generate and characterize a loss-of-function mutation that maps near *ed* and *fred* and phenocopies the *ed* and *fred* rotation and photoreceptor recruitment phenotypes.

# CHAPTER TWO

# The cell adhesion molecules Echinoid and Friend-of-Echinoid coordinate cell adhesion and cell signaling to regulate the rate of ommatidial rotation in the *Drosophila* eye

# Abstract

Directed cellular movements are a universal feature of morphogenesis in multicellular organisms. Differential adhesion between the stationary and motile cells promotes these cellular movements to effect spatial patterning of cells. A prominent feature of *Drosophila* eye development is the 90° rotational movement of the ommatidial precursors within a matrix of stationary cells. Here, we demonstrate that the paralogous cell adhesion molecules, Echinoid (Ed) and Friend-of-Echinoid (Fred), act throughout ommatidial rotation to modulate the degree to which the ommatidial precursors move. We propose that differential levels of Ed and Fred between stationary and rotating cells at the initiation of rotation creates a permissive environment for cell movement, and that uniform levels in these two populations of cells later in the process contribute to slowing the movement. In addition to this expected adhesive role in ommatidial rotation, we demonstrate, using a genetic approach, that *ed* and *fred* impart a second, independent, "brake-like" contribution to this process through the Egfr signaling pathway. Ed and Fred are localized in largely distinct patterns, but both patterns are dynamic throughout rotation. However, *ed* and *fred* are required in only a subset of cells for normal rotation. *ed* and *fred* are required in photoreceptors R1, R7 and R6, cells that, with one exception (*nmo*) have not been linked to a role in TP. Of particular note, this is the first demonstration of a requirement for the cone cells in the ommatidial rotation aspect of TP. *ed* and *fred* also genetically interact with the tissue polarity genes, but affect only the degree of rotation component of the TP phenotype, not the direction of rotation or the specification of the R3 and R4 fates. Significantly, we demonstrate that at least one tissue polarity protein, Stbm, is required in R7 to control the degree of ommatidial rotation.

# Introduction

Cell-cell adhesion is fundamental to metazoan development and to the growth and maintenance of adult tissues. In adult tissues, continuous regulation of cell adhesion underlies events such as spermatid development (Inagaki et al., 2006; Mueller et al., 2003; Ozaki-Kuroda et al., 2002), maintenance of apico-basal polarity (Nelson, 2003; Tsukita et al., 2001) and regeneration of tissues that require constant maintenance, such as the lining of the gut (Hermiston et al., 1996). Throughout metazoan development, cell adhesion plays key roles in events including maintenance of tissue integrity, boundary formation (Kim et al., 2000; Tepass et al., 2002), cell signaling (Jamora and Fuchs, 2002; Perez-Moreno et al., 2003; Sakisaka et al., 2007), and directed cellular movements (Hermiston et al., 1996; Pacquelet and Rorth, 2005). The precise and dynamic control of cell adhesion is also a critical regulator of tissue morphogenesis and patterning. For example, remodeling cell junctions within epithelia enables single cells and groups of cells to slide past their neighbors to reorganize tissues, such as during neural tube closure and convergent extension in vertebrates (Djiane et al., 2000; Formstone and Mason, 2005; Harrington et al., 2007) and ovary maturation and dorsal closure in *Drosophila* (Gorfinkiel and Arias, 2007; Lin et al., 2007; Niewiadomska et al., 1999). Loss-of-function mutations in cell adhesion molecules result in birth defects, including Zlotogora-Agur syndrome and Margarita Island ectodermal dysplasia, and disease states such as metastatic cancer (Matsushima et al., 2003; Naora and Montell, 2005; Pignatelli, 1998; Sozen et al., 2001; Suzuki et al., 1998; Suzuki et al., 2000). The coordinated regulation of cell adhesion also plays a key role in the rotational movement of subsets of cells that polarizes the *Drosophila* eye across its dorsal/ventral (D/V) midline in an event known as

ommatidial rotation. The mechanism by which changes in cell adhesion regulate this morphogenetic movement is poorly understood.

The 800 precisely aligned unit eyes, or ommatidia, of the *Drosophila* compound eye are polarized across the D/V midline of the eye, the equator. This polarity is manifest as two chiral forms of "trapezoids," composed of the photosensitive membranes, or rhabdomeres, of seven of the eight photoreceptor cells. The apex of the trapezoid (R3) points north in the dorsal half and south in the ventral half of the eye (Fig.1; reviewed in (Wolff and Ready, 1993))

Through a series of coordinated morphogenetic movements, the initially unpolarized retinal epithelium acquires polarity during the second half of third larval instar development. Groups of differentiating cells, the ommatidial precursors, rotate independently of their undifferentiated, stationary neighbors, the interommatidial cells (IOCs, (Fiehler and Wolff, 2007)). These patterning events closely follow a moving front of differentiation, marked by the morphogenetic furrow, which moves from posterior to anterior across the eye imaginal disc (Ready et al., 1976). Posterior to the furrow, the photoreceptors assemble into ommatidial units, beginning with R8 and followed by the R2/R5 and then the R3/R4 pairs. Ommatidial rotation begins coincident with assembly of this 5-cell precluster, five rows posterior to the morphogenetic furrow. Rotation continues as the R1/ R6 pair, followed by R7 and then the cone cells, joins the growing ommatidial unit. Ommatidia rotate 90° counterclockwise in the dorsal half of the eye and 90° clockwise in the ventral half. Rotation is complete by row 15 (Fiehler and Wolff, 2007).

Six core planar cell polarity, or tissue polarity (TP) genes govern the establishment of this polarity: *frizzled* (*fz*), *disheveled* (*dsh*), *strabismus* (*stbm*), *prickle*

(*pk*), *diego* (*dgo*), and *flamingo* (*fmi*) (Chae et al., 1999; Feiguin et al., 2001; Klein and Mlodzik, 2005; Klingensmith et al., 1994; Tree et al., 2002; Usui et al., 1999; Wolff and Rubin, 1998). Three phenotypes are evident when TP signaling is disrupted, suggesting three distinct events contribute to the establishment of polarity in the *Drosophila* eye: specification of the R3/R4 fates, direction of rotation (clockwise vs. counter-clockwise), and degree of rotation. While mosaic analyses indicate a requirement for the TP genes in specifying the R3 and R4 cell fates and additional work demonstrates a tight link between fate specification and direction of rotation, the mechanisms that control the degree to which ommatidia rotate are poorly understood (Fanto and Mlodzik, 1999; Strutt et al., 2002; Wolff and Rubin, 1998). The identification of several proteins that affect only the degree of rotation, including the serine/threonine kinase Nemo, DE-cadherin, DN-cadherin, and members of the Egfr signaling pathway (Brown and Freeman, 2003; Choi and Benzer, 1994; Fiehler and Wolff, 2008; Gaengel and Mlodzik, 2003; Mirkovic and Mlodzik, 2006; Strutt and Strutt, 2003), suggests a subset of genes may cooperate with the TP genes to regulate this event.

Genetic evidence reveals the Egfr signaling pathway promotes rotation (Mirkovic and Mlodzik, 2006), even though ommatidia in Egfr pathway mutant eyes can over- or under-rotate, leading to a wide variance in the degree to which individual ommatidia rotate (Brown and Freeman, 2003; Gaengel and Mlodzik, 2003; Strutt and Strutt, 2003). Egfr pathway members signal through two downstream effectors: the Mapk/Pnt transcriptional cascade and Canoe (Cno), the actin binding protein and fly homolog of Afadin/AF-6, which stabilizes adherens junctions (Brown and Freeman, 2003; Gaengel and Mlodzik, 2003). Egfr pathway members also interact genetically with E-cadherin and

N-cadherin during rotation (Mirkovic and Mlodzik, 2006). E-cad and N-cad act in opposite directions in rotation (E-cad promotes and N-cad inhibits rotation), and Egfr signaling pathway members act in the same direction as E-cad (Mirkovic and Mlodzik, 2006). Although recent studies have identified some of the genetic interactions important in rotation, it remains unclear how rotating ommatidia coordinate changes in cell adhesion and cell signaling to initiate, advance, and arrest rotation.

Here, we describe roles for two paralogous cell adhesion molecules (CAMs), Echinoid (Ed) and Friend-of-Echinoid (Fred), in controlling one output of TP, the degree of ommatidial rotation. Ed and Fred are large transmembrane CAMs with extracellular immunoglobin (Ig) C2 repeats and fibronectin type III domains (Bai et al., 2001; Chandra et al., 2003). The work described here demonstrates that Ed and Fred are required at multiple steps during ommatidial rotation and that they participate in two functionally distinct mechanisms to either enable or slow rotation. We propose that in one mechanism, Ed and Fred modulate adhesivity and thereby regulate rotation; in a second mechanism, they regulate rotation via Egfr signaling. Ed and Fred levels must be tightly titrated both initially, to create an environment permissive for rotation, and later, to slow rotation, likely by equalizing levels between rotating and non-rotating populations of cells. In addition, we demonstrate that *ed* and *fred* act in a subset of photoreceptor cells and in the cone cells, perhaps to regulate levels of Egfr signaling, ultimately inhibiting rotation. Notably, this requirement represents the first demonstration of a role for the cone cells in ommatidial rotation. This work also demonstrates that *ed* and *fred* interact with the core tissue polarity genes to control rotation. Finally, we have identified a new and unexpected role for *stbm* in photoreceptor R7 to control the degree to which ommatidia rotate. This

result raises the intriguing possibility that all of the tissue polarity genes function in distinct subsets of cells to control R3/R4 fate specification and the degree of rotation.

# Materials and Methods

## Genetics

Fly lines used: $w^{1118}$; $ed^{1}$; $dsh^{1}$; $fz^{N21}$/TM3; $fz^{J22}$; $stbm^{15cn}$, $stbm^{6cn}$, $stbm^{6cn}$/CyO, $stbm^{153}$, $stbm^{J14}$; $pk^{sple}$; $dgo^{380}$; $aos^{rlt}$/TM6; $fmi^{frz3}$; $w^{1118}$; *PneoFRT42D* $fmi^{192}$/CyO; $w^{1118}$; *PlacWspi*$^{s3547}$/CyO; $cno^{mis1}$; $cno^{2}$/TM3 (gift from U. Gaul); $pnt^{\Delta 88}$/TM3; $w^{1118}$; *PlacWpnt*$^{1277}$; $nmo^{P1}$; *Elp*; *sev*-GAL4; *GMR*-GAL4 (gift from H. Chang); *ro*-GAL4 (gift from J. Fischer); UAS-*ed* (gift from J.-C. Hsu); UAS-$fred^{RNAi}$ (gift from H. Vaessin); *y w eyFlp*; $ed^{K1102}$*FRT40A*/BC, $ed^{1x5}$*FRT40A*/CyO, $ed^{SlH8}$*FRT40A*/CyO, $fred^{l(2)gH10}$*FRT40A*/CyO and $fred^{l(2)gH24}$*FRT40A*/CyO (described in (de Belle et al., 1993)) $fred^{l(2)gH24}$, $ed^{K1102}$*FRT40A*/CyO, UAS-*fred* (gifts from S. Spencer.) All crosses were raised at 25°C. Stocks are available from Bloomington unless otherwise noted.

## Immunohistochemistry

Third instar eye imaginal discs were dissected, fixed and stained as described (Wolff 2000), with the exception of tissue stained with α-Cno, which was fixed in PLP (Matsuo et al., 1999). Discs were incubated in primary antibody overnight at 4°C at the following concentrations: mouse α-Armadillo, 1:10 (Developmental Studies Hybridoma Bank); rabbit α-Ed, 1:1000 (gift from A. Jarman); guinea pig α-Fred, 1:1000 (generous gift from S. Spencer); rabbit α-Cno, 1:500 (generous gift from D. Yamamoto); mouse α-Flamingo, 1:20 (Developmental Studies Hybridoma Bank); rabbit α-Stbm, 1:500; mouse α-dpERK, 1:500 (Sigma); rabbit α-PointedP1, 1:500 (gift from J. Skeath); rat α-DE-cadherin, 1:20 (Developmental Studies Hybridoma Bank). Alexafluor-conjugated secondary antibodies (Molecular Probes) were used at a concentration of 1:300 and

incubated at room temperature for two hours in dark conditions. Discs were mounted in 1:1 N-propylgallate:Vectashield and imaged on a Leica confocal microscope.

**Phenotypic analyses**

Adult eyes were fixed, embedded, and sectioned as described (Wolff, 2000). Degree of rotation was determined using ImageJ software (NIH) to measure angles defined by vectors drawn 1) through the rhabdomeres of photoreceptors R1, R2, and R3, and 2) parallel to the equator. Only ommatidia with a correct complement of eight photoreceptor cells were scored. For all genotypes, 1000-1500 ommatidia from between six and ten eyes were scored. Statistical significance was determined using the Student's t-test (for mean angle of orientation) and F-test (for variance).

Larval rotation phenotypes were scored in third instar eye imaginal discs stained with α-Armadillo to outline cells. ImageJ software was used to measure the rotation angle between two vectors, one drawn between R3 and R4 and through R8, and the second drawn parallel to the equator. Angles of orientation were scored in rows two through 15 in 15 independent eye discs (i.e. one per larva) for each genotype.

**Generation of mitotic clones**

Mitotic clones were generated using the FLP/FRT technique (Xu and Rubin, 1993). Larvae of the appropriate genotypes were heat-shocked for one hour during the first instar to generate hsFlp clones. To generate *ey*FLP clones, larvae were raised at 25°C until the third instar. The following Flp and FRT lines were used: *yw hsFlp*; *w+ FRT40A, w ry eyFlp*; *w+* (GMR-myr-GFP) FRT40A/CyO; $w^{1118}$*, eyFlp*; *w+* (GMR-myr-GFP)

FRT42D. Mutant tissue is marked with $w^-$ in adult eyes and with the absence of GFP in larval discs.

**Mosaic analysis**

Mosaic analysis was performed in *ey*FLP- and hsFLP-generated mitotic clones. Phenotypes and photoreceptor genotypes were scored in adult sections. Wild-type cells in mosaic ommatidia were marked with $w^+$ and therefore identified by the presence of pigment granules at the base of the rhabdomeres. Only ommatidia with a correct complement of eight photoreceptor cells were scored for rotation.

# Results

## *ed* and *fred* mutant ommatidia misrotate

The cell adhesion molecule, *echinoid* (*ed*), was identified as a dominant suppressor of the ommatidial over-rotation phenotype caused by misexpression of the S/T kinase, *nemo (nmo)* (Fiehler and Wolff, 2008). Although loss-of-function alleles of *ed* and *nmo* do not exhibit genetic interactions (data not shown), phenotypic analyses reveal key roles for *ed* and its paralog, *friend-of-echinoid* (*fred*), during ommatidial rotation. Wild-type ommatidia in adult eyes are oriented at almost precisely 90° (90.6°, standard deviation =1.7). In contrast, many *ed* and *fred* mutant ommatidia are oriented at either greater than or less than 90° (Fig 2-1, Table 2-1). While the mean angle of orientation (MAO; see Materials and Methods for method used to determine MAO) for both *ed* and *fred* loss-of-function alleles does not differ significantly from wild type, the variance, a quantifiable measurement of phenotype represented by the standard deviation (SD), differs significantly from wild type (Table 2-1). Furthermore, stronger allelic combinations of *ed* (e.g. the null allele $ed^{k1102}$ *in trans* to the hypomorphic allele $ed^{SlH8}$) exhibit a greater variance (SD=19.6, $P$=0) than do weaker allelic combinations, such as the hypomorph $ed^{l}/ed^{l}$ (SD=10, $P$=0). Loss of *fred* function, as assayed in genetically mutant clones of the hypomorphic allele $fred^{H10}$, yields a similar phenotype with a large variance (SD=13.5, $P$=0) and a MAO close to that of wild type (89.8°).

*ed* and *fred* act cooperatively in R8 specification (Rawlins et al., 2003b; Spencer and Cagan, 2003) and also cooperate to ensure that ommatidia orient at precisely 90° as $fred^{H24}$ dominantly enhances the ommatidial orientation phenotype of $ed^{K1102}/ed^{SlH8}$ transheterozygotes (Fig. 2-1G, Table 2-1). Notably, the *ed* and

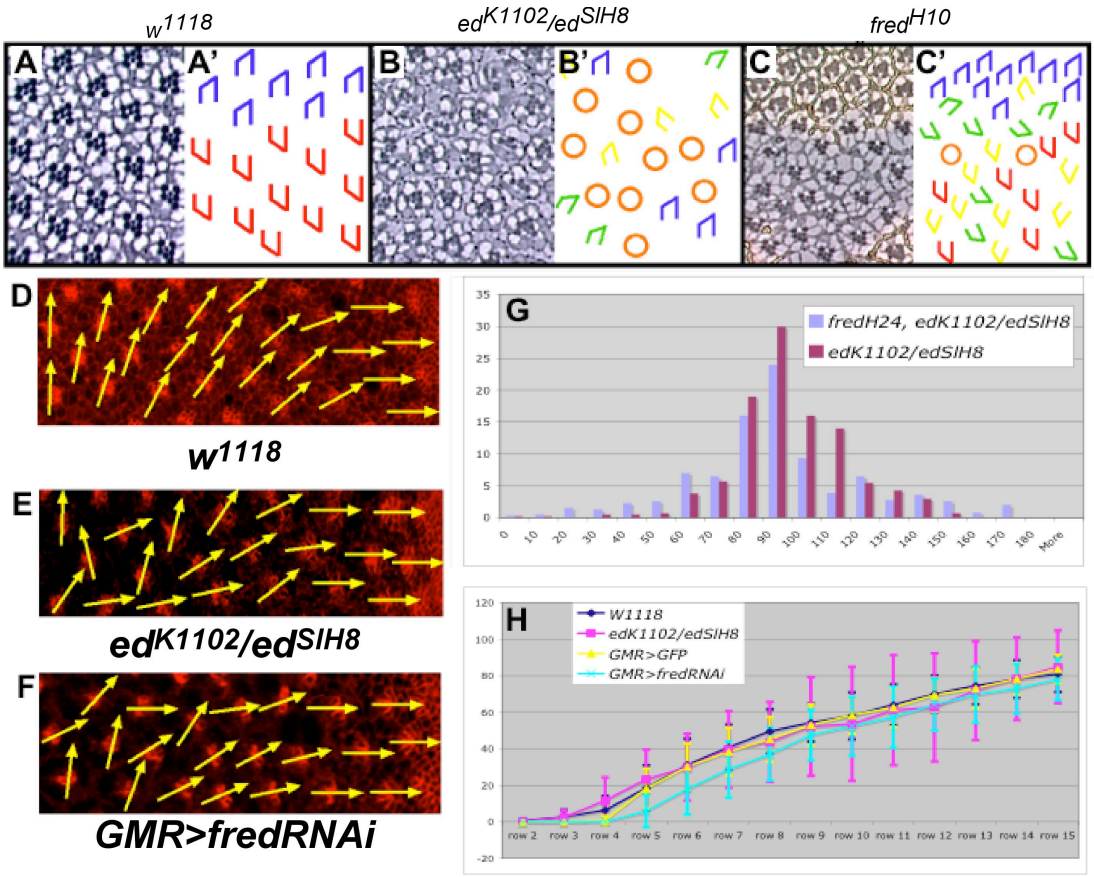


**Figure 2-1. *ed* and *fred* mutant ommatidia misrotate**. (A-C) Tangential sections through adult eyes (left panels) and corresponding schematics (right panels). (A) Wild type. Ommatidia come in two chiral forms, shown as blue in the dorsal and red in the ventral half of the eye. (B) Some $ed^{SIH8}/ed^{K1102}$ ommatidia under- or over-rotate (green and yellow trapezoids, respectively), and some contain an incorrect number of photoreceptors (orange circles). (C) Some ommatidia in $fred^{H10}$ clones rotate correctly while others under- or over-rotate. (D-F) The *ed* and *fred* orientation phenotypes result from aberrant ommatidial rotation. α-Arm (red) outlines cell boundaries. Yellow vectors bisect R8 and run through the R3/R4 interface, highlighting the angle of orientation of each ommatidium. (D) Wild-type ommatidia follow a smooth progression of rotation. Ommatidial precursors in both $ed^{K1102}/ed^{SIH8}$ (E) and *GMR>fredRNAi* (F) knockdown eye discs misrotate. (G) Reduction of *fred* activity enhances the *ed* mutant phenotype;

histogram illustrating the percentage of ommatidia (Y-axis) that are oriented at the angles indicated (X-axis) in $ed^{k1102}/ed^{SlH8}$ and $ed^{K1102}, fred^{H24}/ed^{SlH8}$ eyes. (H) Graphical representation of data from (D-F) plotted as the MAO of ommatidia in each of four genotypes in rows 2-15. Error bars represent the variance (SD). $w^{1118}$ is the control for $ed^{K1102}/ed^{SlH8}$; *GMR>GFP* is the control for *GMR>fredRNAi*. The SD of *ed* and *fred* ommatidia is significantly different from that of the controls between rows 7-15. Key to trapezoid color for all schematics: blue, red, wild-type; green, under-rotated; yellow, over-rotated; black, fail to rotate; orange circles, incorrect number of photoreceptors.

**Table 2-1. List of *ed* and *fred* genetic interactions.**

| | Genotype | Mean Angle Orientation (MAO) | Standard deviation (SD) | *P*-value | N | n |
|---|---|---|---|---|---|---|
| | $w^{1118}$ | 90.6 | 1.85 | | 8 | 1006 |
| | $ed^{1}$ | 87.16 | 10.1 | 0 | 9 | 1383 |
| | $ed^{SIH8}/ed^{K1102}$ | 90.56 | 19.6 | 0 | 6 | 417 |
| | $fred^{H10}$ clones | 89.82 | 13.5 | 0 | 10 | 420 |
| | *GMR>fredRNAi* | 87.65 | 13.14 | 0 | 10 | 1039 |
| | $fred^{H24}$, $ed^{K1102}/ed^{SIH8}$ | 87.1 | 29.71 | 4E-12 | 10 | 384 |
| **Tissue polarity genes** | $fz^{N21}/fz^{J22}$ | 88.38 | 6.54 | | 10 | 1126 |
| | $ed^{1x5}/+;fz^{N21}/fz^{J22}$ | 85.5 | 13.56 | 1.0E-126 | 10 | 1275 |
| | $fred^{H24}/+;fz^{N21}/fz^{J22}$ | 88.49 | 7.69 | 4E-4 | 10 | 1355 |
| | $dsh^{1}/Y$ | 86.16 | 10.7 | | 7 | 899 |
| | $dsh^{1}/Y;ed^{1x5}/+$ | 82.3 | 16.87 | 9E-41 | 6 | 752 |
| | $dsh^{1}/Y;fred^{H24}/+$ | 86.22 | 12.19 | 4E-5 | 9 | 1025 |
| | $stbm^{153}$ | 76.27 | 22.66 | | 11 | 1638 |
| | $ed^{1x5}/+;stbm^{153}$ | 68.29 | 24.95 | 0.15 | 10 | 1199 |
| | $fred^{H24}/+;stbm^{153}$ | 83.01 | 15.4 | 1.0E-45 | 6 | 842 |
| | $pk^{sple}$ | 88.34 | 4.69 | | 10 | 1431 |
| | $ed^{K1102}/+;pk^{sple}$ | 88.99 | 4.52 | 0.49 | 10 | 1505 |
| | $fred^{H24}/+;pk^{sple}$ | 88.02 | 5.03 | 0.29 | 10 | 1430 |
| | $dgo^{380}$ | 88.61 | 11.83 | | 8 | 755 |
| | $ed^{1x5}/+;dgo^{380}$ | 83.9 | 16.37 | 3E-25 | 10 | 1235 |
| | $fred^{H24}/+;dgo^{380}$ | 87.89 | 13.08 | 7E-4 | 10 | 1142 |
| | $fmi^{frz3}$ | 88 | 10.24 | | 6 | 612 |
| | $ed^{1x5}/+;fmi^{frz3}$ | 83.83 | 24.52 | 1.6E-13 | 6 | 627 |
| | $fred^{H24}/+;fmi^{frz3}$ | 85.17 | 15.49 | 1.2E-11 | 9 | 1010 |
| **Egfr pathway** | $aos^{rlt}$ | 77.84 | 40.42 | | 6 | 645 |
| | $ed1^{x5}/+;aos^{rlt}$ | 80.61 | 38.39 | 0.02 | 10 | 1055 |
| | $fred^{H10}/+;aos^{rlt}$ | 78.00 | 39.26 | 0.11 | 10 | 1040 |
| | $ed^{1}$ | 87.17 | 10.13 | 0 | 10 | 1383 |
| | $ed^{1}$, $spi^{s3547}/ed^{1}$ | 89.88 | 5.71 | 1.3E-76 | 10 | 1295 |
| | $cno^{mis1}/cno^{2}$ | 94.30 | 26.28 | | 6 | 728 |
| | $ed^{1x5}/+;cno^{mis1}/cno^{2}$ | 88.39 | 33.48 | 4.9E-25 | 10 | 867 |
| | $fred^{H10}/+;cno^{mis1}/cno^{2}$ | 95.99 | 20.65 | 1.8E-20 | 10 | 1382 |
| | *Elp* | 92.08 | 12.12 | | 5 | 466 |
| | $fred^{h24}/Elp$ | 88.54 | 8.34 | 1E-192 | 5 | 464 |
| | $pnt^{\Delta 88}/pnt^{1277}$ | 85.5 | 16.64 | | 9 | 630 |
| | $ed^{1x5}/+;pnt^{\Delta 88}/pnt^{1277}$ | 83.53 | 20.84 | 2E-6 | 6 | 611 |
| | $fred^{H10}/+;pnt^{\Delta 88}/pnt^{1277}$ | 91.2 | 5.1 | 4E-297 | 8 | 987 |

*P*-values are derived from *F*-test.
*F*-test *P*-values are for a comparison between SD of genotype indicated and its respective baseline (i.e. homozygous phenotype is baseline for modified genotypes).
"N" refers to the number of eyes scored; "n" refers to the number of ommatidia scored.

*fred* ommatidial orientation phenotypes are essentially identical to those of the tissue polarity mutants. However, in contrast to the tissue polarity mutants, which also exhibit chirality and R3/R4 fate specification defects, loss of *ed* or *fred* function disrupts only the degree of ommatidial orientation.

The *ed* and *fred* orientation phenotypes could originate from two non-mutually exclusive patterning events: ommatidial precursors may either fall short of or rotate past the normal 90° stopping point, or the misalignment could result from defects in morphogenetic events that occur during pupal life, such as cell death (Fiehler and Wolff, 2007) or ommatidial stabilization following rotation. To establish whether *ed* and *fred* function during ommatidial rotation, a row-by-row analysis of the degree to which individual ommatidia rotate was conducted between rows 2-15 in third instar eye imaginal discs lacking *ed* or *fred* function and compared to age-matched, wild-type counterparts ($w^{1118}$ or *GMR>GFP*; see Methods for details). Rotation was measured in $ed^{SIH8}/ed^{K1102}$ and *GMR>fredRNAi* eye imaginal discs (*fred* alleles are lethal, necessitating the use of *fredRNAi*; the *GMR>fredRNAi* phenotype is identical to the $fred^{H10}$ phenotype; Table 2-1).

In wild type, ommatidial rotation begins between rows four and five and is complete by row 15. In $ed^{SIH8}/ed^{K1102}$ and *GMR>fredRNAi*, although the MAO is essentially the same as it is in wild type, the variance in the degree of rotation (SD) is greater in the mutants/knockdowns than in wild type (Fig. 2-1D). Importantly, the SD does not become statistically distinct from wild type until 2-3 rows after the initiation of rotation, or row 7: between rows 7 and 15, many ommatidial precursors under- or over-rotate in *ed* and *fred* mutant eye discs relative to wild type (Fig. 2-1E, F). Notably, row 7

marks the time at which the anterior and posterior cone cells are recruited into the ommatidial precursor (Fiehler and Wolff, 2007). These results not only demonstrate a role for *ed* and *fred* in the cellular movements that drive ommatidial rotation, but further indicate they are required for the post-initiation stages of rotation rather than for the initiation of rotation. While *ed* and *fred* may also participate in later patterning events that align ommatidia, their contributions to such events would likely play only a minor role in ommatidial rotation, as the MAO and SD for *ed* and *fred* ommatidia when rotation is complete (row 15) are essentially the same as in their adult counterparts.

## Ed and Fred localize in dynamic and partially overlapping patterns in the eye imaginal disc

Ed was previously described as localizing throughout the eye imaginal disc (Bai et al., 2001; Rawlins et al., 2003b). However, insight into potential mechanisms by which Ed might regulate ommatidial rotation necessitated a more detailed, cell-by-cell and row-by-row analysis of Ed localization. Immunolocalization of the C-terminal, α-Ed antibody reveals that high levels of Ed protein localize at the apical surface of all cells in the morphogenetic furrow. This pattern persists immediately posterior to the furrow, through row 1 (the arc stage; Fig. 2-2A). In row 3**,** Ed remains enriched at the apical membranes of R3, R4, and the mystery cells, but is considerably diminished at the R8/R2/R5 interfaces (Fig. 2-2B). The most striking change in Ed localization coincides with the start of ommatidial rotation (row 4/5) when Ed is reduced specifically within the photoreceptors, the cells that will soon begin to rotate (Fig. 2-2C). The low levels of Ed

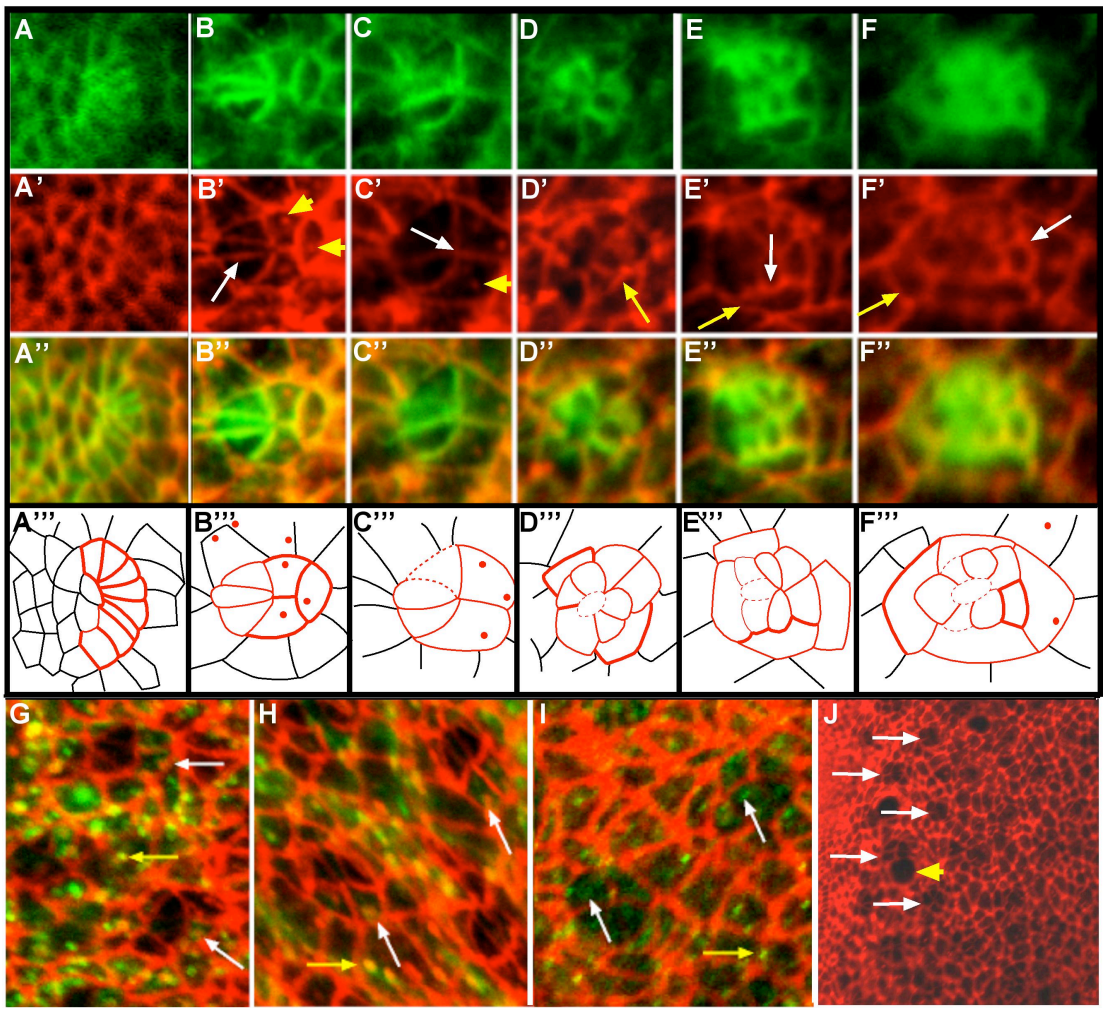


**Figure 2-2. Ed localization is dynamic throughout rotation**. (A - F) α-Arm (green) and (A' - F') α-Ed (red) in sequentially older ommatidial precursors in third instar eye disc. (A''- F'') Merge of α-Arm and α-Ed images. (A'''-F''') Corresponding schematics, with Ed localization in ommatidial precursors represented by solid red lines; Ed localization in cells outside the ommatidial precursors are shown in black. Dashed red lines indicate cell boundaries where Ed is below detectable levels. Intensity of Ed staining correlates with the line weight. (A-A''') In row 1, Ed is localized in all cells. (B-B''') By row 3, Ed levels have diminished in R8, R2 and R5 (white arrow). Ed punctae are visible (yellow arrowheads). (C-C''') Just prior to the start of rotation, Ed levels drop

in the photoreceptor cells (see also J); Ed is visible at the R3/R4 (white arrow), R2/R3, and R4/R5 interfaces and in punctae (yellow arrowhead). (D - D''') Ed levels increase in the photoreceptors as rotation progresses (white arrow). (E-E''') In row 8, Ed remains high in the photoreceptor and cone cells (white arrow), and levels equalize between rotating and non-rotating cells (yellow arrow) (F-F'''). At the completion of rotation, Ed is enriched at the cone cell/IOC (yellow arrow) and the cone cell/photoreceptor cell boundaries (white arrow). Ed (red) vesicles co-localizes with (G) Rab5-GFP (green) and (H) Rab7-GFP-positive (green) punctae in both IOCs (yellow arrow) and photoreceptor cells (white arrows). (I) Vesicular Ed (red) does not co-localize with α-Rab11 (green) in recycling endosomes in either IOCs (yellow arrows) or photoreceptors (white arrows). (J) Low magnification image of an eye imaginal disc stained with α-Ed. Just before rotation begins, ommatidia with low levels of Ed appear as "holes" in the staining pattern (white arrows). Mitotic cells, which also resemble "holes" (yellow arrowhead), are distinct.

in the photoreceptors relative to the robust Ed staining in the IOCs make the photoreceptor clusters appear as holes within the imaginal disc epithelium, a staining pattern that persists until approximately row 7 (Fig. 2-2D, J). The distinct difference in Ed levels between rotating cells (photoreceptors and cone cells) and non-rotating cells (the undifferentiated IOCs; (Fiehler and Wolff, 2007)) at the onset of rotation raises the intriguing possibility that Ed must be downregulated to allow rotating cells to slip past their stationary neighbors. This notion is consistent with Ed's classification as an Ig domain CAM and with the observation that cells with higher levels of Ed adhere more strongly to each other than to cells with lower levels of Ed (Spencer and Cagan, 2003; Wei et al., 2005).

Ed levels are initially high in photoreceptors R1, R6 and R7 when they are recruited into the growing ommatidium in rows 5/6 (Fig. 2-2D, E). They remain high at their interface with the stationary IOCs, yet decrease at the interface with the adjacent photoreceptors (i.e. the R1/R2 and R5/R6 cell boundaries). Shortly following the recruitment of these photoreceptors and the consequent increase in Ed levels at the rotation interface, rotation slows (row 7). Given that Ed is a CAM, and given the close correlation between high levels of Ed and slower rotation, initial and then sustained levels of Ed at the interface between rotating and non-rotating cells may provide a mechanism for slowing/stopping rotation.

When the cone cells are recruited into the ommatidial cluster, there is a dramatic shift in relative levels of Ed within the ommatidia and in the IOCs: Ed becomes prominent in two bands, one at the interface between the cone cells and the photoreceptors and a second at the interface between the cone cells and the IOCs (Fig. 2-

2E, F). Notably, the recruitment of the cone cells and the resulting increase in Ed levels are coincident with the second, slower 45° of rotation (Fiehler and Wolff, 2007). The distinct early and late patterns of Ed localization in rotating vs. stationary cells suggest a model in which adhesion between rotating and non-rotating cells is reduced early to enable cells to slide past one another, and subsequently increased during the slow phase of rotation to slow, and ultimately stop, rotation.

In addition to its membrane localization, Ed is also evident in intracellular vesicles throughout the eye disc (Fig. 2-2B, C). The IOCs contain large Ed punctae that frequently co-localize with either GFP-tagged Rab5 (an early endosome marker, Fig. 2-2G) or Rab7 (a late endosome/lysosome marker, Fig. 2-2H), but not with α-Rab11 (which labels recycling endosomes, Fig. 2-2I). Photoreceptors R8, R2, R5, R3 and R4 often contain Ed punctae before and at the very beginning of rotation and again, the Ed-positive punctae frequently also contain Rab5 or Rab7, but not Rab11, suggesting that Ed is endocytosed and degraded. As noted above, Ed levels in the membranes of R8, R2, R5, R3, and R4 – the first cells to join the ommatidia – are initially high but decrease just before rotation begins (Fig. 2-2C); the presence of Ed in endosomes in these cells prior to the onset of rotation suggests that the cells in the cluster are actively reducing Ed levels, again suggesting that rotation requires different Ed levels in moving and stationary cells. In sharp contrast, Ed is not found in vesicles in photoreceptors R1, R6, and R7 (although Rab5 and Rab7 are prominent in these cells, Fig. 2-2G, H). This is consistent with the observation that Ed remains enriched at the interface between the IOCs and photoreceptors R1, R6, and R7 -- cells that join the cluster just before the second, slower

half of rotation -- and also suggests that Ed may play a distinct role in these cells relative to the other photoreceptor cells in the cluster.

The localization pattern of Fred, as detected by an antibody raised against a peptide in the Fred intracellular domain (Spencer, in preparation), differs markedly from that of Ed. The Fred pattern is strongly reminiscent of those of the tissue polarity proteins Stbm and Fmi, suggesting these proteins may share functions during rotation. Like Ed, Fred protein is abundant in the morphogenetic furrow. In contrast to Ed, early in rotation Fred is enriched in the photoreceptors relative to the surrounding IOCs (Fig. 2-3A, B). In addition, similar to the TP proteins, Fred's localization in R3 and R4 is dynamic during the first half of rotation. At the initiation of rotation (rows 4-5), Fred is localized in a double-horseshoe pattern (UU), outlining photoreceptors R3 and R4 except where they abut R2 and R5 (Fig. 2-3B – B'''). Approximately one row, or 1.5 hours later, in row 6, Fred is restricted to the lateral edge of the R4 cell and the R3/R4 boundary (Fig. 2-3C – C''', D – D'''). Fred levels remain high in R1, R6 and at the R7/R8 interface as they are recruited into the photoreceptor cluster in row 6 (Fig. 2-3; C-C'''). One row further posterior, Fred is not detectable at the R3/R4 boundary but remains at the lateral edge of R4, the R7/R8 interface and in R1 and R6 (Fig. 2-3E – E'''). The relatively high level of Fred in R1, R6 and R7 compared to the other photoreceptor cells during the second half of rotation predicts an important role for Fred in these cells. Following recruitment of the cone cells, the Fred pattern recapitulates the Ed pattern in that bands of Fred are evident at the interfaces between both the cone cells and the photoreceptors and the cone cells and IOCs (Fig. 2-3F – F'''). As described above for Ed, since Fred is also an Ig-

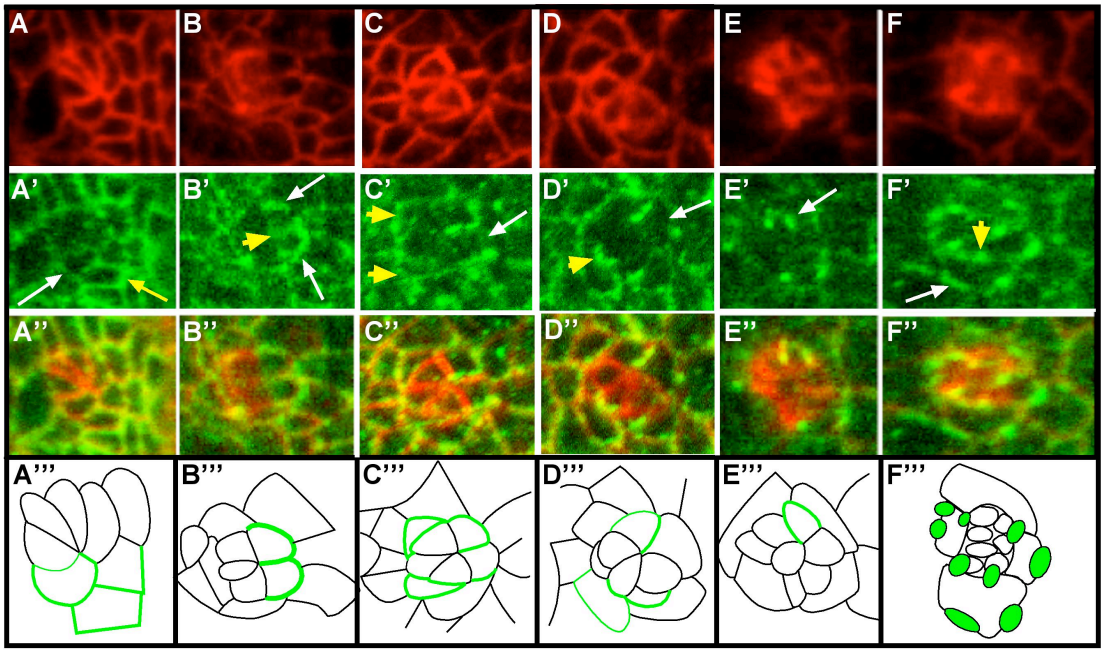


**Figure 2-3. Fred localization is dynamic throughout rotation.** (A-F) α-Arm (red), (A'-F') α-Fred (green), and (A''- F'') merge, in increasingly older ommatidial precursors in third instar eye disc. (A'''- F''') corresponding schematics; Fred localization is represented by green lines, line weight correlates with intensity of Fred staining. (A-A''') In row 3, Fred levels are enriched in R3 (white arrow), R4 (not evident in this image), and the mystery cells (yellow arrow). (B-B''') Just prior to the initiation of rotation, Fred localizes to the lateral edges of R3 and R4 (white arrows) and the R3/R4 boundary (yellow arrowhead). (C-C''') In row 6, Fred begins to disappear from R3 (white arrow), but remains high in R4 and at the R3/R4 boundary. The newly added R1 and R6 contain high levels of Fred (yellow arrowheads). (D-D''') Row 7: Fred disappears from R3 and is still high in R4 and at R3/R4 boundary (white arrow). A bright band of Fred highlights the interface between R7 and R8 (yellow arrowhead), and Fred can still be seen faintly in R1 and R6. (E-E''') By row 9, Fred is no longer present at the R3/R4 boundary, outlining only the periphery of R4 (white arrow). (F-F''') At the end of rotation, Fred is enriched at

the interfaces between the cone cells and the IOCs (white arrow) and also at the boundaries between the photoreceptors and the cone cells (yellow arrow).

containing CAM, the localization pattern at the cone cell/photoreceptor and cone cell/IOC boundaries suggests adhesion increases between these subsets of cells during the second, slower phase of rotation, perhaps serving as a brake for rotating cells.

## Misexpression of *ed* and *fred* generates an under-rotation phenotype

The dynamic localization of Ed and Fred in rotating and stationary cells suggest that *ed* and *fred* must be tightly regulated in time and space to achieve normal rotation. To test this hypothesis, cell-specific drivers were used to manipulate Ed and Fred levels in the photoreceptors and IOCs to either artificially equalize levels between rotating and non-rotating cells or to force high levels of expression in cells where Ed and Fred are not normally elevated, and to subsequently evaluate the effect on rotation.

Ommatidial precursors rotate more slowly when driving *UAS>ed* or *UAS>fred* with the following drivers: *sev>Gal4* (R3, R4, R1, R6, R7 and the cone cells); *ro>Gal4* (R8, R2, and R5); and *GMR>Gal4* (all cells posterior to the morphogenetic furrow). Interestingly, despite the distinct Ed and Fred localization patterns, the consequence of mis-expression is similar for both *ed* and *fred*. When either *ed* or *fred* is driven under the *sev* promoter, ommatidia under-rotate, on average, and exhibit a significant variance (Table 2-1, Fig. 2-4A, B). A similar phenotype results from mis-expression of *UAS>fred* driven by *ro>Gal4*, although driving *UAS>ed* with *ro>Gal4* does not cause a rotation phenotype (Fig. 2-4E, F). (Note that some *ro >ed* ommatidia do have the expected missing photoreceptor phenotype due to an effect on Egfr signaling (Rawlins et al., 2003b; Spencer and Cagan, 2003). In the genotypes that under-rotate, aberrant rotation is evident from the start of rotation, or between rows 4 and 5 (Fig. 2-4G). By row 15, when

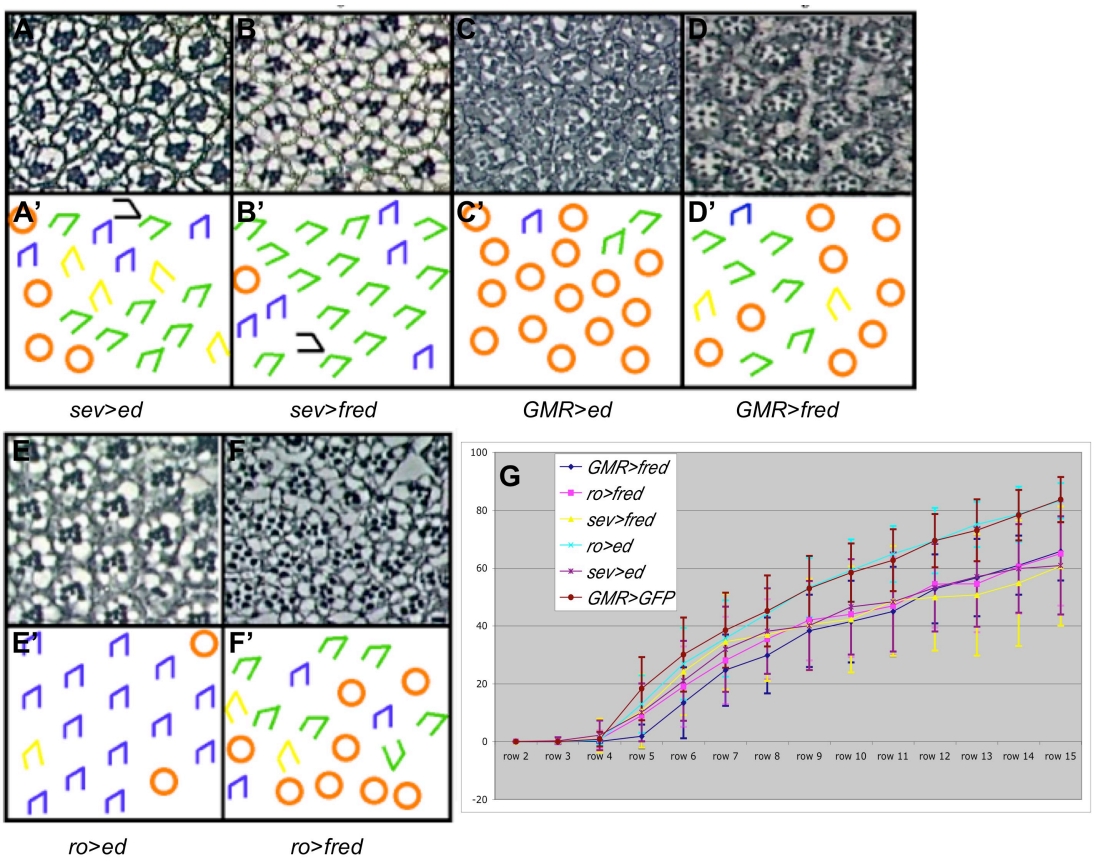


**Figure 2-4. Misexpression of *ed* or *fred* results in under-rotation**. (A-F) Sections through adult eyes and corresponding schematics of *ed* and *fred* misexpression lines. (A, B) *sev>ed* and *sev>fred* ommatidia frequently under-rotate; very few ommatidia are missing photoreceptors. (C) *GMR>ed* tissue is severely disrupted, precluding analysis of angles of orientation. (D) Most ommatidia in *GMR>fred* adult eyes under-rotate. (E) Most ommatidia rotate 90° in *ro>ed* eyes; some ommatidia are missing photoreceptors. (F) In contrast, many ommatidia under-rotate in *ro>fred* eyes. (G) Graph of larval rotation, or MAO, for ommatidia in rows 2-15; Y-axis, degree of rotation. Ommatidia in misexpression lines are under-rotated in rows 4-15 compared to controls. Error bars represent the SD.

rotation is complete in wild type, ommatidia in these mis-expression backgrounds have only rotated approximately 60° (Fig. 2-4G). Overall, these data indicate that excess *ed* and *fred* activity early in rotation and forced equalization of levels in rotating vs. non-rotating cells interferes with rotation, suggesting that dissimilar Ed and Fred levels in rotating and non-rotating cells are vital for the progression of rotation.

## *ed* and *fred* are required in a subset of cells for ommatidial rotation

Ed and Fred are dynamically localized in multiple cell types in the eye disc during rotation, including both motile and stationary cells (Fig. 2-2, Fig. 2-3). Since *ed* and *fred* have pleiotropic effects, the localization patterns of the proteins do not definitively identify those cells that require *ed* and *fred* for normal rotation, particularly since Ed and Fred regulate the reiterative Egfr signaling necessary for photoreceptor recruitment (Freeman, 1997; Spencer and Cagan, 2003; Spencer et al., 1998) at a time coincident with their role in ommatidial rotation. To identify the single photoreceptor or subsets of photoreceptor cells in which Ed and/or Fred function to regulate ommatidial rotation, we conducted a mosaic analysis. The FLP/FRT system (Xu and Rubin, 1993) was used to generate clones of either $ed^{1x5}$ or $fred^{H10}$ mutant ommatidia. The degree of rotation of mosaic ommatidia, those with a mixture of genetically mutant and genetically wild-type photoreceptors, was then assessed to evaluate the function of Ed or Fred in both individual photoreceptor cells and in specific groups of photoreceptors. Mosaic ommatidia mutant for *ed* (or *fred*) in a given photoreceptor were compared to mosaic ommatidia wild-type for *ed* in that photoreceptor; the genotypes of the remaining photoreceptors were not factored in. Parallel analyses were conducted for

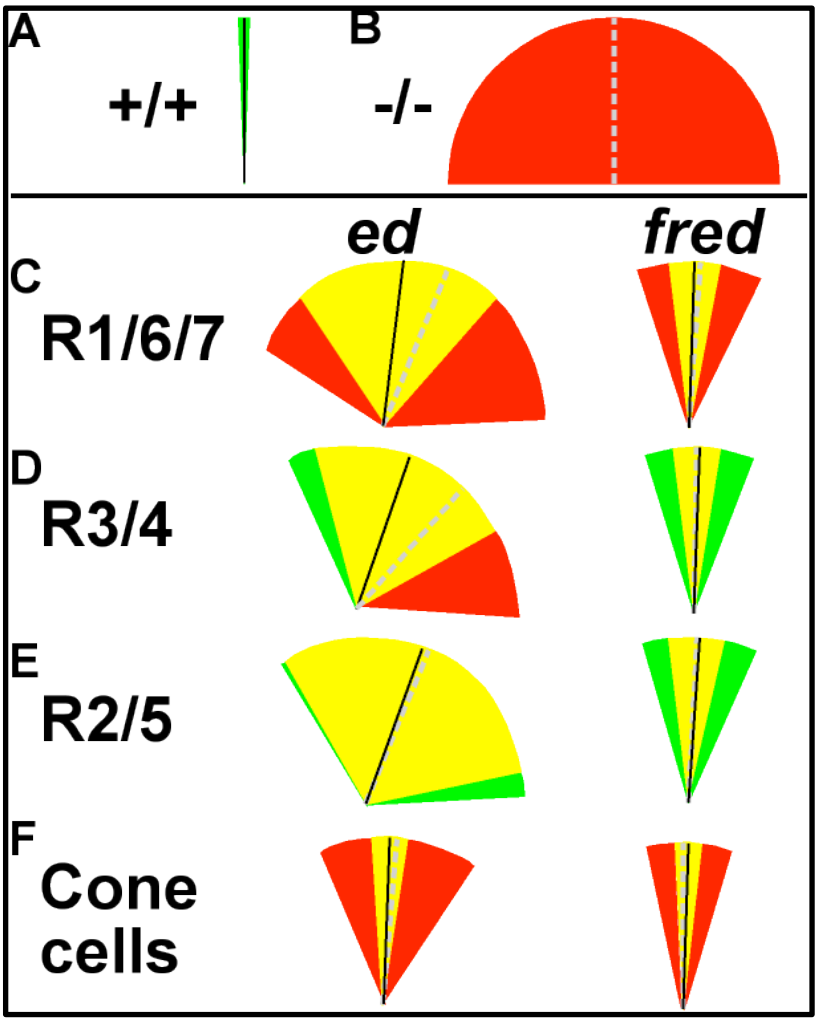


**Figure 2-5. *ed* and *fred* are required in R1, R6, R7 and the cone cells for correct ommatidial rotation.** (A) Schematic representation of wild-type MAO (black line; 90.6°) and wild-type variance (SD, green wedge; 1.7). (B) Schematic representation of hypothetical mutant MAO (dashed grey line) and SD (red wedges). In C-F, black line: MAO when designated cells are genetically wild-type for *ed* or *fred*; dashed gray line: MAO when designated cells are genetically mutant for *ed* or *fred*; genetically wild-type SD: green wedges; genetically mutant SD: red wedges; overlap: yellow wedges. (C, F) *ed* and *fred* are required in photoreceptors R1, R6 and R7, and the cone cells for rotation. (D, E) *ed* and *fred* are not required in R3/R4 or R2/R5 for rotation.

three groups of photoreceptors: R3/R4, R2/R5, and R1/R6/R7 and significant changes in the variance between each paired data set were identified. This analysis demonstrated that both *ed* and *fred* are required in R1, R6, and R7 for correct rotation: mosaic ommatidia genotypically wild-type for *ed* or *fred* in R1, R6, and R7 are more likely to have a smaller variance than mosaic ommatidia in which R1, R6 and R7 are genotypically mutant (Fig. 2-5A). Although a requirement for *fred* in R3 and R4 seemed likely given the prominent expression of Fred in R3 and R4 at a critical period of rotation, the mosaic analysis did not identify a requirement for either *ed* or *fred* in R3, R4, R8, R2, or R5 (Fig. 2-5B, C).

The mosaic analyses indicate a requirement for Ed and Fred in R1, R6 and R7, yet wild-type *ed* or *fred* in these three cells does not completely rescue rotation. Furthermore, ommatidia with a full complement of genotypically wild-type photoreceptors can still misrotate. These observations suggest that *ed* and *fred* function in additional, non-photoreceptor cells to regulate ommatidial rotation. The most compelling candidates are the cone cells, as they express high levels of Ed and Fred until well after the completion of rotation. To explore a potential role for Ed and Fred in the cone cells, mosaic ommatidia were evaluated in mid-pupal $ed^{1x5}$ and $fred^{H10}$ eyes (40 hrs after puparium formation at 25°). This analysis revealed that mosaic ommatidia with wild-type photoreceptors and mutant cone cells misrotate (for $ed^{1x5}$ MAO = 83°, SD = 30, $P$<5E-17; for $fred^{H10}$ MAO = 92°, SD = 18, $P$<3E-9; Fig. 2-5D), thus defining unambiguous roles for Ed and Fred in the cone cells for ommatidial rotation. Notably, these results provide the first demonstration of a role for the cone cells in ommatidial rotation.

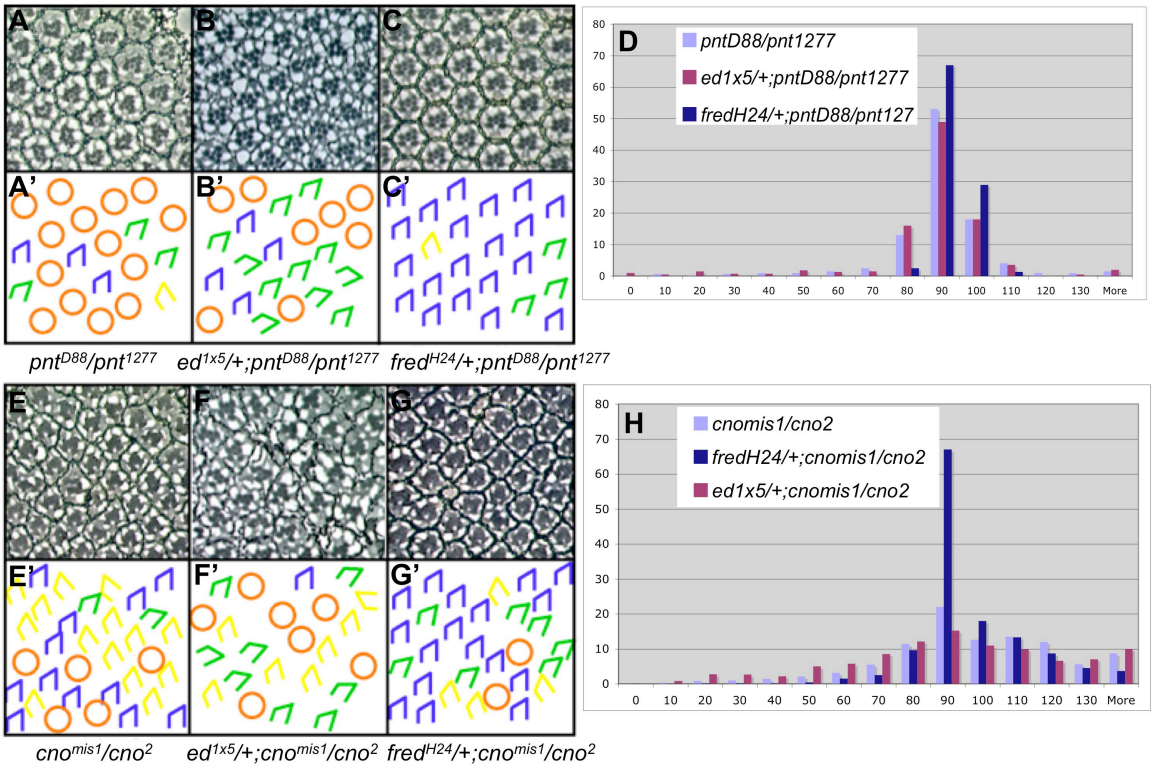


**Figure 2-6. *ed* and *fred* interact genetically with *pnt* and *cno*.** (A-C) Sections through adult eyes and corresponding schematics. (A) $pnt^{1277}/pnt^{\Delta 88}$ mutant eyes exhibit both over- and under-rotated ommatidia. (B) $ed^{1x5}/+$, $pnt^{\Delta 88}/pnt^{1277}$; reducing *ed* activity enhances the *pnt* phenotype (i.e. the SD increases). C) $fred^{H24}/+$, $pnt^{\Delta 88}/pnt^{1277}$; reducing *fred* activity suppresses the *pnt* phenotype virtually to wild type. (D) Histogram of angles of ommatidial orientation for $pnt^{\Delta 88}/pnt^{1277}$, $ed^{1x5}/+$, $pnt^{\Delta 88}/pnt^{1277}$, and $fred^{H24}/+$, $pnt^{\Delta 88}/pnt^{1277}$. X-axis, MAO; Y-axis, percentage. (E-G) Sections and corresponding schematics for adult eyes of genotypes as follows. (E) In $cno^{mis1}/cno^{2}$ mutant eyes, most ommatidia over-rotate. (F) $ed^{1x5}/+$, $cno^{mis1}/cno^{2}$; reducing *ed* activity enhances the *cno* phenotype. (G) $fred^{H24}/+$; $cno^{mis1}/cno^{2}$; reducing *fred* activity suppresses the *cno*

phenotype. (H) Histogram of angles of ommatidial orientation in $cno^{mis1}/cno^{2}$, $ed^{1x5}/+$, $cno^{mis1}/cno^{2}$, and $fred^{H24}/+$; $cno^{mis1}/cno^{2}$ adult eyes. X-axis, MAO; Y-axis, percentage.

## *ed* and *fred* interact with Egfr signaling pathway members to regulate ommatidial rotation

The *ed* and *fred* ommatidial rotation phenotypes strongly resemble phenotypes observed in mutants of members of the Egfr signaling pathway. Furthermore, *ed* inhibits Egfr signaling (Bai et al., 2001; Rawlins et al., 2003b; Spencer and Cagan, 2003). To determine if Ed and/or Fred cooperate with Egfr signaling, we tested *ed* and *fred* for their ability to interact with Egfr pathway members and found that *ed* and *fred* dominantly modify the rotation phenotypes of *Elp, pnt,* and *cno*. However, whereas *ed* and *fred* cooperate to regulate ommatidial rotation (Fig. 2-1G), they oppose one another in their interactions with *Elp*, *pnt*, and *cno*. Both $fred^{H10}$ and $fred^{H24}$ dominantly suppress the eye size and rotation phenotypes of the dominant Egfr gain-of-function allele, *Ellipse* (*Elp*; Table 2-1); the effect of $ed^{1x5}$ on the *Elp* rotation phenotype could not be scored, as *ed* significantly enhances the photoreceptor number phenotype of *Elp*, severely reducing the number of ommatidia with a normal complement of photoreceptors (data not shown). $ed^{1x5}$ enhances while $fred^{h24}$ strongly suppresses the phenotype of both $pnt^{\Delta 88}/pnt^{1277}$ and $cno^{mis1}/cno^{2}$ (Table 2-1, Fig. 2-6).

In the context of R8 selection, *ed* is upstream of *Ras*, at the level of the receptor (Rawlins et al., 2003b; Spencer and Cagan, 2003), and *fred* functions upstream of *ed* (Spencer, in preparation). Standard epistasis analysis cannot be employed to unambiguously order *ed*, *fred* and these *Egfr* pathway genes in a linear pathway because 1) null alleles of each of these genes are lethal and 2) the ommatidial rotation phenotypes resulting from mutations in these genes are indistinguishable. The data presented above

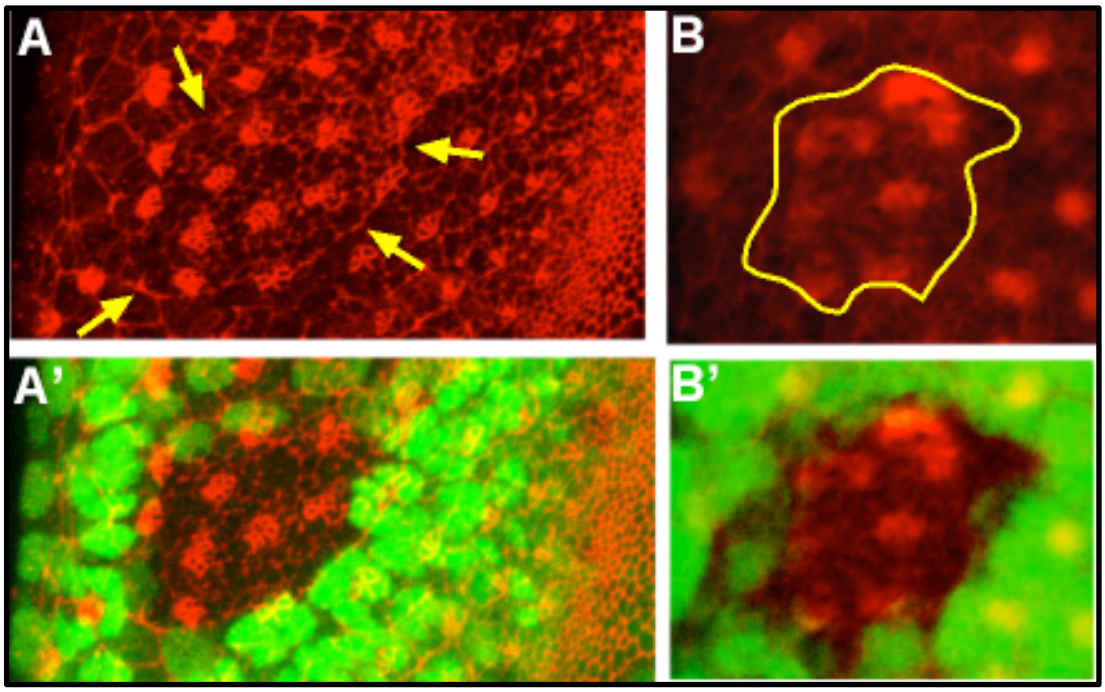


**Figure 2-7. Ed does not physically interact with Cno in the eye.** (A, A') Cno localization (red) in an $ed^{1x5}$ clone, marked by the absence of GFP (A'). There are no detectable changes in Cno localization within *ed* clones, although Cno does form a "cable" of strong staining around the periphery of the clones, at the boundary between wild-type and mutant cells (yellow arrows), similar to the actin cable described in ((Laplante and Nilson, 2006), fig 2A'). (B, B') Phalloidin localization (red) in *ed* null clone (outlined in yellow; marked by absence of green in B'). Phalloidin staining appears normal in *ed* mutant clones.

do, however, indicate that in the simplest scenario, *ed* and *fred* also function upstream of *Ras*, since *ed* and *fred* interact with *Elp* as well as both branches (*cno* and *pnt*) of the Egfr pathway. These results further suggest that *ed* and *fred* likely regulate rotation at least partly through control of Egfr signaling.

In the wing, Ed tethers Cno to the membrane via its physical interaction with the PDZ domain of Cno (Wei et al., 2005). However, in the eye the basis of the *ed*/*cno* genetic interaction in rotation is distinct, as Cno localization is unchanged in clones of the null allele $ed^{lx5}$ (Fig. 2-6A, A'). Furthermore, Cno anchors the cytoskeleton to adherens junctions (Matsuo et al., 1997; Miyamoto et al., 1995), yet at least at a gross level, the actin cytoskeleton does not appear to be disrupted in *ed* mutant tissue (Fig. 2-6B, B'). In light of the absence of a direct physical interaction between Ed and Cno, the genetic link between *ed*/*fred* and Egfr signaling likely has its basis in regulating upstream signaling events, perhaps at the level of the Egf receptor.

## *ed* and *fred* interact with different subsets of tissue polarity genes

The TP genes control three events: specification of the R3 and R4 cell fates (Fanto et al., 1998; Fanto and Mlodzik, 1999; Wolff and Rubin, 1998), the direction of rotation with respect to the ommatidium's dorsal or ventral location in the eye, and the degree of rotation. Of these three events, *ed* and *fred* regulate only the degree to which ommatidia rotate, suggesting they may cooperate with the TP genes in this event. The observation that the Fred localization pattern mimics those of Stbm and Fmi lends support to this hypothesis. Genetic assays designed to identify a possible link between *ed* and *fred* and TP signaling revealed that *ed* and *fred* interact genetically with largely non-

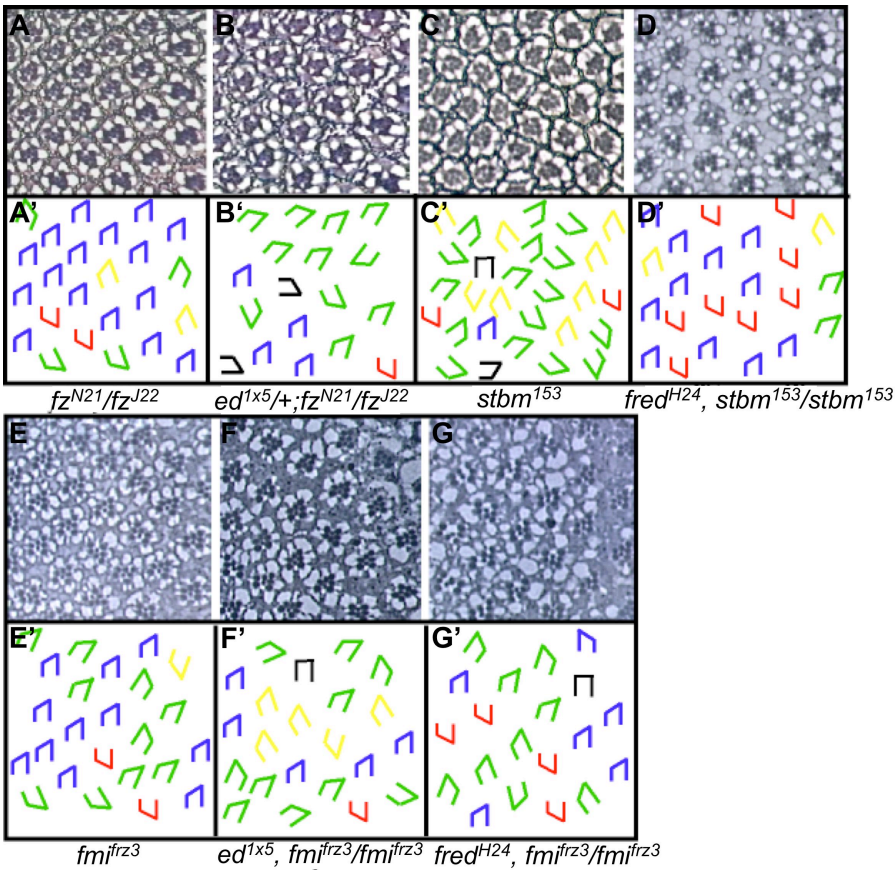


**Figure 2-8. *ed* and *fred* interact genetically with different subsets of the TP genes.** (A-G) Adult eye sections and corresponding schematics. Red trapezoids (Fig. 8 only): dorsoventral inversions. (A) $fz^{N21}/fz^{J22}$ mutant eyes exhibit both over- and under-rotated ommatidia. *ed* interacts specifically with the subset of TP genes required in R3: *fz*, *dgo* and *fmi*. (B) $ed^{1x5}/+; fz^{N21}/fz^{J22}$ ; reducing *ed* activity enhances the *fz* rotation phenotype without affecting the chirality phenotype. *fred* interacts with two TP genes that are required in R4 for correct polarity: *stbm* and *fmi*. (C) $stbm^{153}$ mutant eyes exhibit both over- and under-rotated ommatidia. (D) $fred^{H24}/+$, $stbm^{153}/stbm^{153}$; reducing *fred* activity strongly suppresses the *stbm* rotation phenotype. The $fmi^{frz3}$ phenotype (E) is enhanced by both loss of *ed* function (F) $ed^{1x5}/+$, $fmi^{frz3}/fmi^{frz3}$ and loss of *fred* function (G) $fred^{H24}/+$, $fmi^{frz3}/fmi^{frz}$.

overlapping sets of the six core TP genes, as follows. *ed* dominantly enhances the mutant phenotypes of the genes that function in R3: *fz*, *dsh*, *dgo*, and *fmi*, whereas *fred* dominantly interacts with genes that function in R4: *fred* suppresses the hypomorphic *stbm* phenotype and enhances the *fmi* phenotype (Table 2-1; Fig. 2-8).

These striking findings not only reveal a distinct association between *ed* and *fred* and the R3- and R4-specific tissue polarity genes, respectively, but they are also unexpected in light of the mosaic analysis data, which identify roles for *ed* and *fred* in R1, R6, and R7, but not in R3 and R4 (Fig. 2-5). Furthermore, excess Ed and Fred protein in R3 and R4 at the beginning of rotation slows the process (*sev>ed* and *sev>fred*, Fig. 2-4). These findings raise the intriguing possibility that the TP genes act in unique subsets of cells to control the three distinct events under their control. The localization patterns of the TP proteins are consistent with such a model as several, including Stbm, localize not only at the R3/R4 interface, but also at the interfaces between the R7/R8, the R7/R1 and the R7/R6 photoreceptor cells. Furthermore, like *nmo*, *ed* and *fred* function are clearly required in R7 to regulate ommatidial rotation (see Discussion). While previous mosaic analyses have not uncovered a requirement for the TP genes in any cells other than R3 and R4, these analyses measured the composite phenotype (R3/R4 fate, degree and direction of rotation). Consequently, a role for a subset of photoreceptors in one of these events could have been masked.

We therefore re-examined the requirement for *stbm* in TP, but focused specifically on its role in ommatidial rotation. This analysis revealed a requirement for *stbm* function in photoreceptor R7 in regulating the degree of rotation. Remarkably, loss of *stbm* function in R7 can account for almost all of the degree-of-rotation errors in

mosaic *stbm* ommatidia: when R7 is genotypically wild-type for *stbm*, the variance in the degree of rotation, SD=5, is very close to that of wild type, SD=1.7; when R7 is genotypically mutant for *stbm*, the variance is significantly greater (SD=15; see Table 2-2). These results provide the first demonstration 1) of a genetic requirement for any TP gene outside the R3/R4 pair, and 2) that the TP genes act in distinct subsets of cells to control the genetically separable aspects of the TP phenotype. This novel result, in

| | MAO | *P* value | SD | *P* value |
|---|---|---|---|---|
| R1 wt | 89.23 | | 12.37 | |
| R1 mut | 88.38 | 0.51 | 12.94 | 0.55 |
| R2 wt | 88.51 | | 15.02 | |
| R2 mut | 88.75 | 0.87 | 11.46 | 0.0002 |
| R3 wt | 89.55 | | 12.36 | |
| R3 mut | 88.46 | 0.48 | 12.84 | 0.69 |
| R4 wt | 89.04 | | 12.04 | |
| R4 mut | 87.88 | 0.43 | 14.18 | 0.03 |
| R5 wt | 89.45 | | 12.06 | |
| R5 mut | 87.93 | 0.23 | 13.33 | 0.16 |
| R6 wt | 91.1 | | 10.42 | |
| R6 mut | 86.73 | 4.00E-04 | 14.02 | 4.00E-05 |
| R7 wt | 89.27 | | 5.6 | |
| R7 mut | 88.33 | 0.39 | 15.72 | 1.05E-35 |

**Table 2-2. *stbm* is required in R7 for degree of rotation.**

conjunction with the localization of Stbm at the tip of R7 and in the cone cells, provides an exciting new perspective as to how the TP complex may regulate the degree to which ommatidia rotate.

The Ed, Fred and core TP proteins localize to the R3/R4 boundary at approximately the same stage of development (Bastock et al., 2003; Strutt et al., 2002; Strutt, 2002). In addition, the Fred, Stbm, and Fmi localization patterns during rotation bear a strong resemblance to one another (Rawls and Wolff, 2002). While these

observations raise the possibility that the tissue polarity proteins may influence Ed and Fred localization, or vice versa, molecular epistasis analyses failed to uncover such a link, as Stbm and Fmi localization are unaffected in *ed* and *fred* mutant clones, and Ed and Fred are not mislocalized in clones of the tissue polarity genes *stbm* and *fmi* (data not shown). Since protein localization does not appear to be the mechanism whereby the tissue polarity complex modulates Ed/Fred activity, an alternative possibility is that the core TP genes may act in a pathway parallel to *ed* and *fred*, indirectly regulating these two genes.

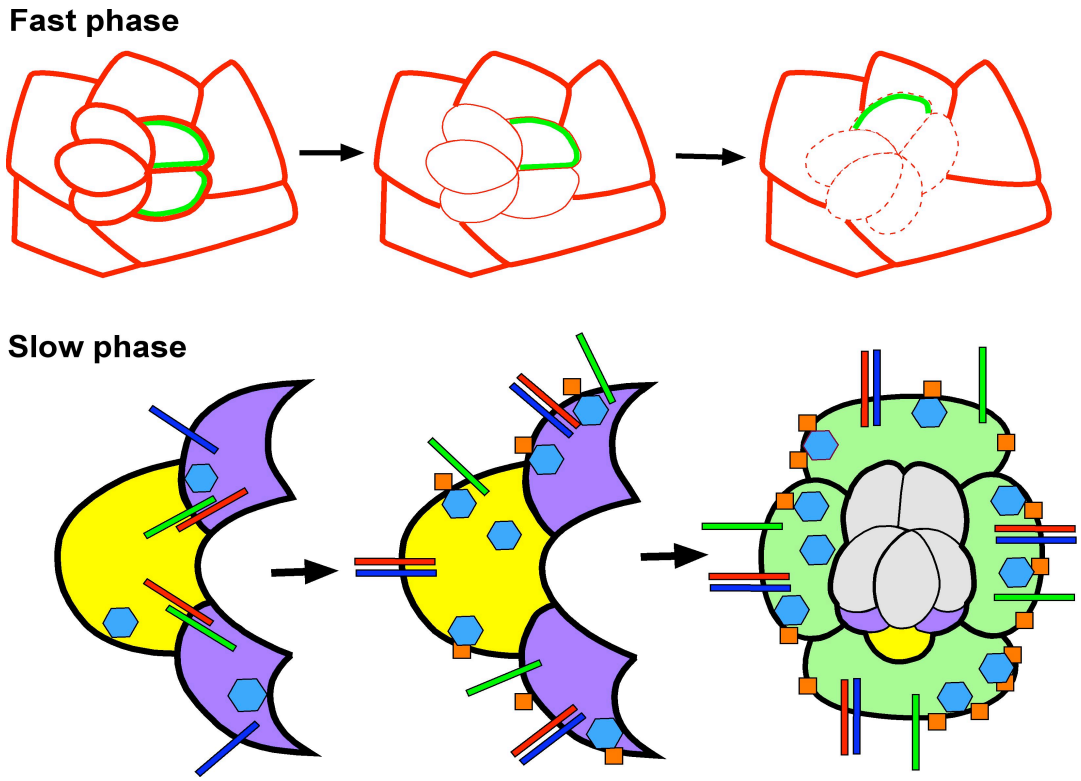


**Figure 2-9. Ed and Fred contribute to both phases of rotation.** (A) Differential levels or expression domains of Ed and Fred, respectively, in rotating and non-rotating cells create a permissive environment for the faster phase of rotation. Levels of Ed are equivalent in cells within nascent ommatidial preclusters and IOCs (depicted as solid red lines of equal line weight in left panel). Immediately before rotation, cells that will rotate actively reduce their levels/distribution of Ed and Fred (center panel: reduced Ed levels, thin red line; reduced number of cells expressing Fred (green)). A decrease in adhesion (dashed red line, right panel) between rotating and stationary cells enables rotation to proceed. (B) Ed and Fred regulate Egfr signaling during the slow phase of ommatidial rotation. When photoreceptors R1, R6 (purple cells) and R7 (yellow cell) join the cluster, they contain high levels of both Ed (red bars) and Fred (green bars). During the fast

phase, Ed/Fred binding reduces Ed's inhibition of the Egf receptor (blue bars, left panel). Robust Egfr signaling inhibits Cno (blue hexagons) activity, consequently few stable AJs form (orange squares). Concurrent with the slower phase of rotation, Ed levels increase in R1, R6 and R7. Ed associates with the Egf receptor, inhibiting Egfr signaling (middle panel). As a result, Cno activity increases and stable AJs form between moving and stationary cells, effectively applying a brake at the rotation interface (middle panel). Rotation-specific signaling events shift to a new rotation interface upon recruitment of the cone cells (light green) into the cluster. At the completion of rotation, levels of AJ proteins (Ed, Fred, Cno, and Arm) are high, an indication that these two subsets of cells adhere strongly to one another.

# Discussion

Here, we demonstrate that *ed* and *fred* have partially overlapping functions during the two phases of ommatidial rotation. In the first phase, we propose that different levels of Ed and Fred in rotating and non-rotating cells modulate the adhesivity of these cells, a prerequisite for rotation to occur. In the second half of rotation, Ed and Fred are required in R1, R6, R7, and the cone cells, where they likely regulate the Egf receptor to contribute to the slowing of rotation. The Egfr effector Cno inhibits rotation, and is itself inhibited in response to Egfr signaling.

There are two phases of rotation, distinguishable by the rate at which ommatidia rotate (Fiehler and Wolff, 2007). The initial phase is fast and persists from row 4 to row 7; during this phase, ommatidia rotate between 10-15° per row. During the second, slow phase, between rows 7 and 15, ommatidia rotate 5-10° per row. The data presented here demonstrate that Ed and Fred function during both phases, and that they play unique roles in each of these phases.

In the first phase, we propose that the tight regulation of Ed and Fred levels between rotating and stationary cells creates an environment that is permissive to rotation. Immediately before rotation starts, Ed begins to be endocytosed in the rotating cells – the ommatidial precluster cells. Concurrently, Ed levels fall dramatically in these cells while remaining high in the stationary IOCs. This rapid drop in Ed levels effectively sets up an imbalance in levels of Ed between these two populations of cells. We propose that the resulting differential adhesion between these two cell populations enables the rotating cells to slide past their stationary neighbors, according to the parameters of

Malcolm Steinberg's differential adhesion hypothesis (DAH; (Steinberg, 2007)). The DAH proposes that populations of cells maximize the strength of adhesive bonding between them and minimize the adhesive free energy, and uses tension generated by adhesion between cells to drive events such as cell rearrangements during morphogenesis. Differential adhesion underlies multiple morphogenetic events, including epithelial-mesenchymal transitions, cell intercalation (Lecuit, 2005), somite segmentation (Murakami et al., 2006) and invasion by malignant cells (Winters et al., 2005), an event that bears similarities to ommatidial rotation. In the case of rotation, those cells with the same levels of Ed (or Fred) adhere more tightly to one another and cell adhesion is reduced between cells with different levels of Ed (or Fred) ((Spencer and Cagan, 2003), Spencer, in preparation), thereby enabling the two groups to slide past one another. In support of this hypothesis, we showed that artificially equalizing levels of Ed or Fred significantly slows rotation.

The second phase of rotation, between rows 7-15, is slower than the first, with ommatidial precursors rotating at a rate of 5-10° per row (Fiehler and Wolff, 2007). The data presented here are consistent with Ed and Fred playing two key roles in this phase by both directly and indirectly (via Egfr signaling) affecting the physical component of the process. We suggest that the outputs in both cases produce adhesive forces that slow/stop rotation. Ed and Fred are required in photoreceptors R1, R6 and R7 and the cone cells for normal ommatidial rotation. These cells do not become fully integrated into the ommatidial cluster until the second half of rotation. Furthermore, photoreceptors R1, R6 and R7 constitute the rotation interface until the cone cells are recruited, at which point the cone cells co-opt this position and role. Consequently, Ed and Fred are required in the

right place (the subset of cells that lie at the rotation interface) and at the right time (the slower phase of rotation) to play a role in slowing rotation.

We propose that Ed and Fred activity in R1, R6, R7 and the cone cells regulates Egfr signaling in these cells to slow/stop rotation, as follows. Egfr signaling promotes rotation via the Ras/Cno and Ras/Mapk/Pnt effectors (Brown and Freeman, 2003; Gaengel and Mlodzik, 2003), so its output must be dampened to slow rotation. Ed binds and inhibits the Egf receptor (Bai et al., 2001; Rawlins et al., 2003b; Spencer and Cagan, 2003), whereas Fred binds Ed and interferes with this inhibition (Spencer, in preparation). Therefore, cooperation between Ed and Fred precisely titrates Egfr activity in the cells in which Ed and Fred function. As R1, R6 and R7 are recruited into the ommatidial cluster, Ed levels are high in these cells, thereby decreasing Egfr signaling at their side of the rotation interface, thus impeding rotation. This inhibitory role switches to the cone cells when they are recruited and create a new rotation interface.

One plausible means by which rotation may be slowed through Egfr signaling activity is through one of its effectors, Cno. Cno is the fly homolog of Afadin, an actin-binding adherens junction protein (Mandai et al., 1997; Matsuo et al., 1997; Miyamoto et al., 1995; Ooshio et al., 2007). In mammals, Afadin and its binding partners, nectins and α-actinin, build and stabilize those dynamic AJs that undergo remodeling (Ooshio et al., 2007; Takahashi et al., 1999). In our hands, the majority of *cno* mutant ommatidia over-rotate, indicating that Cno inhibits ommatidial rotation (Fig. 2-6E, H). Given that Egfr signaling promotes rotation and Cno inhibits rotation, Egfr signaling likely suppresses Cno activity during rotation. To inhibit Cno activity, activated Ras may bind Cno, thereby blocking stable junction formation. In this scenario, high levels of Egfr would be

required during the early phase of rotation to prevent Cno from promoting stable junctions between rotating and non-rotating cells. Consistent with this hypothesis, levels of Ed, an Egfr inhibitor, are very low in ommatidial cells both when rotation commences and during the fast phase of rotation.

In this model, early in the second half of rotation, we propose that higher levels of Ed activity are necessary to repress Egfr signaling at the rotation interface, thereby increasing the amount of active Cno and consequently increasing the number of stable AJs between the moving and stationary cells. The more tightly the cells adhere to one another, the less permissive the environment is for movement, and the slower (and more difficult) rotation becomes. As previously noted, Ed levels are high in the cells in which it would need to be high -- R1, R6, R7 and the cone cells -- and Ed is required in these cells. Once rotation is complete, Ed and Fred are at high levels at the cell-cell boundaries between the interommatidial and ommatidial cells, an indication that stable AJs now cement the fully-rotated ommatidia in place.

Ed's closest mammalian orthologs are the nectins, CAMs with extracellular Ig domains and a C-terminal PDZBM that binds the PDZ domains of Afadin and Par-3 (the Bazooka homolog, (Takahashi et al., 1999; Takekuni et al., 2003). In the *Drosophila* wing, this interaction localizes Cno at the AJs to build and stabilize these junctions (Wei et al., 2005). However, a direct, physical Ed/Cno interaction is not necessary for Cno localization in the eye, as Cno is not mislocalized in *ed* null clones. Furthermore, the AJs are stable in the eye since β-catenin and E-cadherin staining are normal in *ed* null clones (this is in contrast to E-cad clones, in which the tissue is disrupted and neither Arm nor

Ed localize properly, data not shown), so in the *Drosophila* eye, something other than Ed binds Cno and stabilizes the AJs.

*ed* and *fred* genetically interact with the R3 and R4 genes, respectively, modifying only the degree-of-rotation aspect of the TP phenotype. Our genetic and molecular epistasis data suggest that *ed* and *fred* act in a pathway either downstream of or parallel to the TP genes. First, Ed and Fred localization do not require the TP complex, nor do the TP proteins require Ed and Fred for their localization. Second, mutations in *ed* and *fred* affect only one aspect of the TP phenotype.

Nectins and afadins have been implicated in numerous human diseases and developmental defects, including breast cancer, metastasis, and cleft palate. Defective cell-cell adhesion and cell-cell signaling also underlie these problems. Our data suggest a new role for an RTK, the Egf receptor, in inhibiting AJ formation by interfering with Cno activity. Given the conservation between these genes, a similar mechanism may also underlie at least some of the human diseases associated with nectin and afadin disruption. For example, decreasing AJs and increasing cell motility underlie cancer metastasis, so understanding the interaction between RTKs and AJ formation may yield profound insights into potential therapeutic strategies for these diseases.

# Acknowledgements

We are grateful to A. Rawls, S. Arur and J. Skeath for critical comments on the manuscript. We thank R. Fiehler and B. Grillo-Hill for helpful discussions, A. Jarman and K. Takahashi for antibodies, and J.C. Hsu, H. Vaessin, U. Gaul and the Bloomington Stock Center for fly stocks. This investigation was supported by NIH grant R01 EY13136 to T.W.

# CHAPTER THREE

# Identification of a new tissue polarity mutation that affects ommatidial rotation

# Abstract

Tissue polarity is essential for the correct patterning of many epithelia. The *Drosophila* eye, a highly polarized structure, is an excellent system for studying the mechanisms by which epithelial tissues organize themselves within the plane of the epithelium. Although for a long time tissue polarity in the *Drosophila* eye was viewed as a single entity, recent work suggests that it may be broken down into three genetically separable components. Here, I identify and describe a GMREP transgenic line that specifically enhances one class of tissue polarity errors, and find that this line contains three separate EP insertions, all on the second chromosome. Furthermore, I investigate the phenotype of three genes that may be affected by the insertions, and determine that none of these genes is involved in setting up any aspect of tissue polarity.

I generate an imprecise excision event using this original EP line and isolate a loss-of-function mutant line that has a rough eye and a tissue polarity phenotype. I characterize this mutation as having photoreceptor number errors, defects in the degree of rotation, and possible cell fate errors. Using a mapping strain and deficiency stocks, I mapped the phenotype's causative mutation to the 2L, between 24C3 and 25A1. Although the deficiency that spans this region removes the coding regions of the cell adhesion molecule *echinoid* (*ed*) and the atypical cadherin *fat* (*ft*), both known tissue polarity genes (see chapter 1 and chapter 2), I ruled out the possibility of mutations in either gene being the causative mutation of the phenotype.

# Introduction

Proper development of multicellular organisms requires the precise organization of cells into tissues. Apicobasal polarity is well characterized in epithelia. In many organisms, epithelial tissue can also be organized along an axis perpendicular to the apicobasal axis, such that cellular structures and cells are polarized within the plane of the epithelium. This latter form is called tissue polarity, or planar cell polarity. Tissue polarity is necessary for the correct placement of cellular structures such as the stereocilia in the inner ear hair cells in the mammalian cochlea, as well as the orientation of hair follicles in the vertebrate epidermis (Guo et al., 2004; Lewis and Davies, 2002; Montcouquiol et al., 2003). In addition to setting up patterning, tissue polarity also affects the convergent extension movements that drive gastrulation and neural tube closure (Djiane et al., 2000; Formstone and Mason, 2005; Goto and Keller, 2002; Jessen et al., 2002). Defects in tissue polarity can have catastrophic consequences for an organism, and have been associated with developmental defects and disease states such as hearing loss and spina bifida.

The pathways that set up tissue polarity are conserved throughout metazoans. Much initial work has been done using *Drosophila* as a model system, as this was the first organism in which tissue polarity was identified. Polarized tissues in *Drosophila* are easily visible in the adult and include the abdomen, the wing, the leg, and the eye. In the abdomen and leg, sensory organ bristles orient along an anterior-posterior and proximal-distal direction, respectively. Similarly, in the wing, actin-based “hairs” extend from the distal tip of each cell and align along a proximal-distal axis (Mlodzik, 2005).

The compound *Drosophila* eye is a highly polarized epithelial structure. Polarity in this tissue is manifest by the arrangement of the ommatidia, or unit eyes, and is evident in the adoption of one of two chiral forms of photoreceptor arrangement. The rhabdomeres, the light-sensing organelles of the photoreceptors, form a trapezoid. In all ommatidia on the dorsal half of the eye, the point of the trapezoid (the R3 cell) faces the dorsal pole, and on the ventral half of the eye, the point faces toward the ventral pole (Wolff and Ready, 1993).

Mutations in any member of a group of six genes, called the core tissue polarity genes, result in tissue polarity phenotypes in the eye. These genes include *flamingo* (*fmi*), *frizzled* (*fz*), *disheveled* (*dsh*), *strabismus* (*stbm*), *prickle* (*pk*), and *diego* (*dgo*) (Chae et al., 1999; Feiguin et al., 2001; Klein and Mlodzik, 2005; Klingensmith et al., 1994; Tree et al., 2002; Usui et al., 1999; Wolff and Rubin, 1998). The adult pattern derives from events that occur during the third larval instar. After their recruitment into the ommatidia, two cells undergo a fate specification event in which the polar cell in the R3/R4 pair adopts the R3 fate and the equatorial cell adopts the R4 fate. Ommatidia then initiate rotation in either a clockwise (ventral ommatidia) or counterclockwise (dorsal ommatidia) and continue to rotate through 90° from their initial position (Wolff and Ready, 1993).

In the eye, mutations in tissue polarity genes give rise to three general classes of defect (Fig. 3-1): 1) symmetrical errors, in which the cell fate decision does not occur properly and both cells of the R3/R4 pair become R3 or R4; 2) chirality errors, including anterior-posterior (A/P) inversions, dorso-ventral (D/V) inversions, and AP/DV inversions. A/P inversions arise when the wrong cell adopts the R3 fate, but rotates

correctly given that ommatidium's location in the eye (counterclockwise if it is a dorsal ommatidium, for example). D/V inversions occur when both the cell fate decision and the direction of rotation occur incorrectly. Finally, AP/DV errors result when the correct cell fate decision occurs, but the ommatidium rotates in the wrong direction based on its location in the eye. The third class of errors includes rotation defects, in which ommatidia rotate either greater than or less than 90°(Wolff et al., 2007).

While the three components of tissue polarity have historically been viewed as a unit, recent work indicates that they are separable (Wolff et al., 2007). For example, certain genes (see chapter 1 and chapter 2) can specifically affect degree of rotation without influencing either cell fate or rotation direction and vice versa. The fate decision and the direction of rotation are also genetically separable: mutations exist that affect one class or the other. However, the mechanisms by which tissue polarity genes orchestrate all three events are still unclear.

To address these problems, a collection of GMREP lines was screened for lines with the ability to specifically modify different classes of errors in a *sev-stbm* misexpression background. Initially, I worked with five of these lines to identify the genes involved. In this chapter, I present work on one of these EP lines. After locating the EP insertion and identifying the gene affected, I characterized its phenotype and its interactions with other misexpression tissue polarity backgrounds. From this line, I generated a loss-of-function line that specifically affects degree of rotation, symmetrical errors, and photoreceptor recruitment, and mapped the mutation to between 24C3 and 25A1. I also show that this line interacts with the tissue polarity genes, and I rule out two candidate genes.

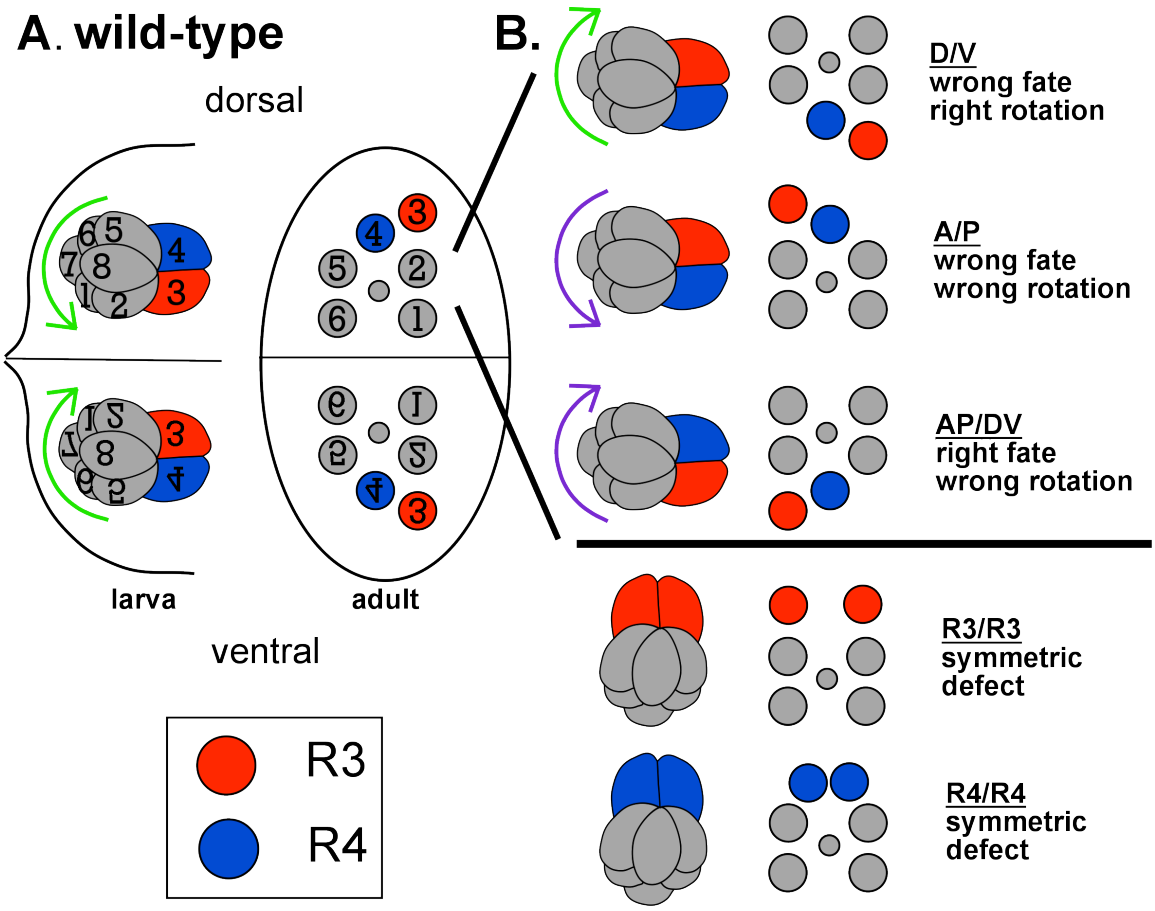


**Figure 3-1. Origin of different classes of tissue polarity errors.** (A) In wild-type discs, ommatidia rotate 90° counter-clockwise in the dorsal half of the eye and clockwise in the ventral half (green arrows). Final adult forms are shown as trapezoids. (B) Corresponding mutant forms of ommatidial precursors and adult trapezoids from dorsal half of the eye. D/V inversions arise from the wrong fate choice, but correct rotation with respect to that fate. A/P inversions occur when the fate choice is incorrect, and rotation occurs in the wrong direction for that fate. AP/DV ommatidia result when the fate decision occurs properly but the ommatidia rotate the wrong direction for that fate. Wolff T, Guinto JB, Rawls AS (2007) Screen for Genetic Modifiers of stbm Reveals that Photoreceptor Fate and Rotation Can Be Genetically Uncoupled in the Drosophila Eye. PLoS ONE 2(5): e453. doi:10.1371/journal.pone.0000453

# Materials and Methods

**Fly strains used:**

EP1658, EP43, EP382, EP564, EP677 (gifts of B. Hay). *sev-stbm*$^{14\text{-}1}$, *sev-dsh*, *sev-fz*, *stbm*$^{153}$, *fmi*$^{192}$, *fmi*$^{frz3}$, *pk*$^{sple}$, *dsh*$^{1}$, *dgo*$^{380}$, *coro*$^{ex11}$ (gift from L. Shashidhara), *hil*, mapping strain *nub,b,rdo,hk,pr,cn*; Df702, and the Bloomington second chromosome deficiency kit. All stocks from Bloomington Stock Center, unless otherwise noted. All crosses raised at 25°C.

**Plasmid rescue:** Plasmid rescue to identify the GMREP insertion site was performed as described in (Hay et al., 1997). Genomic DNA was isolated from 50 adult heads using standard procedures BamH1, Sau3A, and Bgl II were used to digest DNA. Sequencing off the 3' end of the GMREP element was done with a sequencing primer (Hay et al., 1997) on an ABI Prism 3000.

***In situ* hybridization:** To study the expression levels of candidate genes, *in situ* hybridization was performed. Third instar eye discs were dissected and processed as described in (Rawls et al., 2007). DIG-labeled sense and antisense RNA probes for *fu2* and *fu10* were generated from the following ESTs, respectively: RE67956 and GM02347 (DGC). Labeled probe was made from the manufacturer's protocol (Roche Molecular Biochemicals). *In situ* hybridization was performed as described (Rawls et al., 2007), using 1ug DIG-labeled RNA probe.

**Imprecise excision**: GMREP elements are marked with *w*+. To generate the excision line, EP1658 males were crossed to Δ2-3 virgin females. Female progeny with variegated eyes were crossed to Adv/CyO males. White-eyed males were isolated, and mapped with using Adv/Cyo and TM3/TM6 to chromosome X, 2, or 3. The extent of the excision was confirmed using PCR with primers flanking the *fu2* insertion. Forward primer sequence: 5' – AAT GTG GAC GCT GTC CCT AC – 3'. Reverse primer sequence: 5' – AAT GGA CAA AAA GCG ACG AC – 3'.

**Phenotypic analyses**: Adult eyes were fixed, embedded, and sectioned as described (Wolff and Rubin, 1998). Ommatidia were scored and classed as follows: A/P inversions, D/V inversions, AP/DV inversions, R3/R3 symmetrical errors, R4/R4 symmetrical errors, extra photoreceptors, missing photoreceptors, and failure to rotate. For each genotype, 100 ommatidia from 10 individual flies were scored.

# Results

To identify potential genetic interactors of *stbm*, a collection of GMREP-lines (Hay et al., 1997) was screened to identify those lines that modify the *stbm* misexpression background *sev>stbm* (Wolff et al., 2007). These lines each contained an enhancer-promoter element inserted randomly in the genome, which had the ability to affect gene expression in one of three ways: 1) inserting into a coding region, 2) inducing expression of a nearby gene via the promoter element, or 3) inducing expression of genes up to 10kb away via the enhancer element (Fig. 3-2). The enhancer/promoter element contained the enhancer from the gene *GMR*, which is expressed in all cells posterior to the morphogenetic furrow. Particular attention was paid to those GMREP lines that modified different tissue polarity classes. For example, certain lines specifically enhanced or suppressed the number of A/P inversions, D/V inversions, AP/DV inversions, or symmetrical errors.

Initially, I selected five lines to follow up with: EP1658, EP43, EP382, EP564, and EP677 because they each enhanced different classes of polarity errors in the *sev-stbm*$^{14\text{-}1}$ background (Table 3-1). I chose to concentrate on EP1658 because of its strong enhancement of the *sev-stbm* D/V errors and also because the insertion, when homozygosed, produces a rough eye phenotype. Sections through adult EP1658 homozygous eyes reveal a strong tissue polarity phenotype (Fig. 3-3). These eyes contained ommatidia with all three classes of chirality defects, cell fate errors, and misrotated ommatidia. Approximately 46% of ommatidia had some sort of tissue polarity error, a very strong tissue polarity phenotype.

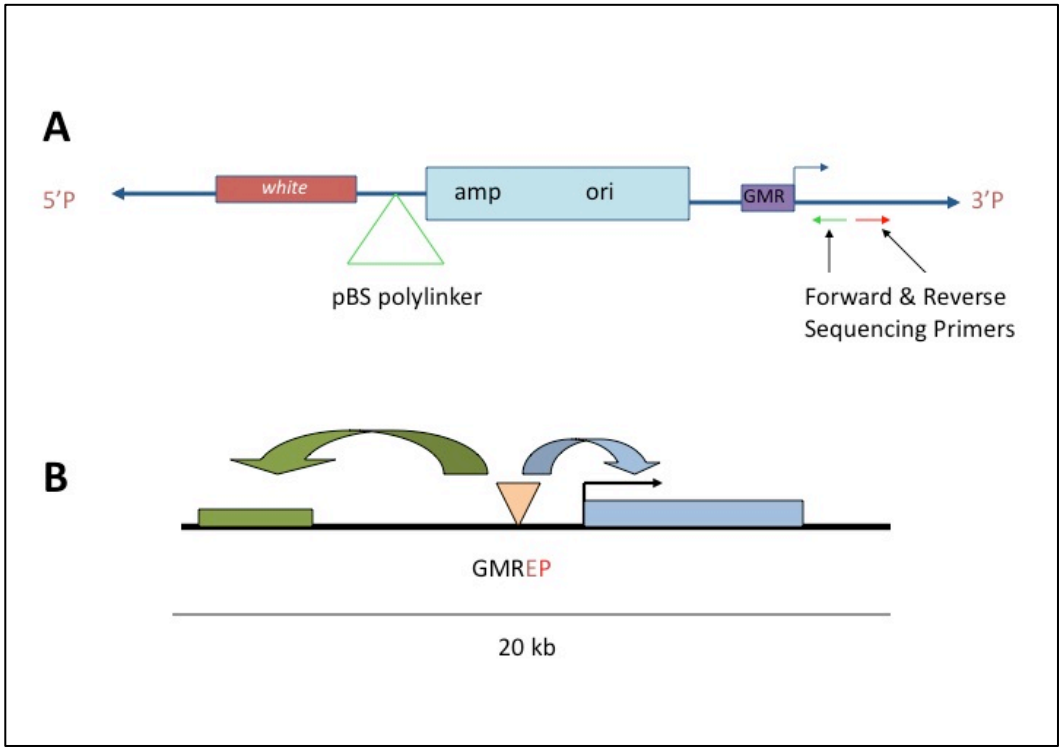


**Figure 3-2. The GMREP element design**. (A) The GMREP element is marked with w+ and contains the pBS polylinker. The GMR minimal enhancer is immediately adjacent to a promoter sequence. After the transcription start site are located the sequences to prime both forward and reverse sequencing to enable the rapid identification of the insertion site. (B) The GMREP can affect gene expression by inserting into a coding region, driving expression of a gene immediately adjacent by virtue of the Hsp70 promoter (blue arrow) or driving expression of a gene within 10 kb upstream or downstream of the insertion site with the GMR enhancer (green arrow).

| Polarity errors | **EP43 / *sev-stbm*** | **EP1658 / *sev-stbm*** | **EP-382 / *sev-stbm*** | **EP564 / *sev-stbm*** | **EP677 / *sev-stbm*** | ***sev-stbm* / +** |
|---|---|---|---|---|---|---|
| **D/V** | 33% (489/1500) | 34% (274/816) | 14% (119/829) | 9.4% (93/991) | 12% (143/1239) | 8.6% (112/1309) |
| **A/P** | 12% (175/1500) | 11% (91/816) | 3.7% (21/829) | 5% (50/991) | 4.3% (53/1239) | 1.4% (19/1309) |
| **AP/DV** | 4.2% (63/1500) | 4.5% (37/816) | 6.3% (52/829) | 2% (20/991) | 2.3% (28/1239) | 4.7% (61/1309) |
| **R3/R3** | 3.3% (50/1500) | 3.9% (32/816) | 15% (123/829) | 1.4% (14/991) | 4.3% (53/1239) | 0.6% (8/1309) |
| **R4/R4** | 4.1% (62/1500) | 4.3% (53/816) | 15% (120/829) | 3.4% (34/991) | 1.7% (21/1239) | 0.7% (9/1309) |
| **Extra R** | 0 | 0.6% (5/816) | 0.2% (2/829) | 0 | 0 | 0 |
| **Missing R** | 0 | 0.3% (2/816) | 2.3% (18/829) | 0.4% (4/991) | 0 | 0 |
| **Fail to rot.** | 0.8% (12/1500) | 0 | 3.1% (26/829) | 2.2% (22/991) | 0 | 0 |
| **Total error** | 57% (856/1500) | 64% (520/816) | 60% (500/829) | 24% (236/991) | 24% (299/1239) | 16% (209/1309) |

**Table 3-1. Five GMREP lines strongly enhance different types of polarity errors in a *sev-stbm* misexpression background.** Particularly striking enhancements are in red.

In order to identify the gene affected by the transgene, I needed to locate the EP element insertion. The GMREP transgene was designed to facilitate this by containing sequences that forward and reverse priming sequences at the 3' end of the GMREP element. Therefore, to find the insertion site, I performed inverse PCR on genomic DNA isolated from EP1658 adults. The EP element inserted into the genome at 29D1, immediately 5' to the uncharacterized C2H2 transcription factor *fu2*. The only other predicted gene within 10kb was the uncharacterized gene *fu10*.

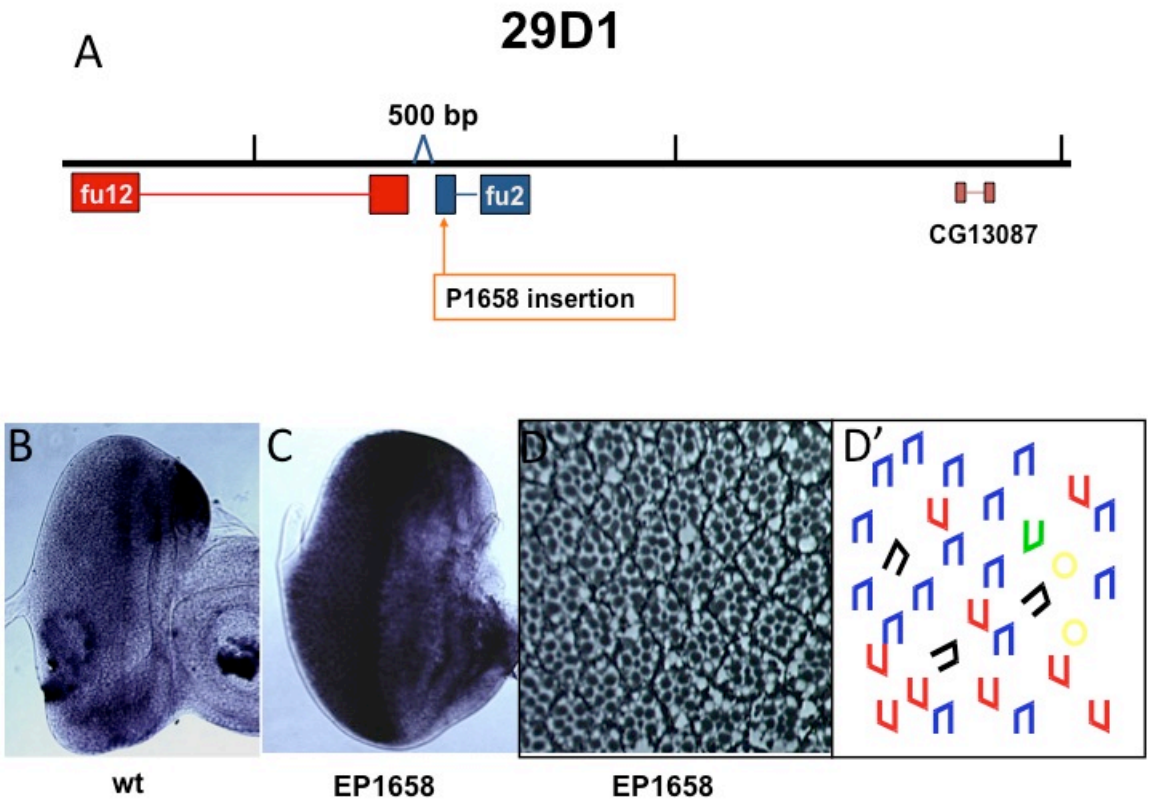


**Figure 3-3. The GMREP element in EP1658 drives misexpression of *fu2*.** (A) A schematic representation of the site of the GMREP insertion in EP1658 and the surrounding gene region. The P-element is inserted into the 5' UTR of *fu2*. In situ hybridization with (B) sense control and (C) antisense probe against fu2 reveals that fu2 is highly expressed in the GMR pattern in EP1658. (D) A cross section through the adult eye and (D') corresponding schematic reveals that EP1658 homozygous eyes have a strong tissue polarity phenotype. Blue trapezoids: wild type; red trapezoids: D/V inversions; green trapezoids: AP/DV inversions; black trapezoids: A/P inversions; yellow circles: R4/R4 symmetrical error.

To determine which gene the EP element affected, I performed *in situ* hybridization with probes designed against the *fu2* mRNA and the *fu10* mRNA. *fu2* showed significantly enhanced expression in the GMR pattern compared to the sense control (Fig. 3-3B,C). In contrast, *fu10* expression levels remained unchanged compared to the sense controls, thus confirming that *fu2* was in fact the affected gene (data not shown).

## Imprecise excision provides a loss-of-function line

The *in situ* hybridization data indicated that the EP1658 adult phenotype resulted from misexpression of *fu2*. The precise pattern of the *Drosophila* eye is extremely sensitive, and phenotypes resulting from gene misexpression could stem from causes outside of the gene's true biological function. For example, excessive amounts of protein could result in polarity errors simply by interfering with signaling events and the formation of protein complexes, and not necessarily by enhanced performance of the gene product.

Therefore, to confirm that *fu2* regulates tissue polarity, I generated an imprecise excision event in the EP1658 line to isolate a line that would excise part or all of the *fu2* gene region. The goal of this experiment is to create a loss-of-function allele, whose phenotype would be more representative of the biological function of *fu2*. I isolated one line, called Δ75, and confirmed using PCR that the entire *fu2* coding region was excised in this line.

The Δ75 line was subviable: only a small number of homozygous mutant escapers survived. While these escaper flies had rough eyes, a cross section through the

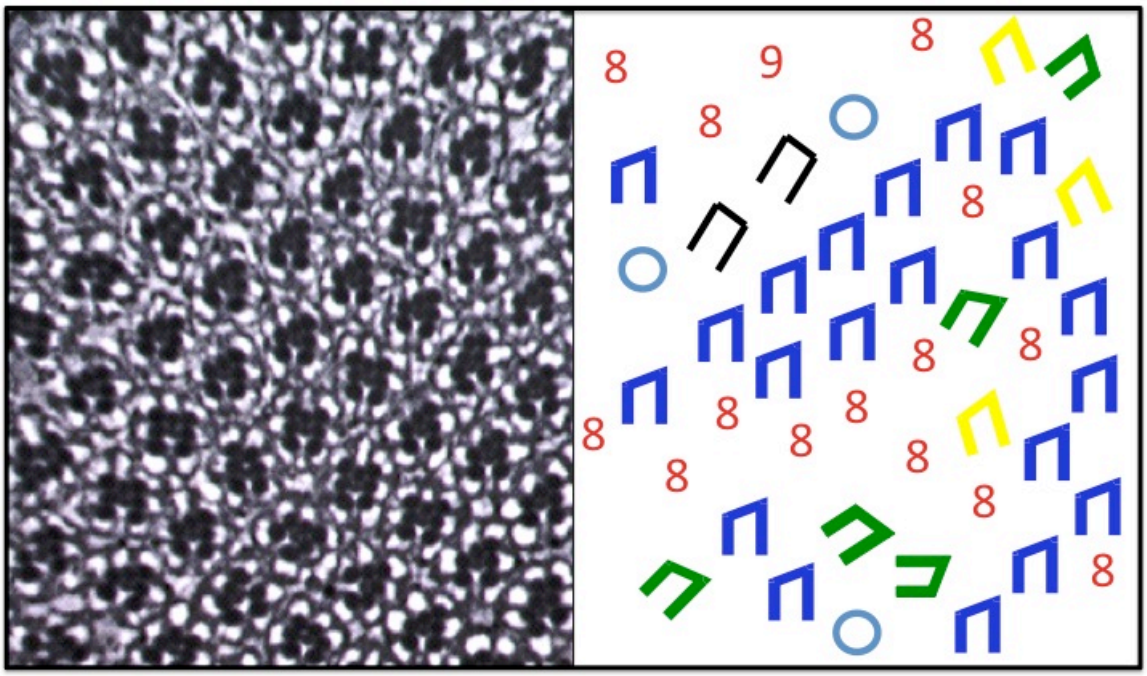

**Figure 3-4. Δ75 mutant eyes have a tissue polarity phenotype.** A cross-section and corresponding schematic through Δ75 adult eyes reveal several errors, including photoreceptor number defects, misrotated ommatidia, and symmetrical defects. Blue trapezoids: wild type ommatidia. Green trapezoids: under-rotated ommatidia. Yellow trapezoids: over-rotated ommatidia. Black rectangles: R3/R3 symmetrical errors. Blue circles: R4/R4 symmetry errors. Numbers represent ommatidia with photoreceptor number defects.

adult Δ75 eye revealed a strikingly different phenotype than that of the EP1658 misexpression line (Fig. 3-4). Very few ommatidia had any chirality defects, although a few had what appeared to be symmetrical defects. Many ommatidia had one extra outer photoreceptor cell. Finally, many ommatidia were misoriented.

## Δ75 is not an allele of *fu2*

Since the entire coding *fu2* region was deleted, I assumed this was a genetic and protein null allele of *fu2*. To confirm this, I performed a genetic test, by placing Δ75 in *trans* to a deficiency chromosome that covered the region. A stronger phenotype than the homozygous *fu2* phenotype would indicate that Δ75 is a hypomorphic allele, and an identical phenotype would indicate a genetic null allele. Δ75 in *trans* to a deficiency chromosome uncovering the region is entirely wild-type.

This result revealed that *fu2*, despite being deleted from the Δ75 line, was not the causative gene of the Δ75 phenotype. The most likely explanation was that a second EP element was inserted into the original EP1658 line, and that the excision of gene near that insertion caused the phenotype. Chromosomal *in situ* hybridization (Todd Laverty, personal communication) revealed that EP1658 contained three separate EP elements: the *fu2* insertion at 29D1, an insertion at 42D6, and a third insertion at 57A7.

To isolate these insertions, I out-crossed the original EP1658 line and isolated three line, each with one EP insertion. The insertion at 42D6 was immediately 5' of the actin and metal ion binding gene *coronin* (Bharathi et al., 2004), and 57A7 insertion was immediately 5' of the zinc ion binding gene *hillarin* (Ji et al., 2005). Because loss-of-

function alleles of both *coronin* and *hillarin* are available, I tested these to see if either gene was allelic to Δ75, but both genes complemented Δ75. From these data, I concluded that none of the genes affected by the original insertions in the EP line caused the Δ75 phenotype.

## The Δ75 mutation maps to chromosomal region 24C3 – 25A3

In order to find the gene affected in the Δ75 line, I used a mapping strain to pinpoint the location of the mutation. This genetic mapping indicated that the mutation associated with the Δ75 phenotype is located distal to 31D. To narrow the region, I tested deficiency chromosomes covering this whole region for failure to complement Δ75. One deficiency line, Df702, failed to complement Δ75. Df702 uncovers region 24D3 – 25A3, far from any of the EP insertions. Again, this combination is subviable; these escapers phenocopy the Δ75 escapers.

Df702 deletes a region that contains the genes *echinoid* (*ed*) (see chapter 2) and *fat*, both of which are tissue polarity genes. Therefore, both are excellent candidates to be the gene mutated in the Δ75 strain. A deficiency that specifically removes the *fat* gene region complements Δ75. This was not surprising, given that *fat* and Δ75 have completely different phenotypes. However, Δ75 and *ed* have very similar phenotypes. Therefore, I tested the $ed^{K1102}$ allele and found that it, too, complemented Δ75.

## Δ75 genetically interacts with the tissue polarity genes.

The Δ75 phenotype strongly resembles that of certain genes that interact with the tissue polarity genes, including *ed* and *fred*. To determine if Δ75, too, interacted with

the tissue polarity genes I used a genetic approach to look for interaction and found that the Δ75 allele enhances the *dsh* and *stbm* mutant phenotypes but did not enhance the *pk* or *dgo* phenotypes. In contrast, *dsh*, *stbm*, *pk*, and *dgo* suppress the Δ75 phenotype (Table 3-2).

| | Total omm. | % errors | % DV | % AP | % AP&DV | % R3R3 | % R4/R4 | % extra R |
|---|---|---|---|---|---|---|---|---|
| *Δ75H* | 1401 | 26.6 | 0.26 | 1.3 | 0.16 | 3.2 | 5.6 | 12.3 |
| *Δ75,dgo$^{380}$/Δ75* | 327 | 15 | 0 | 0 | 0.9 | 1.8 | 5.1 | 4.5 |
| *Δ75,stbm$^{6cn}$/Δ75* | 337 | 12.5 | 0 | 0 | 0 | 0.2 | 2.65 | 8.7 |
| *Δ75,stbm$^{153}$/Δ75* | 1419 | 3.8 | 0 | 0.11 | 0 | 0.51 | 0.69 | 1.96 |
| *Δ75,fmi$^{192}$/Δ75* | 322 | 5.87 | 0.7 | 0.8 | 0 | 0.28 | 0.28 | 2.19 |
| *Δ75, pk$^{sple}$/Δ75* | 916 | 5.8 | 0.2 | 0.3 | 0 | 0.7 | 1 | 1.6 |
| *stbm$^{153}$* | 1769 | 37.75 | 19.5 | 11.375 | 2.9 | 0.81 | 2.39 | 0 |
| *Δ75,stbm$^{153}$/stbm$^{153}$* | 2116 | 47.3 | 19.64 | 10.16 | 3.23 | 3.05 | 5.49 | 0 |
| *dgo$^{380}$* | 952 | 45 | 0.64 | 5.72 | 1.02 | 6.26 | 30.5 | 0 |
| *Δ75,dgo$^{380}$/dgo$^{380}$* | 842 | 41.3 | 2.32 | 5 | 0.35 | 9.4 | 24.5 | 0 |
| *stbm6cn* | 2033 | 44 | 23.6 | 9.1 | 3.9 | 2.3 | 2.1 | 0 |
| *Δ75,stbm$^{6cn}$/stbm$^{6cn}$* | 648 | 60.5 | 26 | 6.125 | 6.9 | 6.7 | 14.4 | 0.45 |
| *pk$^{sple}$* | 1259 | 46 | 38 | 2 | 1.8 | 1.6 | 2.2 | 0.2 |
| *Δ75, pk$^{sple}$/pk$^{sple}$* | 2854 | 41 | 39 | 1.1 | 0.5 | 0.5 | 0.7 | 0 |
| *dsh$^{1}$/Y;Δ75/+* | 1972 | 43 | 8.9 | 5.24 | 4.26 | 12.5 | 11 | 0.11 |
| *dsh$^{1}$/Y* | 994 | 24.3 | 4.2 | 5.85 | 4.53 | 5.45 | 3.86 | 0 |

**Table 3-2. Δ75 interacts with the tissue polarity genes.**

# Discussion

In this work, I phenotypically characterize one GMREP line and present evidence that it genetically interacts with misexpression lines of tissue polarity genes. I provide further evidence that there are three GMREP insertions in this line, that one insertion results in greatly increased gene expression of the transcription factor *fu2*, and that none of the genes affected by these insertions actually influence tissue polarity. I generate a loss-of-function mutation that specifically affects ommatidial rotation and photoreceptor recruitment, and which phenocopies mutations in *ed* and *fred*. I map this mutation to between 24D3 and 25A1, and determine that neither *ed* nor *fat* are allelic to Δ75.

The initial GMREP line EP1658 enhanced the D/V class of error to a greater extent than any other, and had a tissue polarity eye phenotype. However, the work I did characterizing this line demonstrated that none of the genes that were affected by the EP element actually had a role in tissue polarity. Therefore, I conclude that the original genetic enhancements and the eye phenotype were due to an excess of protein or mRNA that interfered with proper tissue polarity signaling.

The mutation in the Δ75 line remains of interest. First, it interacts genetically with the tissue polarity genes. Second, the phenotype of the adult escapers suggests that while this mutation acts differently that the original EP1658 results led me to expect, it still provided a new mutant line that affects one aspect of tissue polarity (degree of rotation). Some ommatidia also appear to have symmetrical errors, suggesting an affect on the cell fate decision, but this observation has not been confirmed looking at a molecular marker for R3/R4 fate.

The phenotype of Δ75 is strikingly like that of *ed* and *fred*. Furthermore, a deficiency in the region of *ed* and *fred* fails to complement the Δ75 mutation. These observations made it seem extremely likely that *ed* may be the gene mutated in the Δ75 line. However, the molecular null allele $ed^{K1102}$ complements Δ75. I have not performed complementation analysis with *fred* loss-of-function alleles because these lines were not available before I ended this project. However, it would be interesting to test Δ75 against *fred* loss-of-function alleles for complementation. If *fred* fails to complement Δ75, the Δ75 line would be a useful reagent: the first *fred* allele that is homozygous semi-viable.

# Acknowledgements

I thank T. Laverty, who performed the chromosome *in situs*. B. Hay generated the GMREP collection and donated it to the lab.

# CHAPTER FOUR

# Future Directions

# Further exploration of Ed's role in rotation

## Endocytosis and degradation

My work suggests that prior to rotation initiation, Ed is visible in punctae in the ommatidial precursor cells. These vesicles are frequently Rab5-GFP and Rab7-GFP positive, indicating that Ed, either the full-length protein or the cleaved Ed intracellular domain (ICD), is endocytosed and shuttled into lysosomes for degradation (Kramer, 2002). In this experiment, GMR-Gal4 drives Rab5-GFP or Rab7-GFP in an otherwise wild-type background that also contains endogenous Rab5 and Rab7; in other words, these data are based on misexpression studies. Therefore, these results need to be validated with immunohistochemistry using antibodies against endogenous Rab5 and Rab7 and confirming that Ed colocalizes with these proteins in a statistically significant manner.

In my model, immediately before ommatidial rotation, ommatidia actively endocytose Ed, reducing Ed levels in ommatidial membranes to levels significantly lower than in the IOCs; the resulting minimal adhesion between the two cell populations provides an environment permissive for ommatidial rotation. To test the hypothesis that endocytosis causes the reduction in Ed levels seen in rows 3 – 6, endocytosis could be blocked using the *shibire* mutation and the consequent effect on Ed levels assessed. This temperature- sensitive allele of Dynamin prevents endocytosis when larvae are subjected to heat shock (Lloyd et al., 2002). Using the α-Ed antibody, levels of membrane-associated Ed at the surface of the ommatidial cells could be assessed in eye discs from *shi* larvae dissected immediately after heat shock. If my hypothesis is correct, I would

expect to see high levels of Ed in ommatidia in rows 3 – 6 in these discs. *shi* mutant ommatidia have both photoreceptor number and ommatidial rotation defects, indicating that endocytosis itself is necessary for ommatidial rotation(Lloyd et al., 2002).

## Structure/function analysis

My work suggests that Ed plays two roles during the regulation of rotation: 1) reducing adhesion between ommatidial cells and IOCs during the fast phase of rotation and 2) inhibiting Egfr signaling during the slow half of rotation. However, the molecular mechanism by which Ed performs its functions remains unclear. The extracellular domain (ECD), rich in protein-protein interaction domains, is essential for regulating cell-cell adhesion. The ECD has also been implicated in the direct physical interaction between Ed and the Egf receptor, and is required for the homotypic and heterotypic *trans* dimerization necessary to retain Ed at the cell membrane (Spencer and Cagan, 2003). However, Ed's ICD contains two important protein-protein interaction domains as well: the C-terminal PDZBM and a Jar-interacting region (Lin et al., 2007; Wei et al., 2005). It is unknown whether any part of the Ed ICD is necessary during ommatidial rotation.

To investigate the ICD's role in ommatidial rotation, a structure/function analysis could be performed, generating a transgenic line containing an Ed construct lacking the ICD and testing it for the ability to rescue the *ed* loss-of-function ommatidial rotation phenotype. If the ICD proves to be indispensable in ommatidial rotation, further investigation, creating transgenic lines carrying constructs deleting the ICD's known functional motifs and testing for ability to rescue the *ed* phenotype could lend further insight into the molecular mechanism underlying Ed's role in ommatidial rotation. For

example, if Ed's PDZBM is necessary for ommatidial rotation, this would indicate that Ed interacts with an as yet unknown intracellular molecule to regulate ommatidial rotation. Such a result could indicate that Ed may act in a protein complex, possibly keeping molecules localized to the membrane. Alternatively, Ed's PDZBM may bind to a protein that either facilitates or blocks cleavage and endocytosis of the ICD. In the wing, Cno's PDZ domain binds Ed's PDZBM (Wei et al., 2005), but my work demonstrates that this relationship is not true in the *Drosophila* eye. Therefore, it will be necessary to identify the protein that does bind Ed's PDZBM.

## Identifying physical interactors of Ed

If Ed's PDZBM proves to be important in ommatidial rotation, the identity of the PDZ protein that binds Ed remains unknown. One potential candidate is Bazooka (Baz), the *Drosophila* homolog of Par-3(Kuchinke et al., 1998). In the wing, Ed's PDZBM binds Baz's PDZ domain; Baz competes with Cno for binding to Ed(Wei et al., 2005). Although Baz has not been shown to play a role in rotation, it is a component of adherens junctions and therefore an excellent candidate for Ed's binding partner during rotation (Muller and Wieschaus, 1996). First, I would test for genetic interactions between *baz* and *ed* to confirm that these genes interact in ommatidial rotation. If so, the next step would be molecular epistasis, assessing whether Baz localizes properly to the cell membranes in *ed* null clones, using an α-Baz antibody. If Baz does not bind Ed, or if Ed is not necessary for Baz to localize to adherens junctions in the eye, a screen for physical interactors similar to that performed by (Wei et al., 2005) could turn up novel candidates, or proteins previously not implicated in ommatidial rotation.

## Identification of a regulator of Ed activity

Ed levels are initially high in the ommatidial precluster but drop to nearly undetectable levels in the ommatidia immediately preceding and during the fast stage of ommatidial rotation. However, after approximately row 7, Ed levels rise in the ommatidial cells until they equal levels within the IOCs. At the end of ommatidial rotation, Ed is enriched at the photoreceptor/cone cell boundary and again at the cone cell/IOC boundary. It is entirely unknown what causes so dramatic a reduction in Ed levels before ommatidial rotation, and also what triggers Ed levels to rise after row 7.

What is that signal? To answer this question, I would first use a candidate gene approach. One potential candidate is the N regulatory gene *scabrous* (*sca*). Sca is a secreted fibrinogen-related glycoprotein found at high levels along the morphogenetic furrow and also up to 6 – 8 rows behind the MF (Baker et al., 1990; Chou and Chien, 2002; Lee et al., 1996; Lee et al., 2000). Sca has been shown to function during ommatidial rotation, although there is some controversy as to its role. Published data suggest that *sca* loss-of-function mutations result in over-rotated ommatidia, from which the authors concluded that Sca functions as a brake (Chou and Chien, 2002). My unpublished work (Fig. 4-1) demonstrates that *sca* loss-of-function ommatidia actually under-rotate, suggesting that Sca promotes rotation. According to multiple sources, secreted Sca protein is observed up to 8 rows past the MF (Chou and Chien, 2002; Lee et al., 1996). Therefore, it localizes to exactly the right place and time to act as the signal that ultimately results in reduction of Ed levels and, therefore, rotation initiation.

Although *fred* interacts genetically with *sca* (discussed below), an interaction between *ed* and *sca* has not been tested. Therefore, I would first use a genetic approach to see if loss of one copy of *ed* dominantly modifies the *sca* phenotype. If so, I would use next use molecular epistasis to determine whether or not Ed levels drop in ommatidial cells in *sca* mutant tissue. If my hypothesis is correct, and Sca is the signal that induces Ed endocytosis, I would predict that in *sca* mutant clones, Ed levels would not decrease in ommatidial cells.

If there is an interaction between *ed* and *sca*, Ed may act as a receptor for Sca, and the signal is the result of Sca binding the Ed ECD. To test this, I would perform binding assays using cell extracts to see if Ed and Sca physically interact. It is possible, due to Sca's known role as a modifier of *N* signaling, that any potential *ed*/*sca* genetic interaction could have a basis in *N* signaling. This is unlikely, however, because *ed* does not interact genetically with *N* or *Dl* in ommatidial rotation (data not shown), and only co-localizes randomly with *N* and *Dl* in ommatidia cells (data not shown).

# Further investigation of Fred in rotation

## Structure/function analysis

Fred has no known intracellular functional motifs, and a number of extracellular protein-protein interaction domains (Chandra et al., 2003). Fred's ECD is necessary for Fred to form *trans* heterodimers with Ed (Spencer, in preparation). It remains unknown whether Fred's ICD plays a role in regulation of ommatidial rotation. Performing a structure/function analysis like that described above for Ed could identify potential

regions of the Fred protein that may be important for Fred function or localization. Transgenic lines would be generated containing a Fred construct that lacks the Fred ICD, and these could be assayed for ability to rescue the *fred* loss-of-function ommatidial rotation phenotype. If the ICD proves to be important in ommatidial rotation, further constructs need to be generated to identify the precise region of the ICD involved in activity. The ICD may be required for the physical interaction between Fred and an unknown protein, possibly to set up a protein complex.

In addition, the ICD may play an important role in Fred localization. The Ed and Fred localization patterns are strikingly different, although *in situ* hybridization indicates that both genes are ubiquitously expressed throughout the eye disc ((Chandra et al., 2003) and data not shown). This indicates that the difference in localization patterns is due to manipulation of the protein post-translationally and not due to *ed* and *fred* transcription occurring in different cells. Furthermore, the protein sequences of the Ed and Fred ICDs have little similarity (only 30% identical), although their ECDs are highly homologous (70% identical)(Chandra et al., 2003). Taken together, these observations lead me to predict that Fred's ICD dictates its distinct and dynamic localization pattern, and is therefore necessary for rotation.

## Identification of Fred binding partners

Fred currently has no known physical interactors besides Ed. Fred's localization pattern is intriguingly reminiscent of the Stbm and Fmi localization patterns (Rawls and Wolff, 2003). While Fred localization does not depend on Stbm or Fmi function (chapter 2, data not shown), the identical localization patterns suggest the possibility that Fred

may bind one or both of these proteins in a complex. Therefore, the first method to identify interactors will be a candidate protein approach, starting with Stbm and Fmi. Binding assays, using cell extracts from eye discs, will determine whether or not Fred binds either of these proteins in the eye. If Fred does not bind either Fmi or Stbm a general physical interaction screen, such as in (Wei et al., 2005) could identify possible regulators or effectors of Fred activity. Although Fred has no obvious protein-protein interaction motifs, that does not rule out the possibility of the Fred ICD binding some protein. For instance, the region of the Ed ICD that binds Jaguar (Jar), the fly homolog of myosin VI, is not a known protein-protein interaction domain (Lin et al., 2007).

## Identifying a regulator of Fred activity

Like Ed, Fred localization is continually in flux during ommatidial rotation. Again, to understand the mechanism by which Fred regulates ommatidial rotation, it is important to learn how Fred itself is regulated during this process. Currently, the means of Fred regulation is not clear. Again, to investigate this I would initially take a candidate gene approach. A prime candidate for regulator of Fred function is Sca. My work shows that *fred* and *sca* genetically interact, and in fact that loss of one copy of *fred* strongly suppresses the *sca* phenotype (Fig. 4-2). One model leading from this data is that Sca directly binds Fred, preventing Fred from binding Ed, and allowing Ed to bind and inhibit the Egf receptor. This model can be tested using pulldown assays with cell extracts to determine whether Fred and Sca physically interact.

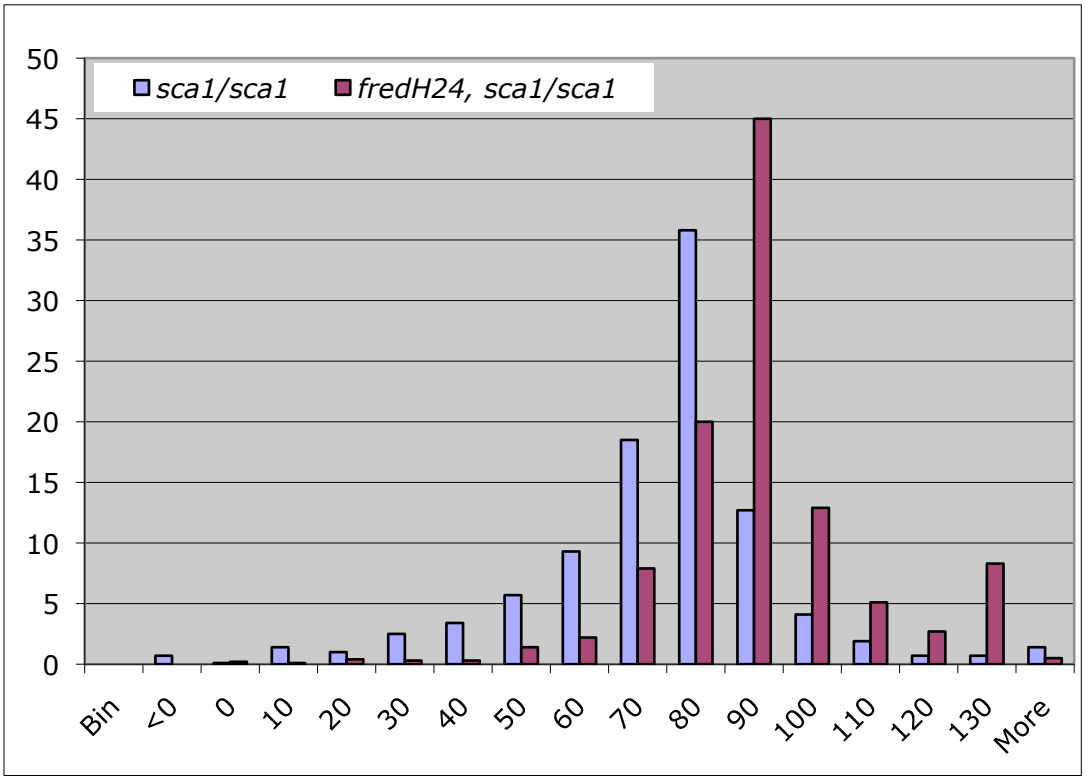


**Figure 4-1. *fred* suppresses the *sca* mutant phenotype.** Histogram representing the percentage of ommatidia (Y-axis) that are oriented at a particular angle (X-axis). In the *sca* background (light purple bars), ommatidia underrotate and there is a wide variance. Removing one copy of *fred* from this background (pink bars) suppresses the underrotation phenotype and, to a lesser extent, the variance.

# Further investigation of Cno in rotation

## Cno mosaic analysis and misexpression

My work demonstrates that Cno inhibits ommatidial rotation, and work from other groups indicates that Egf signaling promotes ommatidial rotation. These observations lead to the model that Egf signaling inhibits Cno activity, and that a reduction in Egf signaling releases this inhibition, thus slowing ommatidial rotation. Cno's localization pattern is identical to that of Armadillo, or β-catenin, and is found at high levels in the membranes of all photoreceptor cells (data not shown). Because of Cno's localization pattern, and the genetic interactions between *cno* and *ed* and *fred* (chapter 2), I hypothesize that Cno acts in photoreceptors R1, R6, R7, and the cone cells to slow ommatidial rotation; in other words, the cells that join the cluster after ommatidial rotation has already begun and which become fully integrated at the start of the slow phase of ommatidial rotation. To test this hypothesis, I would to perform a standard mosaic analysis in adult eyes (for the photoreceptors) and in pupal eyes (for the cone cells).

Cno is the Drosophila homolog of Afadin/AF-6 (Matsuo et al., 1997; Miyamoto et al., 1995). In mammals, Afadin binds members of the nectin family (the closest mammalian relatives of Ed and Fred) to initiate AJ formation (Rikitake and Takai, 2008; Takahashi et al., 1999; Takai et al., 2008). This recruits E-cadherin, β-catenin, and α-actinin via Afadin's interaction with α-actinin and stabilizes the junction and, therefore, adhesion between adjacent cells (Sakisaka et al., 2007; Tachibana et al., 2000). Although Cno localization does not depend on Ed in the eye, Cno still must slow rotation by

building AJs and anchoring the actin cytoskeleton at AJs which would impede the movement of ommatidial cells past IOCs. If this is the case, I would expect that misexpressing Cno at high levels in the eye disc, thereby overwhelming Egfr inhibition and increasing the number of AJs, would result in dramatically slowed ommatidial rotation. To test this, I would use eye-specific drivers (*sev*-Gal4, GMR-Gal4, and *ro*-Gal4) to drive UAS-*cno* in an otherwise wild-type background and assess the resulting affect on ommatidial rotation. If my hypothesis is correct, the mean angle of orientation of ommatidia in these eyes should be dramatically less than 90°. It may even be possible, by misexpressing *cno*, to suppress rotation entirely.

## Analysis of *cno* larval phenotype

While the Cno phenotype includes misrotated ommatidia, it is still unclear when *cno* functions during rotation. My work assessing ommatidial rotation in *ed* and *fred* loss-of-function discs revealed that the *ed* and *fred* phenotypes are statistically significantly different from the controls from row 8 to row 15 (chapter 2). Furthermore, the Freeman lab found that interfering with Egfr signaling between rows 8 and 15 caused rotation defects (Brown and Freeman, 2003). Therefore, I hypothesize that Cno, too, will act during the slow phase of rotation. To confirm this, it will be necessary to measure ommatidial rotation in *cno* mutant larval discs between rows 2 and 15, to see if and when the *cno* phenotype becomes significantly different from wild type.

### Identifying physical interactors of Cno

My work demonstrates that unlike in the wing, Cno localization in the eye is not dependent on Ed binding. However, Cno is tightly membrane associated in the eye disc and colocalizes with β-catenin at the AJs, meaning that some protein must be anchoring Cno to AJs. Since AJ formation is likely vital for inhibition of ommatidial rotation, it will be important to identify which protein acts in concert with Cno to form these junctions. A first attempt should involve molecular epistasis with candidate genes, assessing Cno localization in clones of loss-of-function alleles of genes whose products resemble the Cno localization pattern. Potential candidates include E-cad, β-catenin, and α-actinin, the last of which is a known Cno binding partner (Tachibana et al., 2000).

## Further investigation of the tissue polarity genes and rotation

### Mosaic analysis of additional tissue polarity proteins

The *stbm* mosaic analysis provided new and exciting evidence that at least one of the tissue polarity genes functions in a cell outside of R3/R4 to regulate one aspect of tissue polarity, degree of rotation. The mechanism by which Stbm acts in R7 to regulate this process is entirely unclear. Furthermore, Stbm's requirement in R7 suggests that the other TP genes, too, may act outside of R3 or R4.

Mosaic analyses of the additional tissue polarity genes would determine whether they, too, function outside of R3/R4 to regulate degree of rotation. I hypothesize that Stbm and Fmi would be necessary in R7, and that perhaps Fz, Dsh, and Dgo may be

required in R1/R6. In general, localization of Fz/Dsh/Dgo and Stbm/Pk are mutually exclusive. Stbm, Fmi, and Pk (the Stbm complex) are required in R4 and Fz, Dsh, Dgo, and Fmi (the Fz complex) are required in R3 for correct fate specification (Strutt et al., 2002; Wolff and Rubin, 1998). At the R3/R4 boundary, the Fz complex localizes to the R3 side of the interface, excluding the Stbm proteins. Similarly, the Stbm complex localizes to the R4 side of the interface, thus blocking the Fz complex from this part of the R4 cell(Strutt, 2002). Furthermore, in the wing Fz, Dsh, and Dgo localize to the distal face of the wing cell, and Stbm and Pk localize to the proximal side (Fmi localizes to both sides) (Bastock et al., 2003; Strutt, 2001). Therefore, mutually exclusive localization and activity of the Stbm complex and the Fz complex is a conserved aspect of tissue polarity. Stbm functions in R7, and is localized at the tip of R7/R8 interface. From this, I predict that Fz, Dsh, and Dgo will prove to be required in R1 and R6 to regulate ommatidial rotation. I expect Fmi to be required in all three cells. However, Pk (which does not have a rotation phenotype, data not shown) would be unlikely to be required in any of these cells during ommatidial rotation.

## Molecular epistasis with Egf signaling components

My work demonstrates that the Ed/Fred and TP protein interaction does not have its basis in protein localization. Various TP genes have been shown to interact genetically with members of the Egf signaling pathway, and the Fmi localization pattern is irregular in *aol*$^{rlt}$ mutant discs(Gaengel and Mlodzik, 2003). One potential role of the TP pathway in ommatidial rotation is to regulate Egf signaling. If this is the case, levels of Egfr

activity may be altered in TP mutant tissue. To address this, I would perform molecular epistasis analysis of dpErk levels in clones of TP mutant tissue.

It is possible that instead of acting in a linear pathway, the TP signaling pathway and the Egf signaling pathway may be acting in parallel pathways that converge at some unknown downstream effector. Both the Egf signaling pathway and the TP gene *stbm* enhance the phenotype of *shotgun*, an allele of the Egf receptor (Gaengel and Mlodzik, 2003). Therefore, Stbm may regulate levels of E-cadherin-based adhesion specifically in R7. This hypothesis is supported by the observation that E-cad levels are irregular in clones of RhoA mutant tissue; RhoA is an effector of TP signaling (Gaengel and Mlodzik, 2003).

.

# REFERENCES

**Adler, P. N.** (2002). Planar signaling and morphogenesis in Drosophila. *Dev Cell* **2**, 525-35.

**Bai, J., Chiu, W., Wang, J., Tzeng, T., Perrimon, N. and Hsu, J.** (2001). The cell adhesion molecule Echinoid defines a new pathway that antagonizes the Drosophila EGF receptor signaling pathway. *Development* **128**, 591-601.

**Baker, N. E., Mlodzik, M. and Rubin, G. M.** (1990). Spacing differentiation in the developing Drosophila eye: a fibrinogen-related lateral inhibitor encoded by scabrous. *Science* **250**, 1370-7.

**Bastock, R., Strutt, H. and Strutt, D.** (2003). Strabismus is asymmetrically localised and binds to Prickle and Dishevelled during Drosophila planar polarity patterning. *Development* **130**, 3007-14.

**Bharathi, V., Pallavi, S. K., Bajpai, R., Emerald, B. S. and Shashidhara, L. S.** (2004). Genetic characterization of the Drosophila homologue of coronin. *J Cell Sci* **117**, 1911-22.

**Boutros, M. and Mlodzik, M.** (1999). Dishevelled: at the crossroads of divergent intracellular signaling pathways. *Mech Dev* **83**, 27-37.

**Brown, K. E. and Freeman, M.** (2003). Egfr signalling defines a protective function for ommatidial orientation in the Drosophila eye. *Development* **130**, 5401-12.

**Brown, K. E., Kerr, M. and Freeman, M.** (2007). The EGFR ligands Spitz and Keren act cooperatively in the Drosophila eye. *Dev Biol* **307**, 105-13.

**Casci, T., Vinos, J. and Freeman, M.** (1999). Sprouty, an intracellular inhibitor of Ras signaling. *Cell* **96**, 655-65.

**Chae, J., Kim, M. J., Goo, J. H., Collier, S., Gubb, D., Charlton, J., Adler, P. N. and Park, W. J.** (1999). The Drosophila tissue polarity gene starry night encodes a member of the protocadherin family. *Development* **126**, 5421-9.

**Chandra, S., Ahmed, A. and Vaessin, H.** (2003). The Drosophila IgC2 domain protein Friend-of-Echinoid, a paralogue of Echinoid, limits the number of sensory organ precursors in the wing disc and interacts with the Notch signaling pathway. *Dev Biol* **256**, 302-16.

**Cho, E. and Irvine, K. D.** (2004). Action of fat, four-jointed, dachsous and dachs in distal-to-proximal wing signaling. *Development* **131**, 4489-500.

**Choi, K. W. and Benzer, S.** (1994). Rotation of photoreceptor clusters in the developing Drosophila eye requires the nemo gene. *Cell* **78**, 125-36.

**Chou, Y. H. and Chien, C. T.** (2002). Scabrous controls ommatidial rotation in the Drosophila compound eye. *Dev Cell* **3**, 839-50.

**Clark, H. F., Brentrup, D., Schneitz, K., Bieber, A., Goodman, C. and Noll, M.** (1995). Dachsous encodes a member of the cadherin superfamily that controls imaginal disc morphogenesis in Drosophila. *Genes Dev* **9**, 1530-42.

**Cooper, M. T. and Bray, S. J.** (1999). Frizzled regulation of Notch signalling polarizes cell fate in the Drosophila eye. *Nature* **397**, 526-30.

**Curtin, J. A., Quint, E., Tsipouri, V., Arkell, R. M., Cattanach, B., Copp, A. J., Henderson, D. J., Spurr, N., Stanier, P., Fisher, E. M. et al.** (2003). Mutation of

Celsr1 disrupts planar polarity of inner ear hair cells and causes severe neural tube defects in the mouse. *Curr Biol* **13**, 1129-33.
**Darken, R. S., Scola, A. M., Rakeman, A. S., Das, G., Mlodzik, M. and Wilson, P. A.** (2002). The planar polarity gene strabismus regulates convergent extension movements in Xenopus. *Embo J* **21**, 976-85.
**de Belle, J. S., Sokolowski, M. B. and Hilliker, A. J.** (1993). Genetic analysis of the foraging microregion of Drosophila melanogaster. *Genome* **36**, 94-101.
**Djiane, A., Riou, J., Umbhauer, M., Boucaut, J. and Shi, D.** (2000). Role of frizzled 7 in the regulation of convergent extension movements during gastrulation in Xenopus laevis. *Development* **127**, 3091-100.
**Dominguez, M., Wasserman, J. D. and Freeman, M.** (1998). Multiple functions of the EGF receptor in Drosophila eye development. *Curr Biol* **8**, 1039-48.
**Eaton, S.** (2003). Cell biology of planar polarity transmission in the Drosophila wing. *Mech Dev* **120**, 1257-64.
**Escudero, L. M., Wei, S. Y., Chiu, W. H., Modolell, J. and Hsu, J. C.** (2003). Echinoid synergizes with the Notch signaling pathway in Drosophila mesothorax bristle patterning. *Development* **130**, 6305-16.
**Fanto, M., Mayes, C. A. and Mlodzik, M.** (1998). Linking cell-fate specification to planar polarity: determination of the R3/R4 photoreceptors is a prerequisite for the interpretation of the Frizzled mediated polarity signal. *Mech Dev* **74**, 51-8.
**Fanto, M. and Mlodzik, M.** (1999). Asymmetric Notch activation specifies photoreceptors R3 and R4 and planar polarity in the Drosophila eye. *Nature* **397**, 523-6.
**Feiguin, F., Hannus, M., Mlodzik, M. and Eaton, S.** (2001). The ankyrin repeat protein Diego mediates Frizzled-dependent planar polarization. *Dev Cell* **1**, 93-101.
**Fiehler, R. W. and Wolff, T.** (2007). Drosophila Myosin II, Zipper, is essential for ommatidial rotation. *Dev Biol* **310**, 348-62.
**Fiehler, R. W. and Wolff, T.** (2008). Nemo is required in a subset of photoreceptors to regulate the speed of ommatidial rotation. *Dev Biol* **313**, 533-44.
**Formstone, C. J. and Mason, I.** (2005). Combinatorial activity of Flamingo proteins directs convergence and extension within the early zebrafish embryo via the planar cell polarity pathway. *Dev Biol* **282**, 320-35.
**Freeman, M.** (1997). Cell determination strategies in the Drosophila eye. *Development* **124**, 261-70.
**Gabay, L., Scholz, H., Golembo, M., Klaes, A., Shilo, B. Z. and Klambt, C.** (1996). EGF receptor signaling induces pointed P1 transcription and inactivates Yan protein in the Drosophila embryonic ventral ectoderm. *Development* **122**, 3355-62.
**Gaengel, K. and Mlodzik, M.** (2003). Egfr signaling regulates ommatidial rotation and cell motility in the Drosophila eye via MAPK/Pnt signaling and the Ras effector Canoe/AF6. *Development* **130**, 5413-23.
**Ghiglione, C., Carraway, K. L., 3rd, Amundadottir, L. T., Boswell, R. E., Perrimon, N. and Duffy, J. B.** (1999). The transmembrane molecule kekkon 1 acts in a feedback loop to negatively regulate the activity of the Drosophila EGF receptor during oogenesis. *Cell* **96**, 847-56.
**Golembo, M., Schweitzer, R., Freeman, M. and Shilo, B. Z.** (1996). Argos transcription is induced by the Drosophila EGF receptor pathway to form an inhibitory feedback loop. *Development* **122**, 223-30.

**Gorfinkiel, N. and Arias, A. M.** (2007). Requirements for adherens junction components in the interaction between epithelial tissues during dorsal closure in Drosophila. *J Cell Sci* **120**, 3289-98.
**Goto, T. and Keller, R.** (2002). The planar cell polarity gene strabismus regulates convergence and extension and neural fold closure in Xenopus. *Dev Biol* **247**, 165-81.
**Gubb, D., Green, C., Huen, D., Coulson, D., Johnson, G., Tree, D., Collier, S. and Roote, J.** (1999). The balance between isoforms of the prickle LIM domain protein is critical for planar polarity in Drosophila imaginal discs. *Genes Dev* **13**, 2315-27.
**Guo, N., Hawkins, C. and Nathans, J.** (2004). Frizzled6 controls hair patterning in mice. *Proc Natl Acad Sci U S A* **101**, 9277-81.
**Harrington, M. J., Hong, E., Fasanmi, O. and Brewster, R.** (2007). Cadherin-mediated adhesion regulates posterior body formation. *BMC Dev Biol* **7**, 130.
**Hay, B. A., Maile, R. and Rubin, G. M.** (1997). P element insertion-dependent gene activation in the Drosophila eye. *Proc Natl Acad Sci U S A* **94**, 5195-200.
**Hermiston, M. L., Wong, M. H. and Gordon, J. I.** (1996). Forced expression of E-cadherin in the mouse intestinal epithelium slows cell migration and provides evidence for nonautonomous regulation of cell fate in a self-renewing system. *Genes Dev* **10**, 985-96.
**Inagaki, M., Irie, K., Ishizaki, H., Tanaka-Okamoto, M., Miyoshi, J. and Takai, Y.** (2006). Role of cell adhesion molecule nectin-3 in spermatid development. *Genes Cells* **11**, 1125-32.
**Ishikawa, H. O., Takeuchi, H., Haltiwanger, R. S. and Irvine, K. D.** (2008). Four-jointed is a Golgi kinase that phosphorylates a subset of cadherin domains. *Science* **321**, 401-4.
**Jamora, C. and Fuchs, E.** (2002). Intercellular adhesion, signalling and the cytoskeleton. *Nat Cell Biol* **4**, E101-8.
**Jenny, A., Reynolds-Kenneally, J., Das, G., Burnett, M. and Mlodzik, M.** (2005). Diego and Prickle regulate Frizzled planar cell polarity signalling by competing for Dishevelled binding. *Nat Cell Biol* **7**, 691-7.
**Jessen, J. R., Topczewski, J., Bingham, S., Sepich, D. S., Marlow, F., Chandrasekhar, A. and Solnica-Krezel, L.** (2002). Zebrafish trilobite identifies new roles for Strabismus in gastrulation and neuronal movements. *Nat Cell Biol* **4**, 610-5.
**Ji, Y., Rath, U., Girton, J., Johansen, K. M. and Johansen, J.** (2005). D-Hillarin, a novel W180-domain protein, affects cytokinesis through interaction with the septin family member Pnut. *J Neurobiol* **64**, 157-69.
**Kibar, Z., Vogan, K. J., Groulx, N., Justice, M. J., Underhill, D. A. and Gros, P.** (2001). Ltap, a mammalian homolog of Drosophila Strabismus/Van Gogh, is altered in the mouse neural tube mutant Loop-tail. *Nat Genet* **28**, 251-5.
**Kim, S. H., Jen, W. C., De Robertis, E. M. and Kintner, C.** (2000). The protocadherin PAPC establishes segmental boundaries during somitogenesis in xenopus embryos. *Curr Biol* **10**, 821-30.
**Klein, D. E., Nappi, V. M., Reeves, G. T., Shvartsman, S. Y. and Lemmon, M. A.** (2004). Argos inhibits epidermal growth factor receptor signalling by ligand sequestration. *Nature* **430**, 1040-4.
**Klein, T. J. and Mlodzik, M.** (2005). PLANAR CELL POLARIZATION: An Emerging Model Points in the Right Direction. *Annu Rev Cell Dev Biol* **21**, 155-76.

**Klingensmith, J., Nusse, R. and Perrimon, N.** (1994). The Drosophila segment polarity gene dishevelled encodes a novel protein required for response to the wingless signal. *Genes Dev* **8**, 118-30.
**Kramer, H.** (2002). Sorting out signals in fly endosomes. *Traffic* **3**, 87-91.
**Kuchinke, U., Grawe, F. and Knust, E.** (1998). Control of spindle orientation in Drosophila by the Par-3-related PDZ-domain protein Bazooka. *Curr Biol* **8**, 1357-65.
**Kumar, J. P., Tio, M., Hsiung, F., Akopyan, S., Gabay, L., Seger, R., Shilo, B. Z. and Moses, K.** (1998). Dissecting the roles of the Drosophila EGF receptor in eye development and MAP kinase activation. *Development* **125**, 3875-85.
**Laplante, C. and Nilson, L. A.** (2006). Differential expression of the adhesion molecule Echinoid drives epithelial morphogenesis in Drosophila. *Development* **133**, 3255-64.
**Lecuit, T.** (2005). Adhesion remodeling underlying tissue morphogenesis. *Trends Cell Biol* **15**, 34-42.
**Lee, E. C., Hu, X., Yu, S. Y. and Baker, N. E.** (1996). The scabrous gene encodes a secreted glycoprotein dimer and regulates proneural development in Drosophila eyes. *Mol Cell Biol* **16**, 1179-88.
**Lee, E. C., Yu, S. Y. and Baker, N. E.** (2000). The scabrous protein can act as an extracellular antagonist of notch signaling in the Drosophila wing. *Curr Biol* **10**, 931-4.
**Lewis, J. and Davies, A.** (2002). Planar cell polarity in the inner ear: how do hair cells acquire their oriented structure? *J Neurobiol* **53**, 190-201.
**Lin, H. P., Chen, H. M., Wei, S. Y., Chen, L. Y., Chang, L. H., Sun, Y. J., Huang, S. Y. and Hsu, J. C.** (2007). Cell adhesion molecule Echinoid associates with unconventional myosin VI/Jaguar motor to regulate cell morphology during dorsal closure in Drosophila. *Dev Biol* **311**, 423-33.
**Lloyd, T. E., Atkinson, R., Wu, M. N., Zhou, Y., Pennetta, G. and Bellen, H. J.** (2002). Hrs regulates endosome membrane invagination and tyrosine kinase receptor signaling in Drosophila. *Cell* **108**, 261-9.
**Mahoney, P. A., Weber, U., Onofrechuk, P., Biessmann, H., Bryant, P. J. and Goodman, C. S.** (1991). The fat tumor suppressor gene in Drosophila encodes a novel member of the cadherin gene superfamily. *Cell* **67**, 853-68.
**Mandai, K., Nakanishi, H., Satoh, A., Obaishi, H., Wada, M., Nishioka, H., Itoh, M., Mizoguchi, A., Aoki, T., Fujimoto, T. et al.** (1997). Afadin: A novel actin filament-binding protein with one PDZ domain localized at cadherin-based cell-to-cell adherens junction. *J Cell Biol* **139**, 517-28.
**Matsuo, T., Takahashi, K., Kondo, S., Kaibuchi, K. and Yamamoto, D.** (1997). Regulation of cone cell formation by Canoe and Ras in the developing Drosophila eye. *Development* **124**, 2671-80.
**Matsuo, T., Takahashi, K., Suzuki, E. and Yamamoto, D.** (1999). The Canoe protein is necessary in adherens junctions for development of ommatidial architecture in the Drosophila compound eye. *Cell Tissue Res* **298**, 397-404.
**Matsushima, H., Utani, A., Endo, H., Matsuura, H., Kakuta, M., Nakamura, Y., Matsuyoshi, N., Matsui, C., Nakanishi, H., Takai, Y. et al.** (2003). The expression of nectin-1alpha in normal human skin and various skin tumours. *Br J Dermatol* **148**, 755-62.

**Mirkovic, I. and Mlodzik, M.** (2006). Cooperative activities of drosophila DE-cadherin and DN-cadherin regulate the cell motility process of ommatidial rotation. *Development* **133**, 3283-93.
**Miyamoto, H., Nihonmatsu, I., Kondo, S., Ueda, R., Togashi, S., Hirata, K., Ikegami, Y. and Yamamoto, D.** (1995). canoe encodes a novel protein containing a GLGF/DHR motif and functions with Notch and scabrous in common developmental pathways in Drosophila. *Genes Dev* **9**, 612-25.
**Mlodzik, M.** (2005). Planar cell polarization during development. Amsterdam ; Boston: Elsevier.
**Montcouquiol, M., Rachel, R. A., Lanford, P. J., Copeland, N. G., Jenkins, N. A. and Kelley, M. W.** (2003). Identification of Vangl2 and Scrb1 as planar polarity genes in mammals. *Nature* **423**, 173-7.
**Montero, J. A., Carvalho, L., Wilsch-Brauninger, M., Kilian, B., Mustafa, C. and Heisenberg, C. P.** (2005). Shield formation at the onset of zebrafish gastrulation. *Development* **132**, 1187-98.
**Mueller, S., Rosenquist, T. A., Takai, Y., Bronson, R. A. and Wimmer, E.** (2003). Loss of nectin-2 at Sertoli-spermatid junctions leads to male infertility and correlates with severe spermatozoan head and midpiece malformation, impaired binding to the zona pellucida, and oocyte penetration. *Biol Reprod* **69**, 1330-40.
**Muller, H. A. and Wieschaus, E.** (1996). armadillo, bazooka, and stardust are critical for early stages in formation of the zonula adherens and maintenance of the polarized blastoderm epithelium in Drosophila. *J Cell Biol* **134**, 149-63.
**Murakami, T., Hijikata, T., Matsukawa, M., Ishikawa, H. and Yorifuji, H.** (2006). Zebrafish protocadherin 10 is involved in paraxial mesoderm development and somitogenesis. *Dev Dyn* **235**, 506-14.
**Naora, H. and Montell, D. J.** (2005). Ovarian cancer metastasis: integrating insights from disparate model organisms. *Nat Rev Cancer* **5**, 355-66.
**Nelson, W. J.** (2003). Adaptation of core mechanisms to generate cell polarity. *Nature* **422**, 766-74.
**Niewiadomska, P., Godt, D. and Tepass, U.** (1999). DE-Cadherin is required for intercellular motility during Drosophila oogenesis. *J Cell Biol* **144**, 533-47.
**Ooshio, T., Fujita, N., Yamada, A., Sato, T., Kitagawa, Y., Okamoto, R., Nakata, S., Miki, A., Irie, K. and Takai, Y.** (2007). Cooperative roles of Par-3 and afadin in the formation of adherens and tight junctions. *J Cell Sci* **120**, 2352-65.
**Ozaki-Kuroda, K., Nakanishi, H., Ohta, H., Tanaka, H., Kurihara, H., Mueller, S., Irie, K., Ikeda, W., Sakai, T., Wimmer, E. et al.** (2002). Nectin couples cell-cell adhesion and the actin scaffold at heterotypic testicular junctions. *Curr Biol* **12**, 1145-50.
**Pacquelet, A. and Rorth, P.** (2005). Regulatory mechanisms required for DE-cadherin function in cell migration and other types of adhesion. *J Cell Biol* **170**, 803-12.
**Park, M. and Moon, R. T.** (2002). The planar cell-polarity gene stbm regulates cell behaviour and cell fate in vertebrate embryos. *Nat Cell Biol* **4**, 20-5.
**Perez-Moreno, M., Jamora, C. and Fuchs, E.** (2003). Sticky business: orchestrating cellular signals at adherens junctions. *Cell* **112**, 535-48.
**Pignatelli, M.** (1998). Integrins, cadherins, and catenins: molecular cross-talk in cancer cells. *J Pathol* **186**, 1-2.

**Pokutta, S., Drees, F., Takai, Y., Nelson, W. J. and Weis, W. I.** (2002). Biochemical and structural definition of the l-afadin- and actin-binding sites of alpha-catenin. *J Biol Chem* **277**, 18868-74.
**Rawlins, E. L., Lovegrove, B. and Jarman, A. P.** (2003a). Echinoid facilitates Notch pathway signalling during Drosophila neurogenesis through functional interaction with Delta. *Development* **130**, 6475-84.
**Rawlins, E. L., White, N. M. and Jarman, A. P.** (2003b). Echinoid limits R8 photoreceptor specification by inhibiting inappropriate EGF receptor signalling within R8 equivalence groups. *Development* **130**, 3715-24.
**Rawls, A. S., Guinto, J. B. and Wolff, T.** (2002). The cadherins fat and dachsous regulate dorsal/ventral signaling in the Drosophila eye. *Curr Biol* **12**, 1021-6.
**Rawls, A. S., Schultz, S. A., Mitra, R. D. and Wolff, T.** (2007). Bedraggled, a putative transporter, influences the tissue polarity complex during the R3/R4 fate decision in the Drosophila eye. *Genetics* **177**, 313-28.
**Rawls, A. S. and Wolff, T.** (2003). Strabismus requires Flamingo and Prickle function to regulate tissue polarity in the Drosophila eye. *Development* **130**, 1877-87.
**Ready, D. F., Hanson, T. E. and Benzer, S.** (1976). Development of the Drosophila retina, a neurocrystalline lattice. *Dev Biol* **53**, 217-40.
**Rikitake, Y. and Takai, Y.** (2008). Interactions of the cell adhesion molecule nectin with transmembrane and peripheral membrane proteins for pleiotropic functions. *Cell Mol Life Sci* **65**, 253-63.
**Sakisaka, T., Ikeda, W., Ogita, H., Fujita, N. and Takai, Y.** (2007). The roles of nectins in cell adhesions: cooperation with other cell adhesion molecules and growth factor receptors. *Curr Opin Cell Biol* **19**, 593-602.
**Shilo, B. Z.** (2003). Signaling by the Drosophila epidermal growth factor receptor pathway during development. *Exp Cell Res* **284**, 140-9.
**Simon, M. A.** (2004). Planar cell polarity in the Drosophila eye is directed by graded Four-jointed and Dachsous expression. *Development* **131**, 6175-84.
**Sozen, M. A., Suzuki, K., Tolarova, M. M., Bustos, T., Fernandez Iglesias, J. E. and Spritz, R. A.** (2001). Mutation of PVRL1 is associated with sporadic, non-syndromic cleft lip/palate in northern Venezuela. *Nat Genet* **29**, 141-2.
**Spencer, S. A. and Cagan, R. L.** (2003). Echinoid is essential for regulation of Egfr signaling and R8 formation during Drosophila eye development. *Development* **130**, 3725-33.
**Spencer, S. A., Powell, P. A., Miller, D. T. and Cagan, R. L.** (1998). Regulation of EGF receptor signaling establishes pattern across the developing Drosophila retina. *Development* **125**, 4777-90.
**Steinberg, M. S.** (2007). Differential adhesion in morphogenesis: a modern view. *Curr Opin Genet Dev* **17**, 281-6.
**Strutt, D., Johnson, R., Cooper, K. and Bray, S.** (2002). Asymmetric localization of frizzled and the determination of notch-dependent cell fate in the Drosophila eye. *Curr Biol* **12**, 813-24.
**Strutt, D. I.** (2001). Asymmetric localization of frizzled and the establishment of cell polarity in the Drosophila wing. *Mol Cell* **7**, 367-75.
**Strutt, D. I.** (2002). The asymmetric subcellular localisation of components of the planar polarity pathway. *Semin Cell Dev Biol* **13**, 225-31.

**Strutt, H., Mundy, J., Hofstra, K. and Strutt, D.** (2004). Cleavage and secretion is not required for Four-jointed function in Drosophila patterning. *Development* **131**, 881-90.
**Strutt, H. and Strutt, D.** (2003). EGF signaling and ommatidial rotation in the Drosophila eye. *Curr Biol* **13**, 1451-7.
**Suzuki, K., Bustos, T. and Spritz, R. A.** (1998). Linkage disequilibrium mapping of the gene for Margarita Island ectodermal dysplasia (ED4) to 11q23. *Am J Hum Genet* **63**, 1102-7.
**Suzuki, K., Hu, D., Bustos, T., Zlotogora, J., Richieri-Costa, A., Helms, J. A. and Spritz, R. A.** (2000). Mutations of PVRL1, encoding a cell-cell adhesion molecule/herpesvirus receptor, in cleft lip/palate-ectodermal dysplasia. *Nat Genet* **25**, 427-30.
**Tachibana, K., Nakanishi, H., Mandai, K., Ozaki, K., Ikeda, W., Yamamoto, Y., Nagafuchi, A., Tsukita, S. and Takai, Y.** (2000). Two cell adhesion molecules, nectin and cadherin, interact through their cytoplasmic domain-associated proteins. *J Cell Biol* **150**, 1161-76.
**Takahashi, K., Nakanishi, H., Miyahara, M., Mandai, K., Satoh, K., Satoh, A., Nishioka, H., Aoki, J., Nomoto, A., Mizoguchi, A. et al.** (1999). Nectin/PRR: an immunoglobulin-like cell adhesion molecule recruited to cadherin-based adherens junctions through interaction with Afadin, a PDZ domain-containing protein. *J Cell Biol* **145**, 539-49.
**Takai, Y., Ikeda, W., Ogita, H. and Rikitake, Y.** (2008). The immunoglobulin-like cell adhesion molecule nectin and its associated protein afadin. *Annu Rev Cell Dev Biol* **24**, 309-42.
**Takai, Y., Irie, K., Shimizu, K., Sakisaka, T. and Ikeda, W.** (2003). Nectins and nectin-like molecules: roles in cell adhesion, migration, and polarization. *Cancer Sci* **94**, 655-67.
**Takekuni, K., Ikeda, W., Fujito, T., Morimoto, K., Takeuchi, M., Monden, M. and Takai, Y.** (2003). Direct binding of cell polarity protein PAR-3 to cell-cell adhesion molecule nectin at neuroepithelial cells of developing mouse. *J Biol Chem* **278**, 5497-500.
**Tepass, U., Godt, D. and Winklbauer, R.** (2002). Cell sorting in animal development: signalling and adhesive mechanisms in the formation of tissue boundaries. *Curr Opin Genet Dev* **12**, 572-82.
**Tepass, U. and Harris, K. P.** (2007). Adherens junctions in Drosophila retinal morphogenesis. *Trends Cell Biol* **17**, 26-35.
**Theisen, H., Purcell, J., Bennett, M., Kansagara, D., Syed, A. and Marsh, J. L.** (1994). dishevelled is required during wingless signaling to establish both cell polarity and cell identity. *Development* **120**, 347-60.
**Tomlinson, A. and Struhl, G.** (1999). Decoding vectorial information from a gradient: sequential roles of the receptors Frizzled and Notch in establishing planar polarity in the Drosophila eye. *Development* **126**, 5725-38.
**Tree, D. R., Shulman, J. M., Rousset, R., Scott, M. P., Gubb, D. and Axelrod, J. D.** (2002). Prickle mediates feedback amplification to generate asymmetric planar cell polarity signaling. *Cell* **109**, 371-81.
**Tsukita, S., Furuse, M. and Itoh, M.** (2001). Multifunctional strands in tight junctions. *Nat Rev Mol Cell Biol* **2**, 285-93.

**Usui, T., Shima, Y., Shimada, Y., Hirano, S., Burgess, R. W., Schwarz, T. L., Takeichi, M. and Uemura, T.** (1999). Flamingo, a seven-pass transmembrane cadherin, regulates planar cell polarity under the control of Frizzled. *Cell* **98**, 585-95.
**Vinson, C. R., Conover, S. and Adler, P. N.** (1989). A Drosophila tissue polarity locus encodes a protein containing seven potential transmembrane domains. *Nature* **338**, 263-4.
**Wei, S. Y., Escudero, L. M., Yu, F., Chang, L. H., Chen, L. Y., Ho, Y. H., Lin, C. M., Chou, C. S., Chia, W., Modolell, J. et al.** (2005). Echinoid is a component of adherens junctions that cooperates with DE-Cadherin to mediate cell adhesion. *Dev Cell* **8**, 493-504.
**Winter, C. G., Wang, B., Ballew, A., Royou, A., Karess, R., Axelrod, J. D. and Luo, L.** (2001). Drosophila Rho-associated kinase (Drok) links Frizzled-mediated planar cell polarity signaling to the actin cytoskeleton. *Cell* **105**, 81-91.
**Winters, B. S., Shepard, S. R. and Foty, R. A.** (2005). Biophysical measurement of brain tumor cohesion. *Int J Cancer* **114**, 371-9.
**Wolff, T., Guinto, J. B. and Rawls, A. S.** (2007). Screen for Genetic Modifiers of stbm Reveals that Photoreceptor Fate and Rotation Can Be Genetically Uncoupled in the Drosophila Eye. *PLoS ONE* **2**, e453.
**Wolff, T. and Ready, D. F.** (1993). Pattern formation in the *Drosophila* retina. In *The Development of Drosophila melanogaster*, (ed. M. Bate and A. Martinez-Arias). Cold Spring Harbor, New York: Cold Spring Harbor Laboratory Press.
**Wolff, T. and Rubin, G. M.** (1998). Strabismus, a novel gene that regulates tissue polarity and cell fate decisions in Drosophila. *Development* **125**, 1149-59.
**Xu, T. and Rubin, G. M.** (1993). Analysis of genetic mosaics in developing and adult Drosophila tissues. *Development* **117**, 1223-37.
**Yang, C. H., Axelrod, J. D. and Simon, M. A.** (2002). Regulation of Frizzled by fat-like cadherins during planar polarity signaling in the Drosophila compound eye. *Cell* **108**, 675-88.
**Zheng, L., Zhang, J. and Carthew, R. W.** (1995). frizzled regulates mirror-symmetric pattern formation in the Drosophila eye. *Development* **121**, 3045-55.